Analysis of Two Newly Identified Protease-Activated Receptor-2-Interacting Proteins, Jab1 and p24A, and their Role in Receptor Signalling

Dissertation

zur Erlangung des akademischen Grades
(To the acquisition of the academic degree)

doctor rerum naturalium
(Dr. rer. nat.)

genehmigt durch

die Fakultät für Naturwissenschaften

der Otto-von-Guericke-Universität Magdeburg

von **M. Sc. Weibo Luo**
geb. am 21.06.1976 in Zhejiang, China

Gutachter: Prof. Dr. Georg Reiser

Prof. Dr. Uwe-Karsten Hanisch

eingereicht am: 16 November, 2006

verteidigt am: 19 April 2007

ACKNOWLEGEMENTS

I am very grateful to those who gave me all kinds of help and support during this work at the Institute of Neurobiochemistry, Otto-von-Guericke Universität Magdegurg.

First of all, I would like to sincerely thank my supervisor, Prof. Dr. Georg Reiser, for providing me an opportunity to join his lab to complete my Ph.D. work. His invaluable knowledge, constructive discussion, professional guidance and constant support enabled me to achieve my goals efficiently and easily, and to be of great benefit to my scientific career throughout my life. I am happy to be a member of the Graduate School directed by Prof. Reiser, and the wonderful lectures, seminars and practical courses he organized opened my scientific ken and stimulated my idea. Of course, many thanks also to our Graduate School secretary Frau Manuela Dullin-Viehweg, who assisted the nice organization of the scientific and social activities.

I would like to deeply thank Dr. Rolf Stricker and Dr. Theodor Hanck for the introduction of the baculoviral expression system and GST pull-down assays, valuable scientific suggestions and technical supports.

I also appreciate Frau Evelyn Busse for her excellent technical assistance at the late period of this work, as well as other colleagues in the lab, Dr. Fariba Sedehizade, Dr. Abidat Schneider, Frau Petra Grüneberg, Frau Anke Imrich, Dr. Gregor Zündorf, Dr. Stefan Kahlert, Frau Annette Jürgen, Frau Denise Ecke, Frau Ewa Ostrowska, Dr. Elena Sokolova, Dr. Mikhail L. Strokin, Frau Anastasia Galvita, Frau Dorothe Terhardt, Herr Mohan E. Tulapurkar, Frau Claudia Baumann, Dr. Tanuja Rohatgi, Herr Rongyu Li, and Frau Sabine Hein for their cooperation and support, and Frau Ines Klaes, Herr Peter Ehrbarth for their kind support, during the course of this work.

I would like to thank Prof. Dr. Bernhard A. Sabel, Institute of Medical Psychology, who enabled me to come to Magdeburg for study.

Finally, I would express my special gratitude to my close colleague and wife Frau Yingfei Wang for her constant discussions, advice, encouragement and love, and to my parents for their support and understanding.

CONTENTS

1. INTRODUCTION

1.1 Proteases

Mammalian proteases form one of the largest and most diverse families of enzymes known. They are divided into five major classes identified to date: serine proteases (EC 3. 4. 21); cysteine proteases (EC 3. 4. 22); aspartate proteases (EC 3. 4. 23); metalloproteases (EC 3. 4. 24) and threonine proteases (EC 3. 4. 25), according to their mechanisms of cleavage and active sites [1]. Of these, serine proteases constitute one third of all proteases found in eukaryotes, prokaryotes, archaea and viruses. This class of enzymes was originally defined by the presence of three residues, aspartate, histidine and serine in the catalytic site, forming a hydrogen bonding system often referred to as the "charge relay system" or "catalytic triad" [2]. Since serine proteases cleave diverse substrates, they are involved in many important physiological and pathological processes including digestion, hemostasis, reproduction, immune response, as well as signal transduction.

In the brain, serine proteases, e.g. thrombin (EC 3. 4. 21. 5), tissue plasminogen activator (tPA, EC 3. 4. 21. 68) and plasmin (EC 3. 4. 21. 7), regulate the consequences of ischemic stroke, synaptic plasticity, neurodegeneration and neuroregeneration [3, 4]. Preclinical studies demonstrate that thrombin at low concentrations protects neurons from damage by ischemic injury, whereas at higher concentrations, thrombin causes neurodegeneration and brain insults [3, 5]. It was also reported that overexpression of tPA in neurons could enhance long-term potentiation and thereby improve learning and memory [6]. However, some studies have already demonstrated that tPA activates microglia cells, and exogenous administration of recombinant tPA into mice exacerbates injury in several ischemic models [4]. In the clinic, serine proteases have developed as important therapeutic targets. Recombinant tPA has been used to treat ischemic stroke patients in USA, since it is involved in degrading fibrin clots and thereby improves patient outcomes after ischemic stroke [7].

1.2 Protease-activated receptor

Serine proteases regulate cells by activating certain membrane receptors. Protease-activated receptors (PARs) are a unique family of the seven-transmembrane domain G protein-coupled receptors (GPCRs), which mediates the signal transduction to extracellular serine proteases like thrombin and trypsin (EC 3. 4. 21. 4). So far, four members (PAR-1 to PAR-4) of this family have been identified [8-11]. PAR has been shown by reverse transcription-polymerase chain reaction (RT-PCR) and immunochemistry to be ubiquitously

expressed in multiple cell types, including platelets, cardiomyocytes, endothelium, smooth muscle cells, epithelium, fibroblasts, hepatocytes, macrophage, lymphocytes, neutrophils, mesangial cells, kerotinocytes, neurons, astrocytes, oligodendrocytes, and microglia [9, 12-21]. Accumulating evidence reveals that PAR is involved in diverse signalling events with numerous consequences in multiple systems, including the cardiovascular system, respiratory system, gastrointestinal system, immune system, renal system, and nervous system (Reviewed in [20-28]).

1.2.1 Subtypes of PAR

1.2.1.1 PAR-1

Thrombin was originally established as a key mediator in the coagulation process. However, it was observed that thrombin strongly induces platelet aggregation in the absence of other factors of the coagulation cascade, suggesting the potential of cellular effects in addition to a role in clot formation. In addition, several studies found that thrombin has direct effects on a number of cell types, including monocytes, endothelium, smooth muscle cells, lymphocytes, and others [29-34]. Notably, serine protease inhibitors could block the effect of thrombin on cells, suggesting that the protease activity of thrombin is essential for these cellular effects [35]. Although several thrombin-binding proteins like thrombomodulin had been identified [36], a functional thrombin receptor had not been discovered until 1990.

In 1991, Coughlin and colleagues isolated the cDNA clone encoding the thrombin receptor, expressed in *Xenopus* oocytes [9]. Sequencing of this clone revealed a 3.5-kb insert, containing an open reading frame encoding a 425-amino acid (aa) protein. Hydropathy analysis further indicates that this protein belongs to a new family of seven-transmembrane domain GPCRs. Afterwards, this family was termed as PAR family by International Union of Pharmacology Committee on Receptor Nomenclature and Drug Classification, and the thrombin receptor was named PAR-1 [37]. The extracellular N-terminus of human PAR-1 contains an amino-terminal signal sequence, three potential *N*-linked glycosylation sites, a hirudin-like binding domain (DKYEPF) and a putative thrombin cleavage site ($R^{41}\downarrow S^{42}$FLLRN) [9], whereas the intracellular domains of human PAR-1 including intracellular loops and C-tail contain a G protein binding site, two palmitoylation sites, several potential phosphorylation sites and receptor trafficking signal sequences [38-40]. Recent studies demonstrate that human PAR-1 possesses the 8^{th} α-helix that is likely to be the 4^{th} intracellular loop anchored by the 7^{th} transmembrane domain and the dual cysteine palmitoylation sites at the C-tail. This helix domain is essential for $G\alpha_q$ coupling and

subsequent signal transductions [40]. Interestingly, there is an ionic interaction between the 8th helix and the intracellular loop 1 of PAR-1, which is also involved in Gα_q coupling to the PAR-1 [40]. PAR-1 is abundantly expressed in platelets, epithelium, endothelium, smooth muscle cells, fibroblasts, myocytes, neurons, astrocytes, oligodendrocytes, and microglia [9, 12-15, 17, 41-43].

1.2.1.2 PAR-2

PAR-2 was identified by a low-stringency hybridization screening of a mouse genomic library using primers corresponding to the second and sixth transmembrane domains of the bovine substance K receptor [10]. Human PAR-2 was cloned later by using the mouse PAR-2 as a probe [44]. Human PAR-2 contains 397 aa with the typical characteristics of a GPCR and with ~30% homology to human PAR-1. By fluorescence *in situ* hybridization, the human *PAR-2* gene is mapped to chromosomal region 5q13, only 90 kb of DNA away from the *PAR-1* gene [44]. The extracellular N-terminus of human PAR-2 contains an amino-terminal signal sequence, a potential *N*-linked glycosylation site and a trypsin cleavage site ($R^{36}\downarrow S^{37}$LIGKV), but no hirudin-like binding domains [45, 46], whereas G protein binding sites, potential phosphorylation sites and one palmitoylation site are found at the intracellular domains of human PAR-2. Similar to PAR-1, human PAR-2 also possesses a 7-8-1 structure that the 7th transmembrane domain interacts with the 8th helix domain, which in turn binds to the adjacent intracellular loop 1. Distribution studies demonstrate that PAR-2 is abundantly present in epithelium, endothelium, smooth muscle cells, fibroblasts, myocytes, monocytes, neurons, astrocytes, and microglia [10, 12, 13, 15-17, 42-45, 47].

1.2.1.3 PAR-3

Although PAR-1 was shown to mediate thrombin-induced signal transduction, murine platelets which lack PAR-1 still respond strongly to thrombin, but not to PAR-1-activating peptide (AP), suggesting the existence of other thrombin receptors [48]. By using primers corresponding to the conserved regions of PAR-1 and PAR-2, another thrombin receptor PAR-3 was cloned from rat platelets mRNA [11]. PAR-3 is also a typical GPCR, and is found to share 27% sequence homology with human PAR-1 and 28% with human PAR-2. It has been identified that the thrombin cleavage site ($K^{38}\downarrow T^{39}$FRGAP) also locates upstream of the hirudin-like binding domain (FEEFP) at the extracellular N-terminus of PAR-3 [11]. Genomic analysis reveals that the human *PAR-3* gene locates at the chromosome 5q13, like both *PAR-1* and *PAR-2*, and it also contains two exons [49]. The distribution of PAR-3 is also similar to

that of other PARs, mainly in platelets (mouse), endothelium, epithelium, smooth muscle cells, microglia, astrocytes and neurons [13, 50-55]. Although PAR-3 appears to be a second thrombin receptor, PAR-3 AP fails to activate PAR-3 in Jurkat T cells and A-498 cells [56, 57]. It was reported that murine PAR-3 acts as a cofactor to facilitate thrombin binding to low-affinity murine PAR-4 [50]. Therefore, PAR-3 may not be a fully functional thrombin receptor, which is apparently distinct from PAR-1.

1.2.1.4 PAR-4

PAR-4 is the third thrombin receptor, and it was cloned by searching expressed sequence tag libraries [8]. Human PAR-4 is 385 aa in length, has a markedly distinct cleavage site ($R^{47}\downarrow G^{48}$YPGQV) for thrombin and trypsin at the extracellular N-terminus, but lacks a hirudin-binding site [8]. PAR-4 shares 33% sequence homology with other human PAR subtypes, but with some distinct difference in the N- and C-terminus. Human PAR-4, like human PAR-3, lacks cysteine palmitoylation sites at the C-tail and an ionic interaction between the 8th helix and the adjacent intracellular loop 1, implying that human PAR-4 and PAR-3 have less coupling efficacy with $G\alpha_q$ [40]. Although human *PAR-4* has the same two-exon structure as the other *PARs*, it is mapped to a different chromosomal locus-19p12 [8]. Since it has a low affinity for thrombin, PAR-4 activation occurs in the presence of high concentrations of thrombin [8]. Like the other PARs, PAR-4 is also expressed in platelets (human), endothelium, epithelium, myocytes, astrocytes, microglia and neurons [8, 13, 53, 55, 58-61].

1.2.2 Agonists and antagonists of PAR

In addition to the wound repair in the coagulation cascade, thrombin at the picomolar concentration range could activate PAR-1 to mediate cellular signal transduction (Table 1.1) [3]. Thrombin is generated by the cleavage of prothrombin in the presence of activated factors Xa (EC 3. 4. 21. 6) and Va, calcium and membrane phospholipids [62]. Prothrombin is mainly produced in the liver [62]. Now it is known that prothrombin is also expressed in the brain throughout development [63]. Like the other zymogens, prothrombin is essentially inactive and appears to have no biological activity [64]. Besides PAR-1 [9], it was found that thrombin could also activate two additional receptors of the PAR family, PAR-3 (human) and PAR-4, by cleavage of their extracellular N-termini (Table 1.1) [8, 11].

PAR-2 is the second member of the PAR family, and it is activated by multiple trypsin-like serine proteases including trypsin, tryptase (EC 3. 4. 21. 59), but not by thrombin (Table

1.1) [10, 65]. The active trypsin is generated from the zymogen by enteropeptidase (EC 3. 4. 21. 9) in the small intestine [66]. Trypsin mainly contains three isoforms, cationic trypsin, anionic trypsin and mesotrypsin, which are encoded, respectively, by *PRSS* (protease, serine) genes *PRSS1*, *PRSS2*, and *PRSS3* in the pancreas [67, 68]. Although trypsin is the main physiological agonist of PAR-2, it is not present in most tissues such as in the brain. Since mast cells have been found in the choroid plexus, in parenchymal and perivascular areas in the central nervous system, and in close contact with peripheral nerves [69, 70], mast-cell tryptase is a good candidate agonist for PAR-2 in the brain. P22 is another trypsin-like serine protease in the brain that has been found to activate PAR-2 [71]. Recently, it has been shown that trypsin IV (mesotrypsin) is expressed in the brain, and is able to activate PAR-2 and PAR-4 in transfected KNRK cells [72]. However, our recent data indicate that mesotrypsin uniquely activates PAR-1, but not PAR-2 in rat astrocytes [73]. Therefore, it is still an open question which PARs are activated by mesotrypsin.

Besides serine proteases that can activate PARs, it was found that the short peptide with sequences matching that of the tethered ligand domain could also fully activate PARs without proteolytic cleavage (Table 1.1). SFLLR-NH_2 (thrombin receptor agonist peptide, TRAP) could activate PAR-1 to mimic thrombin functions in most cell types [9]. Among these TRAPs, Ala-parafluoroPhe-Arg-Cha-Cit-Tyr-NH_2 (TRag) was developed as the most potent and selective PAR-1 peptide agonist [74, 75]. The EC_{50} value of TRag is 0.01 μM, and it has much higher potency (1000-fold) than $TRAP_{14}$ Ser-Phe-Leu-Leu-Arg-Asn-Pro-Asn-Asp-Lys-Tyr-Glu-Pro-Phe-OH [74]. Moreover, TRag (≤50 μM) selectively activates PAR-1, and does not cross-activate other PARs [75]. However, SFLLR-NH_2 could also activate PAR-2, although it possesses higher potency for PAR-1 [76, 77]. This implies the interaction of PAR-1 with neighboring PAR-2. Similar to TRAP, SLIGKV-NH_2 (human) or SLIGRL-NH_2 (rodent) (PAR-2 AP) and GYPGQV-NH_2 (human), GFPGKP-NH_2 (rat) or GYPGKF-NH_2 (mouse) (PAR-4 AP) are also able to activate their respective receptors [8, 10, 44, 78]. Accumulating evidence demonstrates that PAR-2 AP (SLIGKV-NH_2 or SLIGRL-NH_2) only activates PAR-2, but not PAR-1, because of a lack of an essential aromatic amino acid substituent at position 2 of the activating peptide [79, 80]. Compared to SLIGKV-NH_2, SLIGRL-NH_2 is much more potent for PAR-2 activation [81]. Recently, a new PAR-2 AP 2-furoyl-LIGRLO-NH_2 has been developed, which possesses 10 to 20 times higher potency than SLIGRL-NH_2 [82]. Moreover, this peptide selectively activates PAR-2 and does not cause a non-PAR-2-mediated contraction of murine femoral arteries [82]. Interestingly, PAR-3 does not appear to respond to its activating peptide [56, 57].

Many studies have already shown that other proteases can also cleave and activate PARs (Table 1.1), and may exert their functions *in vivo*. Coagulation factors VIIa (EC 3. 4. 21. 21) and Xa that act upstream of thrombin have been shown to potently activate PAR-1, PAR-2 and PAR-4 when allosterically associated with the integral membrane protein tissue factor [21, 83]. Another coagulation protease, activated protein C (APC) (EC 3. 4. 21. 69) could activate PAR-1, which protects neuronal death [54]. Under inflammatory conditions, leukocytes release some proteases (e.g., cathepsin G, elastase, proteinase-3), which may also activate certain PARs. Now it is known that cathepsin G (EC 3. 4. 21. 20) is released from activated neutrophils and causes platelets aggregation. This effect is mediated by PAR-4 [84]. Another neutrophil-derived protease, proteinase-3 (EC 3. 4. 21. 76) was shown to activate PAR-2 in epithelial cells [85]. Interestingly, it was reported that an integral membrane protein, called membrane-type serine protease 1 (MT-SP1) (EC 3. 4. 21. -), can target PAR-2 and thereby activates it [86]. In addition, a number of nonmammalian proteases from mites, bacteria, and fungi have been found to activate PARs in mammalian cells. Bacterial protease arginine-specific gingipains-R (RgpB) (EC 3. 4. 22. 37) was shown to activate PAR-1 and PAR-2 in human oral epithelial cells, and further induces interleukin (IL)-6 secretion [87]. Similarly, the mite cysteine and serine proteases Der P3 and P9 activate PAR-2 to induce cytokines GM-CSF and eotaxin secretion in lung epithelial cells [88]. Therefore, these interesting data might reveal a mechanism by which some pathogens induce inflammatory reactions in the airway.

Since thrombin is a key agent for atherosclerosis, thrombosis and other diseases, the development of antagonists for thrombin receptor, especially for PAR-1, has been widely studied. To date, several peptides and peptidomimetic compounds derived from PAR-1 tethered ligand domain have been shown to block thrombin's actions on platelets (Table 1.1). The first developed antagonist of PAR-1, 3-mercaptopropionyl-Phe-Cha-Cha-Arg-Lys-Pro-Asn-Asp-Lys-amide, was designed based on SFLLRN domain and was reported to inhibit low concentrations of thrombin-induced calcium mobilization, GTPase activation, phospholipase A_2 activation, Na^+/H^+ exchange activation and platelet aggregation [89]. Later on, this peptide was found to be an agonist for PAR-2 [75]. Similarly, another PAR-1 peptide antagonist *trans*-cinnamoyl-parafluoro-Phe-paraguanidino-Phe-Leu-Arg-NH_2 at micromolar concentrations could inhibit thrombin-induced platelet aggregation, but it likely acts as a PAR-2 agonist as well [90]. The poor specificity of peptide-derived PAR-1 antagonists might be due to the fact that PAR is activated by its tethered ligand domain. Therefore, it might be not the optimal strategy to find out specific PAR-1 antagonists based on the tethered ligand

domain. Another class of antagonists, nonpeptide PAR-1 antagonists have also been developed (Table 1.1). RWJ58259 and RWJ56110 both have a high affinity for PAR-1, and selectively inhibit thrombin-induced platelet aggregation *in vitro* [91, 92]. Moreover, RWJ56110 has been shown to significantly improve the cardiovascular hemodynamic profile *in vivo* [93]. Similarly, RWJ58259 could prevent thrombus formation and vascular occlusion in nonhuman primates [94]. Other nonpeptide PAR-1 antagonists SCH79797 and FR171113 were also shown to strongly inhibit thrombin-induced platelet aggregation [95, 96].

Similar to PAR-1 antagonists, the peptide *trans*-cinnamoyl-Tyr-Pro-Gly-Lys-Phe-NH_2, based on the murine PAR-4 tethered ligand domain, could inhibit PAR-4 AP-induced rat platelet aggregation (Table 1.1) [97]. Interestingly, palmitoylated peptides derived from the intracellular loop 3 of PAR-1 and PAR-4 both act as antagonists of thrombin *in vitro* and *in vivo* (Table 1.1) [98, 99]. *N*-palmitoyl-RCLSSSAVANRS-NH_2 (PAR-1 antagonist) and *N*-palmitoyl-SGRRYGHALR-NH_2 (PAR-4 antagonist) both efficiently inhibit their respective receptor-mediated intracellular calcium rise in platelets [98]. Moreover, both antagonists could strongly block thrombin-induced human platelet aggregation, which is confirmed in the mouse model *in vivo* [98]. These studies provide new insights for the development of small molecule drugs. However, the development of selective and potent PAR antagonists is still a difficult task, and no antagonists for PAR-2 and PAR-3 have been discovered so far.

Table 1.1. Protease-activated receptors: subtypes, agonists, inactivators, and antagonists

	PAR-1	PAR-2	PAR-3	PAR-4
Activating Proteases	Thrombin Trypsin FVIIa FXa APC Granzyme A RgpB	Trypsin Tryptase Trypsin IV P22 FVIIa FXa MT-SP1 Proteinase-3 Acrosien Der P3 and P9 RgpB	Thrombin	Thrombin Trypsin Trypsin IV Cathepsin G FVIIa FXa RgpB
Inactivating Proteases	Cathepsin G Plasmin Elastase Proteinase-3 Chymase	Cathepsin G Elastase Chymase	Cathepsin G	unknown
Cleavage sites	$R^{41}\downarrow S^{42}$FLLRN (h) $R^{41}\downarrow S^{42}$FFLRN (r, m)	$R^{36}\downarrow S^{37}$LIGKV (h) $R^{36}\downarrow S^{37}$LIGRL (r) $R^{34}\downarrow S^{35}$LIGRL (m)	$K^{38}\downarrow T^{39}$FRGAP (h) $K^{37}\downarrow S^{38}$FNGGP (m)	$R^{47}\downarrow G^{48}$YPGQV (h) $R^{58}\downarrow G^{59}$FPGKP (r) $R^{59}\downarrow G^{60}$YPGKF (m)
Activating APs	SFLLR-NH_2 TFLLR-NH_2 [a] TRag [b] TFRIFD	SLIGKV-NH_2 SLIGRL-NH_2 [a] SFLLR-NH_2 *Trans*-cinnamoyl-LIGRLO-NH_2 2-furoyl-LIGRLO-NH_2 [c]	None	GYPGQV-NH_2 GFPGKP-NH_2 GYPGKF-NH_2 AYPGKF-NH_2 [a]
Inactivating APs	FTLLR-NH_2	LSIGRL-NH_2	None	YAPGKF-NH_2
Antagonists	3-mercapto-propionyl-Phe-Cha-Cha-Arg-Lys-Pro-Asn-Asp-Lys-NH_2 *Trans*-cinnamoyl-parafluoro-Phe-paraguanidino-Phe-Leu-Arg-NH_2 *N*-palmitoyl-RCLSSSAVANRS-NH_2 RWJ56110 RWJ58259 SCH79797 FR171113	None	None	*Trans*-cinnamoyl-YPGKF-NH_2 *N*-palmitoyl-SGRRYGHALR-NH_2

NOTE:
a: standard PAR activating peptide.
b: putative and selective PAR-1 peptide agonist.
c: most potent and selective PAR-2 peptide agonist.
h, human; r, rat; m, mouse; ↓, cleavage site.

1.2.3 Mechanisms of PAR activation

The mechanism of PAR activation was initially established for PAR-1 [9] and appears to be a general paradigm for other PARs. The extracellular N-terminus of human PAR-1 contains a sequence of charged amino acids ($D^{50}KYEPF^{55}$) , which resembles a domain of the leech anticoagulant hirudin. This negatively charged domain interacts with an anion binding site on thrombin, facilitating the putative cleavage site ($R^{41}\downarrow S^{42}FLLRN$) to insert into the thrombin catalytic subsite and finally resulting in receptor hydrolysis. The interaction is very critical for efficient cleavage at low concentrations of thrombin. The importance of this negative domain is further clarified on PAR-4 which lacks the hirudin-like domain. PAR-4 requires higher concentrations of thrombin for activation than the other thrombin receptors [8]. Thrombin cleaves the peptide bond between receptor residues Arg 41 and Ser 42 in PAR-1. Cleavage of PAR-1 by thrombin is irreversible, and this cleavage generates a new N-terminus that functions as a tethered ligand domain ($S^{42}FLLRN$). The tethered ligand domain binds intramolecularly to the second extracellular loop of PAR-1 to initiate transmembrane signalling.

1.2.4 PAR-mediated intracellular signal transductions

Upon receptor cleveage by proteases or AP binding to the receptor, PAR's conformation is significantly changed [100], acting as a switch to relay the signal to heterotrimeric G proteins including $G\alpha_i$, $G\alpha_q$, $G\alpha_{12/13}$ [101-104]. Subsequently, diverse signalling pathways are initiated, which result in different biological consequences [20]. The mechanisms of PAR-mediated signalling pathways, especially PAR-1 signalling, have been elucidated in detail and reviewed (Fig. 1.1 A) [21, 105, 106]. One of the important PAR-1 signalling pathways is that $G\alpha_q$ binds to activated PAR-1 and thereby activates the downstream factor phospholipase C (PLC)-β [103, 104]. PLC-β in turn cleaves phosphatidyl inositol 4,5 bisphosphate to generate inositol 1,4,5-trisphosphate (IP_3) that triggers intracellular calcium release by action on its receptor at the endoplasmic reticulum (ER), and diacylglycerol (DAG) that activates protein kinase C (PKC) [107]. Calcium and PKC have been shown to mediate PAR-1-dependent cellular effects. Increase in intracellular calcium and activation of PKC induced by PAR-1 result in proline-rich tyrosine kinase phosphorylation, which causes activation of mitogen-activated protein kinase (MAPK) cascade [108].

The MAPK pathway has been extensively considered in PAR-1 signalling events. The MAPK family consists of three members, the extracellular signal regulated kinase (ERK) 1/2,

c-Jun N-terminal kinase (JNK) and p38 MAPK [109]. Upon thrombin or PAR-1 AP stimulation, all three members could be activated rapidly [20, 110, 111]. The activated ERK1/2 and p38 MAPK subsequently induce cell proliferation and differentiation [111], and release of the proinflammtory factor IL-6 that might trigger inflammation responses [112]. It was shown that PI3 kinase is required for ERK1/2 activation, indicating that PI3 kinase is an upstream factor of ERK1/2 [111]. Interestingly, activation of JNK by PAR-1 leads to the secretion of chemokine growth-regulated oncogene/cytokine-induced neutrophil chemoattractant-1 (GRO/CINC-1) from astrocytes, which prevents cell death induced by C_2-ceramide [110]. Also in this case, PI3 kinase and PKC as upstream factors play the important role in JNK activation [110]. JNK contains three subisoforms JNK1, JNK2 and JNK3 [113]. Wang *et al*. further found that JNK2 and JNK3 both are involved in this PAR-1-dependent protective pathway [114]. However, JNK1 activates the downstream transcription factor c-Jun, which regulates other cellular processes in rat astrocytes [114].

It is well known that c-Jun associates with the other Jun members, the basic leucine-zipper proteins and the Fos proteins, so that the activator protein-1 (AP-1) complex is generated, which could bind to its DNA motif (5'-TGAG/CTCA-3') to regulate gene expression [115]. It has been shown that thrombin induces activation of AP-1 in human 1321N1 astrocytoma cells [116]. PAR-1 agonists could also activate other transcription factors such as nuclear factor-κB (NF-κB) and signal transducers and activators of transcription 1, which lead to cell growth, apoptosis or inflammation reactions [117-119].

PAR-1-mediated signal transductions have been widely investigated, but only relatively few studies about signalling pathways mediated by PAR-2 were done (Fig. 1.1 B). Nevertheless, it is well established that activation of PAR-2 could increase intracellular calcium via PLC-β pathway, similar to PAR-1 [20]. The calcium rise in turn leads to diverse cellular effects including neuropeptide release, kinase activation and ion channel activation [107, 120]. The MAPK cascade is also associated with PAR-2. Similar to the events in PAR-1, the MAPK cascade relays PAR-2 signals to cell proliferation [121] or to inflammatory responses [122]. Our recent study demonstrates that activation of PAR-2 leads to release of GRO/CINC-1 regulated by JNK1, which is obviously different from that in PAR-1 signalling events [114]. Similarly, PAR-2-induced GRO/CINC-1 also protects rat astrocytes from C_2-ceramide-mediated cell death [114]. These results indicate that PAR-1 and PAR-2 could be selectively activated under different pathological conditions to rescue neural cells from death.

Additionally, the effects of PAR-2 agonists on activation of transcription factors have been demonstrated. PAR-2 agonists could induce activation of NF-κB [123] and AP-1 [124, 125] in multiple cell types, which regulate inflammatory responses.

To date, little is known about the signalling pathway mediated by PAR-3 and PAR-4. Murine PAR-3 is a co-factor for PAR-4 and does not respond to thrombin stimulation [11, 50]. Therefore, it appears possible that there are no signalling pathways mediated by PAR-3 in rodents.

Although PAR-4 could be activated by high concentrations of thrombin, PAR-4 has distinct downstream signalling kinetics relative to PAR-1. It was shown that PAR-4 AP (200 μM) induces a prolonged phosphorylation of ERK1/2 with a maximum at 60 min, whereas PAR-1 AP (200 μM) causes a transient ERK1/2 signal in vascular smooth muscle cells [52]. Similar results were also observed recently in mouse microglia cells showing that activation of PAR-4 by PAR-4 AP induces a prolonged ERK1/2 phosphorylation up to 6 h [59]. Also in the case of p38 MAPK, p38 MAPK was shown to be slowly activated by PAR-4 AP in mouse cardiomyocytes [58]. The mechanism of the unique PAR-4 signalling might be due to the slow receptor activation and desensitization kinetics of PAR-4.

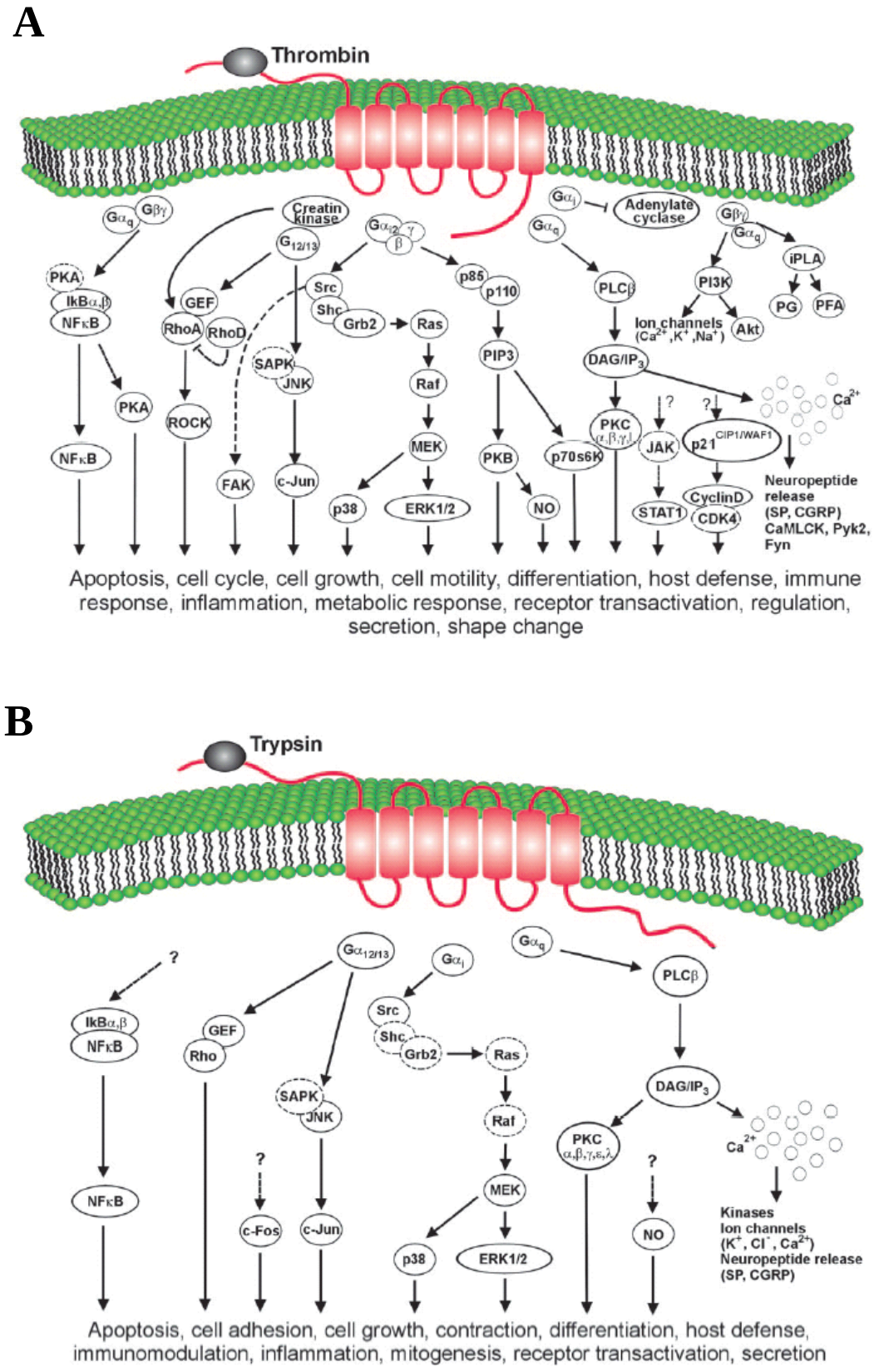

Fig. 1.1. Schematic representation of PAR-1- and PAR-2-mediated intracellular signalling pathways. Upon receptor cleavage by proteases like thrombin (A) and trypsin (B), PAR's conformation is significantly changed that facilitates the coupling with heterotrimeric G proteins. Different G proteins selectively relay PAR signals to their downstream factors, such as PLC-β, MAPK cascade, Rho family, and PI3 kinase. Finally, the cellular effects are triggered in response to agonist stimulation under certain conditions. These diagrams are from literature [105].

1.2.5 Termination of PAR signalling

PAR is activated by a unique mechanism, i.e. proteases cleave the receptor at the special domain. Although proteolysis is important for receptor activation, some proteases can also inactivate PARs (Table 1.1). It was reported that cathepsin G, in addition to the $Arg^{41}\downarrow Ser^{42}$ activation site, mainly cleaves human PAR-1 at $Phe^{43}\downarrow Leu^{44}$ and $Phe^{55}\downarrow Trp^{56}$ sites, which removes the tethered ligand domain and disables the receptor [126]. Also in the case of neutrophil-derived proteases elastase and proteinase-3, both of them can cleave human PAR-1 at the $Val^{72}\downarrow Ser^{73}$ site to inactivate PAR-1 [127]. Similarly, tryptase cleaves human PAR-2 at the $Lys^{41}\downarrow Val^{42}$ site, which inactivates PAR-2 [128]. Therefore, these proteases could remove the tethered ligand domain from the cleaved receptors to terminate the signalling.

The classic GPCR, for example the β_2-adrenergic receptor (β_2-AR), is rapidly desensitized after ligand binding and activation [129, 130]. Likely, signalling by PAR is also rapidly terminated after proteolytic cleavage activation [131], although the tethered ligand domain does not diffuse away. Receptor desensitization is another physiological mechanism to attenuate the signalling by PAR. The rapid desensitization of PAR is regulated by either G protein-coupled receptor kinases (GRKs) or PKC [38, 132]. The C-tails of PAR-1 and PAR-2 contain multiple potential phosphorylation sites, and the phosphorylation in the C-tail of receptors enhances binding to β-arrestin, leading to dissociation of G proteins from receptors, and finally downregulating PAR singalling. PAR-1 is rapidly phosphorylated after thrombin stimulation, and overexpression of GRK3 inhibits intracellular calcium signals induced by PAR-1 [38]. A mutant PAR-1 that lacks all potential phosphorylation sites at the C-tail is resistant to inhibition by GRK3 [38]. In addition, the second messenger kinase PKC could also phosphorylate PAR-1, which might contribute to receptor desensitization [133]. Similar results were also observed with PAR-2. PKC, but not another second messenger kinase, protein kinase A (PKA), mediates desensitization of PAR-2 by receptor phosphorylation, which could be blocked by the PKC inhibitor GF109203X in transfected KNRK cells and hBRIE380 cells [132]. Human PAR-2 contains several PKC consensus sites at intracellular loop 3 and C-tail, as well as one GRK consensus site at intracellular loop 3, suggesting that the intracellular loop 3, besides C-tail, also plays a critical role in receptor desensitization. Interestingly, PAR-4 appears not to be phosphorylated upon thrombin stimulation, and its signalling is shut off less rapidly than PAR-1. Moreover, mutation of all potential phosphorylation sites at the C-tail of PAR-4 does not affect agonist-triggered signalling [134]. PAR-3 has a short C-tail and less phosphorylation sites, and the mechanisms responsible for termination of PAR-3 signalling have not been determined yet.

Distinct from other classic GPCRs, PAR after receptor activation is internalized, and predominantly sorted into lysosomes for degradation [135]. This is another mechanism for permanent termination of PAR signalling. It has been shown that PAR-1 is targeted to lysosomes at 30 min after activation [136, 137]. We found that PAR-2 is colocalized with the lysosomal marker LAMP-1 at 15 min after trypsin stimulation in transfected HEK293 cells. These results suggest that PAR-1 and PAR-2 are rapidly inactivated due to protein degradation in lysosomes. Again, no evidence so far has shown the association of PAR-3 or PAR-4 with lysosomes.

1.2.6 PAR trafficking

Once activated by the receptor ligand, the GPCR is rapidly internalized into intracellular compartments. This represents the important physiological mechanisms that protect against receptor overstimulation [130], and mediate sustained signalling as well [138]. The processes of PAR trafficking, especially for PAR-1 and PAR-2, have been extensively investigated. Similar to other classic GPCRs, PAR-1 and PAR-2, after activation, are rapidly recruited to clathrin-coated pits [136, 139]. The C-tails of PAR-1 and PAR-2 are mainly responsible for this process [39, 138]. It was shown that β-arrestin as an adaptor protein binds to the C-tail of activated PAR-2, and mediates the internalized receptor into clathrin-coated pits [138, 139]. In contrast, β-arrestin is not required for PAR-1 internalization, since agonist-triggered PAR-1 internalization occurs normally in β-arrestin-deficient MEF cells [140]. Recently, it was reported that the tyrosine-based motif (Y*XX*L) that locates at the C-tail of PAR-1 mediates internalization of the activated PAR-1 [39]. The tyrosine-based motif could recognize the μ2 subunit of AP-2 adaptor complex [130], and thereby might mediate translocation of the activated PAR-1 into clathrin-coated pits.

It has been shown that GTPase plays the important role in PAR trafficking. Dynamin is one of such GTPases, and mediates detachment of clathrin-coated pits from the plasma membrane. The detached complex is further translocated into early endosomes [141, 142]. It has been known that another GTPase rab5a mediates trafficking of internalized PAR-2 into early endosomes [143]. Rab5a locates at early endosomes, as well as in the cytosol in unstimulated cells. After 15 min stimulation with trypsin, PAR-2 colocalizes with rab5a in early endosomes. Moreover, overexpression of dominant negative mutants of rab5a (rab5a S34N) impedes internalization of PAR-2 [143].

It is well known that the classic GPCRs, such as the β_2-AR, dissociate from their ligands and are dephosphorylated within endosomes, then recycle back to the cell surface for

signalling again. Totally distinct from the classic GPCR, PAR is a “one-way” receptor. The activated PAR is predominantly sorted to lysosomes for degradation after internalization [137]. The chimeric PAR-1 where its intracellular C-tail is exchanged by the C-tail of substance P receptor recycles back to the cell surface after activation and internalization, behaves like the wild-type substance P receptor. In contrast, the chimeric substance P receptor bearing the C-tail of PAR-1 is sorted to lysosomes and fails to recycle after stimulation with substance P [144]. Therefore, the C-tail of PAR-1 controls the receptor’s fate, degradation in lysosomes, but not recycling after receptor activation and internalization. Some studies have shown that tyrosine- and di-leucine-based motifs and protein ubiquitination are implicated in sorting of membrane receptors to lysosomes [145-147]. However, there is no evidence that they are involved in this process in the PAR-1 case so far. Strikingly, it was shown that the membrane-associated protein sorting nexin 1 interacts with PAR-1 and mediates passage of internalized receptors to lysosomes for degradation [148]. Sorting nexin 1 and its homologous proteins are associated with diverse membrane receptors and might be involved in their intracellular traffickings [149].

Interestingly, a recent report demonstrates that PAR-2 ubiquitination by ubiquitin E3 ligase c-Cbl mediates receptor sorting to lysosomes [150]. Mutant PAR-2 lacking all intracellular lysine residues (PAR-2Δ14K/R) that cannot be ubiquitinated is normally internalized after activation, but remains in early endosomes and fails to be sorted into lysosomes. On the other side, activation of PAR-2 induces c-Cbl phosphorylation and promotes receptor ubiquitination. The dominant negative c-Cbl construct inhibits ubiquitination of PAR-2 and induces retention of internalized receptors in early endosomes.

Although most of the internalized PARs are degraded in lysosomes, PAR still resensitizes to thrombin, trypsin and other proteases within 30-90 min after receptor endocytosis. Receptor resensitization protects cells against prolonged desensitization. PAR resensitization is regulated by the large intracellular PAR stores and newly synthesized proteins [132, 137], although it was found that a few cleaved PARs recycle back to cell surface [151]. The intracellular PAR pools locate in the Golgi apparatus in most cells. In endothelial cells and fibroblasts which have large intracellular PAR-1 stores, the receptor resensitization is rapid and initially independent of new receptor synthesis [137, 152]. In contrast, the recovery of PAR-1 is quite a slow process that depends on the synthesis of new receptor in megakaryoblastic HEL and CHRF-288 cells [151]. Recently, it was shown that the GTPase rab11a as a signal molecule partially mediates resensitization of PAR-2 [143]. Rab11a locates at the Golgi apparatus in KNRK-PAR-2 cells, and translocates to prominent

perinuclear vesicles upon trypsin exposure for 15 min. After 60 min of recovery, rab11a is detected in vesicles containing PAR-2 beneath the plasma membrane. Moreover, the dominant negative construct rab11aS25N causes retention of PAR-2 in the Golgi apparatus after trypsin stimulation in KNRK-PAR-2 cells. However, rab11aS25N does not completely prevent resensitization of PAR-2. Therefore, other adaptor proteins might mediate resensitization of PAR-2.

1.2.7 Post-translational modification of PAR

1.2.7.1 Glycosylation

Most GPCRs are glycoproteins in eukaryote cells. Glycosylation plays an important role in receptor functions such as protein folding, ligand binding, receptor trafficking and signal transduction [153-156]. Protein glycosylation is divided into two classes, *N*-linked glycosylation and *O*-linked glycosylation, based on the binding site of oligosaccharide. *N*-linked glycosylation is most common, and generated co-translationally by the addition of a $Glc_3Man_9GlcNAc_2$ precursor from a dolichol carrier onto the nitrogen in the asparagine side chain of the sequon (Asn-X-Ser/Thr, where X is any amino acid except proline) [157]. Each of the four PAR members possesses this putative *N*-linked glycosylation sequon within their extracellular domains (Table 1.2). It has been shown that *N*-linked glycosylation is important for human PAR-2 expression in HEK293 cells and in the fibroblast cell line Pro5-PAR-2. The glycosylation-deficient mutants of PAR-2 result in a loss of receptor expression by 50% [46]. Moreover, the treatment with tunicamycin that could inhibit the cellular *N*-linked glycosylation process also dramatically reduces cell surface PAR-2 expression in HEK293 cells [158]. Importantly, it was shown that human PAR-2 glycosylated at the extracellular N-terminus is resistant to tryptase stimulation [158]. PAR-1 possesses five potential *N*-linked glycosylation sites, and some reports demonstrate that PAR-1 is also *N*-glycosylated [159], which is confirmed by peptide *N*-glycosidase F (PNGase F) treatment [159]. However, little is known about the effect of glycosylation on PAR-1 functions. To date, no data on the glycosylation of either PAR-3 or PAR-4 were shown, although they possess potential *N*-linked glycosylation sequons.

Meanwhile, oligosaccharides can also be linked through the oxygen of serine or threonine by post-translational sequential enzymatic additions of monosaccharides directly to a protein, normally beginning with *N*-acetyl-galactosamine [157]. This process is so-called *O*-linked glycosylation. The deglycosylated PAR-1 treated with PNGase F migrates at 36-43 kDa shown by western blot analysis [159]. Similar results were also observed with PAR-2

[125]. These results imply that both PAR-1 and PAR-2 might possess *O*-linked glycosylation. However, it is not clear whether *O*-linked glycosylation exerts effects on PAR biological functions.

Table 1.2. Putative *N*-linked glycosylation sequons within human PARs.

	PAR-1	PAR-2	PAR-3	PAR-4
N-terminus	$N^{35}A^{36}T^{37}$ $N^{62}E^{63}S^{64}$ $N^{75}K^{76}S^{77}$	$N^{30}R^{31}S^{32}$	$N^{25}D^{26}T^{27}$ $N^{82}A^{83}T^{84}$	$N^{56}D^{57}S^{58}$
EL1	-	-	-	-
EL2	$N^{252}I^{253}T^{254}$ $N^{262}E^{263}T^{264}$	$N^{222}I^{223}T^{224}$	-	-
EL3	-	-	$N^{331}N^{332}T^{333}$	-

1.2.7.2 Palmitoylation

Protein palmitoylation, also called *S*-acylation, is a reversible post-translational lipid modification, which occurs through covalent linkage of palmitic acid via a labile thioester bond to cysteine residues by palmitoyltransferase or acyltransferase [160]. Palmitoylation has been shown to regulate GPCR functions such as receptor activity, desensitization and internalization [129]. Blockade of palmitoylation of β_2-AR results in an increase of basal receptor phosphorylation and rapid desensitization in response to agonist stimulation [161]. This is due to the fact that receptor palmitoylation masks the neighboring PKA site [162]. It was also reported that palmitoylation regulates serotonin 4A receptor activity [163], and controls $G\alpha_i$ protein coupling to serotonin 1A receptor as well [164]. All PAR members except PAR-3 and human PAR-4 possess one or two putative cysteine palmitoylation site(s) at the C-tail, which results in a fourth intracellular loop [37, 40]. A recent study demonstrates that mutation of palmitoylation sites of PAR-1 causes 4-9 fold increases in the EC_{50} for thrombin and SFLLRN, but does not affect PAR-1 expression and functions [40].

1.3 Scope and aims of project

1.3.1 Background

Protein-protein interactions play a crucial role in controlling and regulating diverse cellular processes. Kinases, phosphatases and transferases bind to their protein substrates to exert the enzymatic function. Protein scaffolds and adaptors interact with kinases, or with activated membrane receptors to transmit signals or to facilitate signal transduction. It is also clear that heterotrimeric G proteins, through their α and $\beta\gamma$ subunits, couple to activated GPCRs and thereby relay extracellular signals to second messengers, such as cyclic AMP, DAG, IP_3, and calcium. These general interactions are also observed with PARs. It has been shown that activated PARs are coupled to $G\alpha_i$, $G\alpha_q$, or $G\alpha_{12/13}$, which trigger diverse intracellular processes [101-104]. Besides the association with G proteins, PARs also interact with other proteins. Several protein kinases such as GRKs and PKC, through interaction with membrane-bound $G\beta\gamma$ subunits and phosphatidylinositol bisphosphate, target to the consensus sequence at intracellular domains of the receptor, and thereby phosphorylate them [38, 132]. The adaptor protein, β-arrestin, binds to phosphorylated PAR-1 and PAR-2, and regulates receptor desensitization and/or internalization [138-140]. Only for PAR-1, two proteins were identified as interacting protein partners (i.e. creatine kinase and Hsp90) [165, 166]. Both proteins specifically bind to PAR-1 C-tail and relay PAR-1 signalling to RhoA, which eventually regulates cell morphological changes. This study provides a clue that multiple proteins might directly interact with PARs and control receptor functions.

PAR is activated by the tethered ligand domain at the extracellular N-terminus of the receptor [9]. Following tethered ligand binding, the transmembrane domains of the PAR undergo conformational changes that result in signals transmitted to intracellular domains [100]. The C-tail is the largest intracellular domain of the PAR. It is accepted that the intracellular C-tail of the PAR is a critical domain that regulates receptor functions [39, 40]. Therefore, the C-tail is considerated as the predominant target of PAR-interacting proteins. However, recent evidence shows that besides the C-tail, the intracellular loops of the PAR are also important for PAR functions [150].

1.3.2 Specific aims

Although PAR-2 has been shown to be significantly involved in proliferation, pain, and inflammatory reactions, its intracellular signalling mechanisms are not completely clear. It is also largely unknown what the role of PAR-2 in the central nervous system (CNS) might be. To improve understanding of PAR-2 functions in the CNS, the plan of the current project was

to perform yeast two-hybrid screening to identify PAR-2-interacting proteins. Then it should be investigated by which mechanisms the interacting proteins regulate PAR-2 functions.

1.3.3 Strategy

To find out protein partners that interact not only with the PAR-2 C-tail, but also with intracellular loops and other domains of PAR-2, here the full-length human PAR-2 was used as bait to fish PAR-2-interacting partners from the human brain cDNA library by the MATCHMAKER GAL4 yeast two-hybrid system.

Further, the candidate interacting protein found in the yeast two-hybrid system should be confirmed to interact with PAR-2 *in vitro* by the GST pull-down assay. Then the domain that is responsible for protein interaction should be also analyzed in the GST pull-down assay.

The final two aims were, firstly, to study whether there is a real physiological interaction in the native system. The interaction of PAR-2 with candidate partners should be tested within mammalian cells under physiological conditions by both immunoprecipitation (IP) and immunostaining. Secondly, and most importantly, the physiological function of the interaction of these proteins with PAR-2 also had to be addressed in the present project.

2. MATERIALS AND METHODS

2.1 Materials

2.1.1 Chemicals and reagents

Z-Phe-Ala-diazomethylketone (ZPAD) and PAR-2 AP (SLIGKV-NH_2) from Bachem.

Linearized BaculoGold virus DNA from BD Bioscience Pharmingen.

HEPES and Tris base from Biomol.

Bio-Rad protein assay dye reagent concentrate from Bio-Rad.

Brefeldin A, cycloheximide and phenylarsine oxide (PAO) from Calbiochem.

Herring testis Carrier DNA from Clontech.

Ammonium peroxodisulfate, sodium azide and paraformaldehyde (PFA) from Fluka.

Protein A Sepharose CL-4B and glutathione-Sepharose 4B from GE Healthcare.

Magnet assisted transfection from IBA GmbH.

Lipofectin from Invitrogen.

Fura-2 AM from Molecular Probes.

TRag (Thrombin receptor agonist peptide) from NeoMPS SA.

DOTAP, protease inhibitor cocktail tablets, trypsin and ponceau S solution (0.2% in 3% acetic acid) from Roche Diagnostics.

Acrylamide (2 ×), N, N'-Methylenbisacrylamide (2 ×), Triton X-100 and Brij 58 from SERVA.

Bromphenol blue, Dimethyl sulfoxide (DMSO), glass beads (425-600 μm, acid-washed), Igepal CA630, β-mercaptoethanol, PAP pen for immunostaining, protein G-Agarose, poly-L-lysine, TEMED, Tween 20, and X-gal from Sigma.

All other chemical reagents from Carl Roth.

2.1.2 Antibodies

2.1.2.1 Primary antibodies

mouse monoclonal anti-EEA1 (BD Transduction Laboratories)

mouse monoclonal anti-LAMP1 (BD Transduction Laboratories)

mouse monoclonal anti-GM130 (BD Transduction Laboratories)

rabbit anti-phospho-c-Jun antibody (Cell signaling technology)

rabbit anti-c-Jun antibody (Cell signaling technology)

mouse monoclonal anti-HA (6E2) antibody (Cell signaling technology)

rabbit polyclonal anti-GFP antibody (Cell signaling technology)

mouse monoclonal anti-myc antibody (Invitrogen)

goat polyclonal anti-PAR-2 (C-17) antibody (Santa Cruz Biotechnology)

mouse monoclonal anti-Jab1 (B-7) antibody (Santa Cruz Biotechnology)

rabbit polyclonal anti-GST antibody (Santa Cruz Biotechnology)

anti-rabbit normal IgG (Santa Cruz Biotechnology)

rabbit polyclonal anti-HA antibody (Sigma)

mouse monoclonal anti-β-tubulin I antibody (Sigma)

rabbit polyclonal anti-p24A serum, a gift from Prof. I. Schulz, Institute of Physiology II, University of Saarland, and Dr. R. Blum, Institute of Physiology, University of Munich.

2.1.2.2 Secondary antibodies

goat anti-mouse-HRP IgG (Dianova, Hamburg, Germany)

goat anti-rabbit-HRP IgG (Dianova, Hamburg, Germany)

mouse anti-goat-HRP IgG (Dianova, Hamburg, Germany)

Alexa Fluor 488 goat anti-mouse IgG (Molecular Probes)

Alexa Fluor 568 goat anti-rabbit IgG (Molecular Probes)

Alexa Fluor 633 goat anti-mouse IgG (Molecular Probes)

2.1.3 Cells, medium and related reagents

2.1.3.1 Mammalian cells

HEK293 cells

DMEM/Ham's F-12 (1:1) supplemented with heat-inactivated 10% fetal calf serum (FCS), 100 U/ml penicillin, 100 µg/ml streptomycin (Biochrom, Berlin, Germany)

Normal primary human astrocytes (Cambrex Bio Science Verviers SPRL, Belgium)

AGM^{TM} astrocytes medium (Cambrex Bio Science Verviers SPRL, Belgium)

Rat primary astrocytes (kindly provided by Yingfei Wang)

DMEM supplemented with heat-inactivated 10% fetal calf serum (FCS), 100 U/ml penicillin, 100 µg/ml streptomycin (Biochrom, Berlin, Germany)

Hank's solution (w/o Ca^{2+} and Mg^{2+}) and Accutase were from PAA. G418 sulphate was from Calbiochem. Puromycin was from Sigma.

2.1.3.2 Insect cells

Spodoptera frugiperda (Sf9) cells

IPL-41 insect medium with L-amino acids (Gibco), supplemented with 10% heat-

inactivated FCS (Biochrom), 2% (v/v) yeast extract (Sigma), 1% (v/v) lipid medium supplements (Sigma), 100 µg/ml gentamycin sulfate (Cell Concepts), and 2.5 µg/ml amphotericine B (Cell Concepts).

2.1.3.3 Bacterial cells

XL 1-Blue cells and DH5*a* cells

LB medium

10 g/l Bacto-tryptone (BD Bioscience), 5 g/l Bacto-yeast extract (BD Bioscience), 10 g/l NaCl, pH 7.0

LB agar plates

LB medium, 18 g/l Bacto-agar (BD Bioscience), appropriate antibiotics (100 µg/ml ampicillin or 50 µg/ml kanamycin)

Hanahan's SOC medium

2% Bacto-tryptone (BD Bioscience), 0.5% Bacto-yeast extract (BD Bioscience), 10 mM NaCl, 2.5 mM KCl, 10 mM $MgCl_2$, 10 mM $MgSO_4$, 20 mM glucose, pH 7.0

2.1.3.4 Yeast cells

AH109 cells and Y187 cells (Clontech)

YPDA medium

20 g/l Difco peptone (BD Bioscience), 10 g/l Bacto-yeast extract (BD Bioscience), 0.003% adenine hemisulfate (Sigma), 2% glucose, 20 g/l Bacto-agar (for plates only) (BD Bioscience), pH 5.8

SD medium

6.7 g/l yeast nitrogen base without amino acids (BD Bioscience), appropriate Dropout powder (Clontech), 2% glucose, 20 g/l Bacto-agar (for plates only) (BD Bioscience), pH 5.8

2.1.4 Vectors

pGBKT7 from Clontech

pEGFP-N1 from Clontech

pcDNA3.1-Myc-His (B) from Invitrogen

pVL1392 from Invitrogen

pDrive from Qiagen

pEAK10, a gift from Dr. T. Koch, Institut für Pharmakologie und Toxikologie, Otto-von-Guericke-Universität Magdeburg

pBL CAT2 and AP-1-driven pBL CAT2, gifts from Dr. J. Kraus, Institut für Pharmakologie und Toxikologie, Otto-von-Guericke-Universität Magdeburg

pEGFP-hP2Y$_1$, a gift from Denise Ecke.

2.1.5 Small interfering RNAs (siRNAs)

Human Jab1 siRNA from Santa Cruz Biotechnology.

Non-silencing siRNA labeled with Alexa Fluor 488 from Qiagen.

2.1.6 Enzymes

All restriction enzymes from MBI Fermentas.

T4 DNA ligase from Invitrogen.

RNase A from Carl Roth.

N-glycosidase F from New England Biolabs.

2.1.7 Markers

Precision Plus Protein All Blue Standard from Bio-Rad.

SeeBlue® Plus2 Pre-Stained Standard from Invitrogen.

GeneRuler™ 1 kb and 100 bp DNA ladders from MBI Fermentas.

2.1.8 Buffers

10 × TE buffer

100 mM Tris/HCl, pH 7.5, 10 mM EDTA

10 × LiAc

1 M Lithium acetate, pH 7.5 with acetic acid

PEG/LiAc solution

40% PEG 4000, 1 × TE buffer, 1 × LiAc

Z buffer

16.1 g/l $Na_2HPO_4 \cdot 7H_2O$, 5.5 g/l $NaH_2PO_4 \cdot H_2O$, 0.75 g/l KCl, 0.246 g/l $MgSO_4 \cdot 7H_2O$, pH 7.0.

X-gal stock solution

20 mg/ml X-gal in dimethylformamide.

Z buffer/X-gal solution

100 ml Z-buffer with 0.27 ml β-mercaptoethanol and 1.67 ml X-gal stock solution

PBS

137 mM NaCl, 2.6 mM KCl, 8.1 mM Na_2HPO_4, 1.4 mM KH_2PO_4, pH 7.4

Yeast lysis buffer

10 mM Tris/HCl, pH 8.0, 100 mM NaCl, 1 mM EDTA, 2% Triton X-100, 1% (w/v) SDS

HEK293 cell lysis buffer

50 mM Tris/HCl, pH 7.5, 1 mM β-mercaptoethanol, 150 mM NaCl, 1% Igepal, and Protease Inhibitor Cocktail (one tablet per 50 ml)

Modified RIPA buffer

50 mM Tris/HCl, pH 7.4, 1% Igepal, 0.25% Na-deoxycholate, 150 mM NaCl, 1 mM EDTA, 1 mM Na_3VO_4, 1 mM NaF and Protease Inhibitor Cocktail

Sf9 lysis buffer

50 mM Tris/HCl, pH 7.5, 150 mM NaCl, 10 mM NaF, 1% Triton X-100, and Protease Inhibitor Cocktail

Sf9 membrane fraction buffer 1

50 mM HEPES, pH 8.0, 300 mM NaCl, 0.1 mM EDTA, 10 mM β-mercaptoethanol, and Protease Inhibitor Cocktail

Sf9 membrane fraction buffer 2

50 mM HEPES, pH 8.0, 300 mM NaCl, 10 mM β-mercaptoethanol, 1% Brij 58, and Protease Inhibitor Cocktail

HBS buffer

20 mM HEPES, pH 7.4, 150 mM NaCl

4 × Laemmli buffer

500 mM Tris/HCl, pH6.8, 8% SDS, 40% glycerol, 0.01% bromphenol blue, 20% β-mecaptoethanol (fresh)

60% Acrylamide/Bis

58.4% Acrylamide (2 ×), 1.6% N,N'-Methylen-bisacrylamide (2 ×)

Resolving buffer

750 mM Tris/HCl, pH 8.8

Stacking buffer

250 mM Tris/HCl, pH 6.8

TBST

20 mM Tris/HCl, pH 7.6, 137 mM NaCl, 0.1% Tween 20

Membrane Stripping buffer

62.5 mM Tris/HCl, pH 6.8, 100 mM β-mercaptoethanol, 2% SDS

Coomassie brilliant blue solution

0.25% Coomassie brilliant blue R 250, 45% methanol, 10% acetic acid

Destaining solution

30% methanol, 10% acetic acid

Coomassie gel fixing solution

20% ethanol, 10% glycerol

4% PFA

4% PFA, 120 mM Na_2HPO_4, pH 7.4, 4% saccharose

Mounting buffer

PBS, 10% glycerol, 0.1% sodium azide

TCM buffer

10 mM Tris/HCl, pH 7.5, 10 mM $CaCl_2$, 10 mM $MgCl_2$

0.5 × TBE buffer

44.5 mM Tris, 44.5 mM Boric acid, 1 mM Na_2EDTA, pH 8.0

1 × TAE buffer

40 mM Tris, 20 mM acetic acid, 1 mM Na_2EDTA

NaHBS buffer

145 mM NaCl, 5.4 mM KCl, 1 mM $MgCl_2$, 1.8 mM $CaCl_2$, 25 mM glucose, 20 mM HEPES, pH 7.4 adjusted with Tris (hydroxymethyl) aminomethane.

2.1.9 Kits

BigDye Terminator Cycle Sequencing Ready Reaction kit (Applied Biosystems)

Supersignal West Pico Chemiluminescent Substrate (Pierce)

HiSpeed Plasmid Midi kit (Qiagen)

HotStarTaq™ Master Mix kit (Qiagen)

MinElute Gel Extraction kit (Qiagen)

MinElute PCR Purification kit (Qiagen)

QIAquick PCR Purification kit (Qiagen)

Omniscript™ Reverse Transcription kit (Qiagen)

RNeasy Mini kit (Qiagen)

CAT ELISA (Roche Diagnostics)

2.1.10 Instruments

ABI PRISMTM^{TM} 310 Genetic Analyzer from Applied Biosystems (CA, USA).

Ultrasonic homogenizer from Bandelin electronic (Berlin, Germany).

T3 Thermocycler from Biometra (Göttingen, Germany).

Electrophoresis power supply, Semi-dry Transfer Cell, GS-800 Calibrated

Densitometer, Gel document system and Gene pulser II from Bio-Rad (Munich, Germany).

LSM510 laser scanning confocal microscope from Carl Zeiss (Jena, Germany).

Thermomixer comfort from Eppendof (Hamburg, Germany).

Mighty Small II and UV/visible Spectrophotometer from GE Healthcare (Munich, Germany).

Biofuge pico and 13 R centrifuges, Megafuge 1.0 R centrifuge, Sorvall® RC-5B Refrigerated Superspeed Centrifuge, Sorvall® discovery^{TM} 90 ultraspeed centrifuge, Heraeus cell culture incubator, and Heraeus refrigerate (-80^{o}C) from Kendro (Hanau, Germany).

HT waterbath shaker from Infors AG (Germany).

Tecnoflow bench from Integra Biosciences (Fernwald, Germany).

Rotator from Labinco BA (The Netherlands).

Waterbath from Bachofer (Reutlingen, Germany).

Refrigerates (4^{o}C and –20^{o}C) from Liebherr (Hamburg, Germany).

Millipore purification system and ultra-pure water system from Millipore (Schwalbach, Germany).

Microplate reader from Molecular Devices (CA, USA).

Innova 4230 refrigerated incubator shaker from New Brunswick Scientific (NJ, USA).

Balance (analytical and preparative) from Sartorius (Göttingen, Germany).

Ca^{2+} imaging system from TILL Photonics GmbH (Gräfelfing, Germany).

Sf9 cell culture incubator from WTC binder (Tuttlingen, Germany).

PH Meter (pH526) from WTW (Weilheim, Germany).

2.2 Methods

2.2.1 RT-PCR

Total RNA was extracted from cultured cells using RNeasy Mini kit (Qiagen). One microgram of RNA was reverse-transcribed using Omniscript™ Reverse Transcription kit (Qiagen), and the resulting cDNA was amplified in the presence of indicated primers (Table 2.1) for 30-35 cycles by PCR using HotStarTaq™ Master Mix kit (Qiagen) for 15 min at 95ºC, followed by repeat cycles of 30 s at 94ºC, 90 s at 51-60ºC, 30-90 s at 72ºC, then a final 10 min extension at 72ºC. The reaction products were analyzed by electrophoresis with 1-2% agarose gel containing ethidium bromide, and visualized by Bio-Rad gel document system (Bio-Rad).

2.2.2 Plasmid constructs

For yeast two-hybrid screening, the full-length human PAR-2 cDNA was amplified by RT-PCR using hsPAR2Y1F and hsPAR2YR primers (Table 2.1) (GenBank™ accession number: AY336105), and cloned into the GAL4 DNA-binding domain vector pGBKT7 (Clontech) at EcoR I/BamH I sites, generating the bait plasmid, pGBKT7-hsPAR-2.

For GST pull-down assays, the GST cDNA was amplified by PCR using GSTFW and GSTRV primers (Table 2.1) and cloned into pDrive cloning vector (Qiagen). The linker sequence (Table 2.1) was hybridized and inserted at the N-terminus of GST. The resulting GST cDNA containing the linker sequence was subcloned into pVL1392 vector at the BamH I site (Invitrogen), generating the C-terminal GST baculoviral expression vector, pVL1392-GST. The cDNA fragments corresponding to the different regions of human PAR-2 (Fig. 3.2.2) were amplified by PCR and subcloned into pVL1392-GST at EcoR I/BamH I sites.

The cDNA fragments of human Jab1, p24A and p23 containing a consensus Kozak sequence upstream of the initiator ATG all were amplified by RT-PCR and cloned into pcDNA3.1mycHis vector (Invitrogen), respectively. The cDNA fragments corresponding to the different regions of human p24A (Fig. 3.4.3 A) were amplified by PCR and subcloned into pEGFP-N1 at Hind III/Sac II sites.

For co-IP, PCR products of the full-length and truncated human PAR-2 with a consensus Kozak sequence upstream of the initiator ATG and the haemagglutinin epitope (YPYDVPDYA, HA) at the C-terminus both were cloned into pEAK10 vector at Hind III/Xba I sites.

The cDNA fragment of human PAR-1 containing a consensus Kozak sequence upstream of the initiator ATG all was amplified by RT-PCR and cloned into pEAK10-HA vector at Hind III/EcoR I sites.

All of the DNA sequences of plasmid constructs were confirmed to be in-frame by ABI 310 sequencer.

2.2.3 Yeast two-hybrid screening

2.2.3.1 Small-scale LiAc yeast transformation

The yeast AH109 cells were transformed using LiAc-mediated methods, according to Clontech yeast protocols handbook. Briefly, one day before transformation, the fresh AH109 yeast was shaken overnight in the YPDA medium at 30^{o}C. On the following day, the overnight culture was further shaken for 3 h in the fresh YPDA medium at 30^{o}C, washed, and suspended in 1.5 ml freshly prepared 1 × TE/1 × LiAc buffer on ice. These fresh competent cells were used for transformation. The bait plasmid pGBKT7-hsPAR-2 (0.1 μg) together with 0.1 mg of herring testes carrier DNA were incubated for 30 min with AH109 competent cells in the presence of PEG/LiAc solution. After adding DMSO, the mixture was heat-shocked for 15 min at 42^{o}C, and separately spread on 100-mm SD/-Trp, SD/-Trp-His and SD/-Trp-Leu-His-Ade media, followed by incubation at 30^{o}C until colonies appear.

2.2.3.2 Yeast mating

The transformed AH109 with pGBKT7-hsPAR-2 was incubated overnight with shaking in the SD/-Trp medium at 30^{o}C, and resuspended in 5 ml 2 × YPDA medium. The concentrated overnight culture of bait strain was combined with commercial pretransformed Y187 cells with human brain MATCHMAKER cDNA library for further gently shaking overnight at 30^{o}C. The entire mating mixture was spread on 150-mm SD/-Trp-Leu-His media, also on 100-mm SD/-Trp, SD/-Leu and SD/-Trp-Leu media for mating efficiency controls. After 6-day incubation at 30^{o}C, $Trp^{+}Leu^{+}His^{+}$ colonies were spread on 150-mm SD/-Trp-Leu-His media again for further selection. Afterwards, the true $Trp^{+}Leu^{+}His^{+}$ colonies were spread on 150-mm SD/-Trp-Leu-His-Ade media, and incubated for 4 days at 30^{o}C.

2.2.3.3 β-galactosidase assay (LacZ colony-lift filter assay)

The fresh colonies grown on SD/-Trp-Leu-His-Ade media were transferred to a sterile clean filter, and permeabilized by liquid nitrogen. The filter sticked with permeabilized colonies was placed on another filter presoaked with Z buffer/X-gal solution, and incubated at

Table 2.1. Oligonuleotides for cloning, PCR and sequencing.

cDNA	Primer name	Primer sequence*	T_m	Application
hsPAR-2	hsPAR2Y1F hsPAR2YR	5' CCGGAATTCAGGATGCGGAGCCCCAGCGCG 3' 5' CGCGGATCCTCAATAGGAGGTCTTAAC 3'	58 °C	cloning
GST	GSTFW GSTRV	5' GATCTGATATCATGTCCCCTATACTAG 3' 5' GAAGATCTTCAATCCGATTTTGGAGGATGGTCGCC 3'	60 °C	cloning
GST linker	GSTlinkerFW GSTlinkerRV	5' GATCCATCGAGGGCCGCGGCGGTGGCGGTTCCGGAGGTGGCGGT TCCGGCGGTGGCGGTTCCGGCGGTGGCGGTTCC 3' 5' GGAACCGCCACCGCCGGAACCGCCACCGCCGGAACCGCCACCTC CGGAACCGCCACCGCCGCGGCCCTCGATG 3'	---	cloning
hsPAR-2	pVLPAR2fw pVLPAR2rev	5' CCGGAATTCGCCACCATGCGGAGCCCCAGCGCG 3' 5' CGCGGATCCATAGGAGGTCTTAAC 3'	58 °C	cloning
hsPAR-2Δ(246-397)	pVLPAR2fw pVLPAR2NTrev	5' CCGGAATTCGCCACCATGCGGAGCCCCAGCGCG 3' 5' CGCGGATCCAGAGAGGAAGTAATTGAAC 3'	58 °C	cloning
hsPAR-2Δ(1-213)	pVLPAR2CTfw pVLPAR2rev	5' CCGGAATTCGCCACCATGGTGAAGCAGACCATC 3' 5' CGCGGATCCATAGGAGGTCTTAAC 3'	58 °C	cloning
hsPAR-2IL1	pVLPAR2fw pVLPAR2IL1rev	5' CCGGAATTCGCCACCATGCGGAGCCCCAGCGCG 3' 5' CGCGGATCCAGGGTGCTTCTTCTTAGTTCG 3'	58 °C	cloning
hsPAR-2IL2	pVLPAR2IL2fw pVLPAR2IL2rev	5' CCGGAATTCGCCACCATGGCTCTTTGTAATGTG 3' 5' CGCGGATCCCTGCTTCACGACATACAAAGG 3'	58 °C	cloning
hsPAR-2IL3	pVLPAR2IL3fw pVLPAR2IL3rev	5' CCGGAATTCGCCACCATGCTCTCTCTGGCCATTG 3' 5' CGCGGATCCATAATGCACCACAAGCAG 3'	58 °C	cloning
hsPAR-2C	pVLPAR2Cfw pVLPAR2rev	5' CCGGAATTCGCCACCATGGTTTCACATGATTTC 3' 5' CGCGGATCCATAGGAGGTCTTAAC 3'	58 °C	cloning
hsPAR-2EL2	pVLPAR2CTfw pVLPAR2NTrev	5' CCGGAATTCGCCACCATGGTGAAGCAGACCATC 3' 5' CGCGGATCCAGAGAGGAAGTAATTGAAC 3'	58 °C	cloning
Jab1	Jab1mychisfw Jab1mychisrev	5' CCCAAGCTTGCCACCATGGCGGCGTCCGGGAGC 3' 5' TCCCCGCGGAGAGATGTTAATTTGATTAAACAG 3'	58 °C	cloning
p24A	RNP24cfw RNP24crev	5' CGGGATCCACCATGGTGACGCTTGCTGAACTG 3' 5' TCCCCGCGGAACAACTCTCCGGACTTC 3'	58 °C	cloning
p23	p23fw p23rev	5' CGGGATCCGCCACCATGTCTGGTTTGTCTGGC 3' 5' TCCCCGCGGCTCAATCAATTTCTTGGCCTTG 3'	58 °C	cloning
p24AΔN	rnpΔNGFPfw RNP24crev	5' CCCAAGCTTGTG GTCCTTTGGTCCTTC 3' 5' TCCCCGCGGAACAACTCTCCGGACTTC 3'	55 °C	cloning
p24AΔC	RNP24cfw rnpΔCmycrev	5' CGGGATCCACCATGGTGACGCTTGCTGAACTG 3' 5' TCCCCGCGGGTAGATCTGTCCCAATGTC 3'	58 °C	cloning
p24AΔCT	rnpΔCGFPfw rnpΔCGFPrev	5' CCCAAGCTTGCCACCATGGTGACGCTTG 3' 5' TCCCCGCGGTCTGCTGTTTGTGTTGTC 3'	58 °C	cloning

Continued

p24AGOLD	rnpΔCGFPfw rnpGOLDGFPrev	5’ CCCAAGCTTGCCACCATGGTGACGCTTG 3’ 5’ TCCCCGCGGAATATCAATGGTGAACATCAC 3’	58 °C	cloning
p24AGL	rnpΔCGFPfw rnp125GFPrev	5’ CCCAAGCTTGCCACCATGGTGACGCTTG 3’ 5’ TCCCCGCGGAGCTTCTGTTTCCATATC 3’	58 °C	cloning
p24AΔGOLD	rnpΔGOLDGFPfw rnpΔGOLDGFPrev	5’ CCCAAGCTTGGGGAGGCTCCAAAAG 3’ 5’ TCCCCGCGGAATATCAATGGTGAACATCAC 3’	58 °C	cloning
p24ASP	SPfw SPrev	5’ GATCTGCCACCATGGTGACGCTTGCTGAACTGCTGGTGCTCCTGG CCGCTCTCCTGGCCACGGTCTCGGGCA 3’ 5’ AGCTTGCCCGAGACCGTGGCCAGGAGAGCGGCCAGGAGCACCAG CAGTTCAGCAAGCGTCACCATGGTGGCA 3’	---	cloning
hsPAR-2HA	peakPAR2kfw hsPAR2peakrev	5’ CCCAAGCTTGCCACCATGCGGAGCCCCAGCGCG 3’ 5’ GCTCTAGATCAAGCGTAGTCTGGGACGTCGTATGGGTAGAATTCA TAGGAGGTCTTAAC 3’	58 °C	cloning
hsPAR-2Δ(1-213)HA	peakPAR2CTfw hsPAR2peakrev	5’ CCCAAGCTTGCCACCATGGTGAAGCAGACCATC 3’ 5’ GCTCTAGATCAAGCGTAGTCTGGGACGTCGTATGGGTAGAATTCA TAGGAGGTCTTAAC 3’	58 °C	cloning
hsPAR-1HA	peakhsPAR1fw peakhsPAR1rev	5’ CCCAAGCTTGCCACCATGGGGCCGCGGCGGCTG 3’ 5’ CCGGAATTCAGTTAACAGCTTTTTGTATATG 3’	58 °C	cloning
hsPAR1	hsPAR1LnF hsPAR1LnR	5’ CGCCTGCTTCAGTCTGTGCGGC 3’ 5’ GGCCAGGTGCAGCATGTACACC 3’	60 °C	PCR
hsPAR2	hsPAR2LnF hsPAR2LnR	5’ GCCATCCTGCTAGCAGCCTCTC 3’ 5’ GATGACAGAGAGGAGGTCAGCC 3’	60 °C	PCR
hsPAR3	hsPAR3LF hsPAR2LCNR	5’ TTGTCAGAGTGGCATGGAA 3’ 5’ TGGCCCGGCACAGGACCTCTC 3’	60 °C	PCR
hsPAR4	hsPAR4LnF hsPAR4LnR	5’ CAGCGTCTACGACGAGAGCGG 3’ 5’ CACTGAGCCATACATGTGACCAT 3’	60 °C	PCR
GAPDH	hGAPfw hGAPrev	5' TCCAAAATCAAGTGGGGCGATGCT 3' 5' ACCACCTGGTGCTCAGTGTAGCCC 3'	60 °C	PCR
Jab1	COP9S5fw COP9S5rev	5’ CATATGAATACATGGCTGCA 3’ 5’ GGCTTCTGACTGCTCTAAC 3’	53 °C	PCR
---	T7fw	5’ TAATACGACTCACTATAGGGA 3’	52 °C	sequencing
---	BGHrev	5’ AACTAGAAGGCACAGTCGAGG 3’	52 °C	sequencing
---	pEAK10fw	5’ TTCTCAAGCCTCAGACAGTGG 3’	52 °C	sequencing
---	pEAK10rev	5’ GATGCAGGCTACTCTAGGGCA 3’	52 °C	sequencing
---	pEGFP N1rev	5’ CGTCGCCGTCCAGCTCGACCAG 3’	52 °C	sequencing
---	pVL1392fw	5’ TATTCCGGATTATTC 3’	52 °C	sequencing
---	pVL1392rev	5’ CAACGACAAGCTTCATCGTGTCG 3’	52 °C	sequencing
---	MATCHMAKER AD LD-Insert fw	5’ CTATTCGATGATGAAGATACCCCACCA 3’	52 °C	sequencing

*The restriction enzyme sites are underlined.

30°C for 8 h. Colonies that turned blue within 8 h were regarded as positive for further analysis.

2.2.3.4 Plasmids isolation from yeast

$His^+Ade^+LacZ^+$ colonies were incubated for 3 days in SD/-Leu medium with shaking at 30°C. Yeast cells were collected and lysed in yeast lysis buffer with the help of acid-washed glass beads. Plasmid DNA was extracted with phenol/chloroform/isoamylalcohol (25:24:1), and precipitated with 1/10 vol of 3 M sodium acetate (pH 5.2) and 0.77 vol of isopropanol. After washing with 70% ethanol, DNA pellet was dried and dissolved in TE buffer.

2.2.3.5 Rescue AD/library plasmids by transformation of *E. coli*

Yeast plasmids were transformed into *E. coli* XL 1-Blue cells by the standard electroporation methods. The plasmid DNA was amplified and isolated from *E.coli* cells using the standard plasmid mini-prep methods. The rescued pACT2 plasmids containing cDNA insert were sequenced, and analyzed with the program BLAST in the GenBank™ database.

2.2.4 Cell culture and transfection

The HEK293 cells were grown in DMEM/Ham's F-12 1:1 medium (Biochrom, Germany) supplemented with 10% heat-inactivated FCS, 100 units/ml penicillin and 100 μg/ml streptomycin at 37ºC and 5% CO_2.

Normal primary human astrocytes (NHA) were obtained from Cambrex Bio Science Verviers SPRL (Verviers, Belgium). These astrocytes were established from normal human brain tissue. NHAs were grown in the AGM™ Astrocyte Medium (Cambrex) at 37ºC and 5% CO_2. NHA cultures were used within 10 passages in the present study, since their characteristic properties are impaired with subsequent passages.

Rat primary astrocytes were prepared, as described previously [110], and grown in DMEM medium (Biochrom, Germany) supplemented with 10% heat-inactivated FCS, 100 units/ml penicillin and 100 μg/ml streptomycin at 37ºC and 10% CO_2. For experiments, cells were used between days 10 and 13 in culture.

Cells (80% confluent) were transfected using DOTAP liposomal transfection reagent, according to the manufacturer's protocol (Roche Diagnostics, Germany). Briefly, one day before transfection the cells were plated on a 6-well plate. On the following day, the subconfluent cells were transfected or co-transfected with the indicated plasmids using

DOTAP. To generate the stable clone, the transfected cells were selected with 500 μg/ml of G418 (for HEK293-Jab1myc, HEK293-p24Amyc, HEK293-p23myc, HEK293-p24A-GFP, HEK293-p24AΔN-GFP, HEK293-p24AΔC-GFP, HEK293-p24AΔCT-GFP, HEK293-p24AGOLD-GFP, HEK293-p24AGL-GFP, HEK293-p24AΔGOLD-GFP, and HEK293-GFP cells), 1 μg/ml of puromycin (for HEK293-PAR-2-HA cells and HEK293-PAR-2Δ(1-213)-HA cells) or both (for HEK293-PAR-2-HA+Jab1myc, HEK293-PAR-2Δ(1-213)-HA+Jab1myc, HEK293-PAR-2-HA+p24Amyc, HEK293-PAR-2Δ(1-213)-HA+p24Amyc, HEK293-PAR-2-HA+p23myc cells, and HEK293-PAR-1-HA+p24Amyc).

2.2.5 PAR-2 activation and inhibitor treatment

To activate PAR-2, cells were rinsed with Hank's solution, and stimulated in serum-free medium with bovine pancreatic trypsin (100 nM, Roche Diagnostics, Germany) as a physiological agonist or with PAR-2 AP SLIGKV-NH_2 (100 μM, Bachem) as a specific agonist. To prevent receptor endocytosis, cells were pretreated with 80 μM phenylarsine oxide (Calbiochem) for 15 min prior to agonist stimulation. To prevent receptor degradation, cells were pretreated with 100 μM Z-Phe-Ala-diazomethylketone (ZPAD, Bachem) for 30 min prior to agonist stimulation. To prevent receptor resensitization, cells were pretreated with 10 μg/ml brefeldin A for 30 min prior to agonist stimulation. To inhibit new protein synthesis, cells were pretreated with 70 μM cycloheximide (Calbiochem) for 30 min prior to agonist stimulation. To study the localization of internalized PAR-2 in lysosomes, cells were pretreated with 10 mM NH_4Cl for 30 min prior to agonist stimulation. The inhibitors were included in the medium throughout the experiments.

2.2.6 GST pull-down assays

The different GST fusion protein constructs were transfected into Sf9 cells, using lipofectin (Invitrogen) in the presence of the linearized BaculoGold™ virus DNA (BD Bioscience Pharmingen). The recombinant baculovirus was amplified and tested for the production of the fusion protein. Cells infected with recombinant baculovirus containing PAR-2-GST, PAR-2Δ(246-397)-GST, or PAR-2Δ(1-213)-GST were homogenized on ice in membrane fraction buffer 1. After centrifugation for 10 min at 1000 g and 4°C, the supernatant was further centrifuged for 1 h at 100000 g and 4°C. Afterwards, pellets were resuspended in membrane fraction buffer 2, sonicated, stirred and centrifuged again for 1 h at 100000 g and 4°C. The resulting supernatant contained the membrane fraction of the

recombinant fusion proteins. On the other hand, cells infected with recombinant baculovirus containing GST, PAR-2IL1-GST, PAR-2IL2-GST, PAR-2IL3-GST, PAR-2C-GST or PAR-2EL2-GST were homogenized in Sf9 lysis buffer. After centrifugation for 5 min at 35000 g and 4^{o}C, the resulting supernatant contained the cytosolic fraction of the recombinant fusion proteins. The recombinant fusion proteins were purified by using glutathione-Sepharose beads (GE Healthcare). The expression of GST fusion proteins was determined by Coomassie blue staining and western blot analysis.

To determine protein-protein interaction *in vitro* and PAR-2 domains responsible for the interaction, equal amounts of GST and full-length or truncated PAR-2-GST fusion proteins immobilized on glutathione-Sepharose beads were incubated overnight at 4^{o}C with either the crude HEK293-Jab1myc cell extracts or the crude HEK293-p24Amyc cell extracts in HEK293 lysis buffer. After washing three times with the HEK293 lysis buffer without protease inhibitor, the bound proteins were separated by SDS-PAGE, and immunoblotted with the anti-myc antibody (1:5000, Invitrogen).

To determine p24A domains involved in interaction with PAR-2, the cell lysates from HEK293-p24A-GFP, HEK293-p24AΔN-GFP, HEK293-p24AΔC-GFP, HEK293-p24AΔCT-GFP, HEK293-p24AGOLD-GFP, HEK293-p24AGL-GFP, HEK293-p24AΔGOLD-GFP, as well as HEK293-GFP cells were incubated overnight with full-length PAR-2-GST fusion proteins immobilized on glutathione-Sepharose beads at 4^{o}C. After washing three times with the HEK293 lysis buffer without protease inhibitor, the bound proteins were separated by SDS-PAGE, and immunoblotted with the anti-GFP antibody (1:5000, Cell signaling technology).

2.2.7 Immunoprecipitation

In the overexpressed systems, equal amounts of cell lysates were rotated with the anti-HA antibody (1:200, Sigma), the rabbit IgG (1:200, Santa Cruz) or the anti-GFP antibody (1:200, Cell signaling technology) for 6 h, followed by incubating with protein A Sepharose beads (GE Healthcare) overnight at 4^{o}C. After washing three times with HEK293 lysis buffer without protease inhibitor, the bound beads were incubated in Laemmli buffer for 60 min on ice (for immunoprecipitating PAR-1-HA, PAR-2-HA and $P2Y_1$-GFP receptor), or boiled in Laemmli buffer for 5 min at 100^{o}C (for immunoprecipitating PAR-2Δ(1-213)-HA), separated by SDS-PAGE, and immunoblotted with the anti-myc antibody (1:5000, Invitrogen). To confirm the specific immunoprecipitation by PAR-1 and PAR-2, the membrane was stripped,

blocked, and reprobed overnight with the anti-HA antibody (1:2000, Cell signaling technology).

In the native systems, equal amounts of cell lysates were rotated with the anti-PAR-2 (C-17) antibody (1:25, Santa Cruz), the anti-GST antibody (1:25, Santa Cruz), the anti-p24A antibody (1:100), or the rabbit IgG (1:100, Santa Cruz) for 6 h, followed by incubating with protein G agarose beads (Sigma) overnight at 4^{o}C. After washing three times with HEK293 lysis buffer without protease inhibitor, the bound beads were incubated in Laemmli buffer for 60 min on ice, separated by SDS-PAGE, and immunoblotted with the anti-Jab1 antibody (1:1000, Santa Cruz), or with the anti-PAR-2 antibody (1:100, Santa Cruz). To confirm that Jab1 was specifically immunoprecipitated by PAR-2, the membrane was stripped, blocked, and reprobed overnight with the anti-PAR-2 antibody (1:100, Santa Cruz).

2.2.8 Western Blot

Cells were rinsed with cold PBS, and lysed on ice for 30 min in the HEK293 lysis buffer. After centrifugation for 15 min at 13000 rpm and 4^{o}C, the resulting supernatant was collected and quantitated by Bradford methods using bovine serum albumin (BSA) as standard. To detect endogenous c-Jun phosphorylation, cells were lysed in the modified RIPA buffer.

To remove *N*-linked oligosaccharides of PAR-2, the whole cell lysates were incubated overnight with *N*-glycosidase F (500 units/reaction, New England Biolabs) at 4^{o}C. The reaction was stopped by dissolving in Laemmli buffer.

The proteins with Laemmli buffer were boiled for 5 min or incubated on ice for 1 h (for detecting PAR-1, PAR-2 and $P2Y_1$ receptor), electrophoresed on a 10% or 12.5% SDS-PAGE gel, and transferred to nitrocellulose membrane. The membrane was blocked and incubated overnight with the primary antibody (anti-GST, 1:80000, Santa Cruz; anti-Jab1, 1:2500, Santa Cruz; anti-phospho-c-Jun (Ser63), 1:1000, Cell signaling technology; anti-c-Jun antibody, 1:1000, Cell signaling technology; anti-HA (6E2), 1:1000, Cell signaling technology; or anti-β-tubulin I, 1:40000, Sigma) at 4ºC, followed by goat anti-rabbit or goat anti-mouse IgG conjugated to HRP for 1 h at room temperature. After washing, the immune complexes were detected by the SuperSignal West Pico Chemiluminescent Substrate (Pierce).

2.2.9 Immunofluorescence analysis

Cells were fixed with 4% PFA for 20 min at room temperature, and permeabilized by incubation in PBS with 0.2% Triton X-100 and 3% BSA for 60 min.

For single staining, cells were incubated overnight with either mouse anti-Jab1 antibody (8 μg/ml, Santa Cruz) or rabbit anti-HA antibody (4 μg/ml, Sigma) at 4ºC, washed, and incubated with respective Alexa Fluor 488 goat anti-mouse IgG antibody (20 μg/ml, Molecular Probes) or Alexa Fluor 568 goat anti-rabbit IgG antibody (20 μg/ml, Molecular Probes) for 120 min at room temperature in the dark.

For double staining, cells were incubated overnight with mouse anti-myc antibody (2 μg/ml, Invitrogen) and rabbit anti-HA antibody (4 μg/ml, Sigma), with mouse anti-Jab1 antibody (8 μg/ml, Santa Cruz) and rabbit anti-HA antibody (4 μg/ml, Sigma), or with mouse anti-GM130 antibody (5 μg/ml, BD) and rabbit anti-HA antibody (4 μg/ml, Sigma) at 4ºC, washed, and incubated with Alexa Fluor 488 goat anti-mouse IgG antibody (20 μg/ml, Molecular Probes) and Alexa Fluor 568 goat anti-rabbit IgG antibody (20 μg/ml, Molecular Probes), or with Alexa Fluor 633 goat anti-mouse IgG antibody (20 μg/ml, Molecular Probes) and Alexa Fluor 568 goat anti-rabbit IgG antibody (20 μg/ml, Molecular Probes) for 120 min at room temperature in the dark.

Mounted slides were observed with a LSM510 confocal laser scanning microscope (Carl Zeiss, Germany).

2.2.10 Reporter gene assays

Cells were transfected with an AP-1-driven chloramphenicol acetyltransferase (CAT) reporter plasmid (a gift from Dr. J. Kraus, Institut für Pharmakologie und Toxikologie, Otto-von-Guericke-Universität Magdeburg) using DOTAP, as described above. Six hours after transfection, the cells were treated with 100 μM PAR-2 AP for 48 h in DMEM/Ham's F-12 medium supplemented with 1% FCS. The CAT activity in cell lysates was analyzed by enzyme-linked immunosorbent assay (ELISA) (Roche Diagnostics, Germany), and normalized to protein concentration. The empty CAT reporter vector was also transfected in parallel, as a negative control.

2.2.11 siRNA

Human Jab1 siRNA was obtained from Santa Cruz Biotechnology, Inc. HEK293-PAR-2-HA cells were transfected with human Jab1 siRNA by using magnet assisted transfection, according to the manufacturer's protocol (IBA GmbH, Germany). Briefly, one day before transfection cells were plated on a 6-well plate. On the following day, the subconfluent cells (80%) were incubated for 15 min with human Jab1 siRNA or scrambled siRNA and magnet

assisted transfection reagents mixture on the magnet plate. Afterwards, transfected cells were cultured for 48 h under normal conditions. Non-silencing siRNA labeled with Alexa Fluor 488 served as a scrambled siRNA control (Qiagen). Jab1 knockdown was assessed by western blot and RT-PCR at 48 h after transfection.

2.2.12 Cytosolic calcium measurements

The free intracellular calcium concentration ($[Ca^{2+}]_i$) was determined using the calcium sensitive fluorescent indicator Fura-2 AM. For dye loading the cells grown on a coverslip were removed from the culture dish and placed in 1 ml NaHBS buffer for 30 min at 37ºC, supplemented with 2 μM Fura-2 AM. Loaded cells were transferred into a perfusion chamber with a bath volume of about 0.2 ml and mounted on an inverted microscope (Zeiss, Axiovert 135). During the experiments the cells were continuously superfused with NaHBS buffer, which was heated to 37ºC. The perfusion system allowed to switch between solutions containing different agonists to be tested.

Single-cell fluorescence measurements of $[Ca^{2+}]_i$ were performed using an imaging system from TILL Photonics GmbH. Cells were excited alternately at 340 nm and 380 nm for 20 to 100 ms at each wavelength with a rate of 0.33 Hz and the resultant emission collected above 510 nm. Images were saved on a personal computer and subsequently the changes in fluorescence ratio ($F_{340\ nm}$ /$F_{380\ nm}$) were determined from selected regions of interest covering a single cell.

2.3 Statistical analysis

Data were expressed as mean ± S.E.M. Differences were examined by Student's *t*-test between two groups or one-way analysis of variance within multiple groups. $p<0.05$ was considered significant.

3. RESULTS

Part I. Identification of interacting proteins of human PAR-2 by using yeast two-hybrid screening

PAR-2, a GPCR, mediates the intracellular signal transduction in response to stimulation with the extracellular proteases trypsin and tryptase. To identify intracellular proteins that are involved in PAR-2 signalling events, a yeast two-hybrid screening was performed. The full-length human PAR-2 cDNA was fused in-frame to the GAL4 DNA binding domain as a bait. The yeast strain AH109 transformed with bait plasmids nicely grew on SD/-Trp media, but not on SD/-Trp-His and SD/-Trp-Leu-His-Ade media, indicating that human PAR-2 protein itself does not autonomously activate the histidine and adenine reporter genes. Further experiments demonstrated that the bait strain grew normally in SD/-Trp liquid medium supplemented with 20 μg/ml kanamycin (OD_{600}: 1.3, after 24 h-incubation), compared to AH109 cells transformed with empty pGBKT-7 vector (OD_{600}: 1.5, after 24 h-incubation). These data suggest that there are no toxic effects of the bait protein on yeast cells. Small-scale yeast mating experiments showed that the mating efficiency between the bait strain and Y187 transformed with GAL4 activation domain vector fused with SV40 large T antigen pTD1-1 (Y187 [pTD1-1]) was about 8.6%. This value is slightly, but not significantly lower than that of the positive control that AH109 cells transformed with pGBKT7-53 were mating with Y187 [pTD1-1] cells (9.7%), suggesting that the bait protein does not affect mating efficiency.

Next, using this bait, a pretransformed human brain cDNA library was screened. From 1.6×10^6 clones screened that were grown on nutritional deficient media and which activated the β-galactosidase, 308 colonies were found positive for the selection markers histidine, adenine and LacZ. Subsequent sequencing and BLAST analysis further revealed that the cDNAs from 34 colonies encoded 19 potential PAR-2-interacting proteins. Many others either encoded mitochondrial proteins (ATP synthase subunit 6, COX3, NADH dehydrogenase subunit 1) and the transcription factor (PAX6) that were unlikely to interact with cell surface receptors under physiological conditions, or they were scrambled sequences that did apparently not encode any proteins.

To further verify the protein interaction in yeast, we transformed yeast Y187 cells with bait plasmids and yeast AH109 cells with candidate prey plasmids isolated from the library, and then performed yeast two-hybrid tests. The transformants grown on SD/-Trp-Leu-His-Ade media were tested by LacZ colony-lift filter assay. 24 colonies that encoded 12 different proteins were found again to activate the LacZ reporter gene, indicating that they are truly

positive in yeast (Table 3.1). Other candidate partners, such as RanBPM, tetraspan 3, tetraspan 5, cysteine-rich with EGF-like domain 1, connexin47 and minor histocompatibility antigen 13, were shown to be negative by LacZ colony-lift filter assay.

Table 3.1. The candidate PAR-2-interacting proteins identified in the yeast two-hybrid screening.

Clone	Insert size (kb)	Protein	Position (aa)	DNA Accession #	Protein Accession #
17/8a	2.3	HUEL	360-568	NM_006345	NP_006336
58/1a	2.0	HUEL	360-568	NM_006345	NP_006336
1/1a	2.0	HUEL	360-568	NM_006345	NP_006336
21/5b	2.3	HUEL	360-568	NM_006345	NP_006336
20/9a	2.0	HUEL	360-568	NM_006345	NP_006336
7/1b	2.3	HUEL	360-568	NM_006345	NP_006336
7/14b	2.3	HUEL	360-568	NM_006345	NP_006336
5/6a	1.3	SLC21A11	470-692	BC000585	AAH00585
42/4c	1.8	MLC1	162-377	NM_015166	NP_055981
12/9b	1.8	Jab1	31-334	BC001859	AAH01859
23/14a	1.0	Jab1	49-334	BC001859	AAH01859
10/15b	1.6	COP9S4	1-406	NM_016129	NP_057213
54/2b	1.6	COP9S4	1-406	NM_016129	NP_057213
54/3c	1.6	COP9S4	1-406	NM_016129	NP_057213
28/6b	1.9	RERE	59-133	NM_012102	NP_036234
28/7b	1.9	RERE	59-133	NM_012102	NP_036234
28/8a	1.9	RERE	59-133	NM_012102	NP_036234
T28/Aa	1.8	RERE	59-133	NM_012102	NP_036234
45/3b	1.5	TM4SF2	115-249	NM_004615	NP_004606
24/9b	1.0	p24A	63-201	NM_006815	NP_006806
36/34b	3.3	MRP7	983-1098*	NM_033450	NP_003170
59/26b	2.4	synaptophysin	52-313	NM_003179	NP_003170
23/6c	2.0	Integrin VLA-4 beta subunit, isoform 1A	572-667*	NM_002211	NP_002202
		Integrin VLA-4 beta subunit, isoform 1B	572-667*	NM_033666	NP_389647
		Integrin VLA-4 beta subunit, isoform 1C-1	572-667*	NM_033667	NP_391987
		Integrin VLA-4 beta subunit, isoform 1C-2	572-667*	NM_033669	NP_391989
		Integrin VLA-4 beta subunit, isoform 1D	572-667*	NM_033668	NP_391988
3/8c	1.4	Reticulon 1, isoform A	609-776	NM_021136	NP_066959
		Reticulon 1, isoform B	189-356	L10334	AAA59951
		Reticulon 1, isoform C	41-208	L10335	AAA59952

*sequenced by MATCHMAKER AD LD-Insert fw only.

Prey plasmids were isolated from $His^+Ade^+LacZ^+$ colonies, amplified in XL-1 Blue *E. coli* cells, and digested with the Hind III enzyme. Afterwards, the insert was sequenced, and analyzed with the program BLAST in the GenBank™ database.

Part II. PAR-2 overexpression in insect and mammalian cells

3.2.1 PAR-2 overexpression in Sf9 cells

To confirm the protein-protein interaction between PAR-2 and candidate interacting partners by GST pull-down assays, we engineered exogenous PAR-2-GST expression in insect Sf9 cells. We generated a novel baculovirus GST expression vector pVL1392-GST in order to facilitate the expression of the transmembrane protein tagged with GST in Sf9 cells, and inserted the full-length human PAR-2 cDNA at the N-terminus of GST. Sf9 cells were transfected with pVL1392-PAR-2-GST in the presence of the linearized BaculoGold virus DNA using lipofectin. Afterwards, the recombinant baculovirus was amplified and tested for the production of the fusion protein. The expression of PAR-2-GST (lane 4) was detectable by Coomassie blue staining with two major bands (~60-70 kDa and ~140-160 kDa) in Sf9 cells (Fig. 3.2.1 A), which was confirmed by subsequent western blot analysis using the antibody against GST (Fig. 3.2.1 B). The high molecular mass band might represent the PAR-2 homodimer.

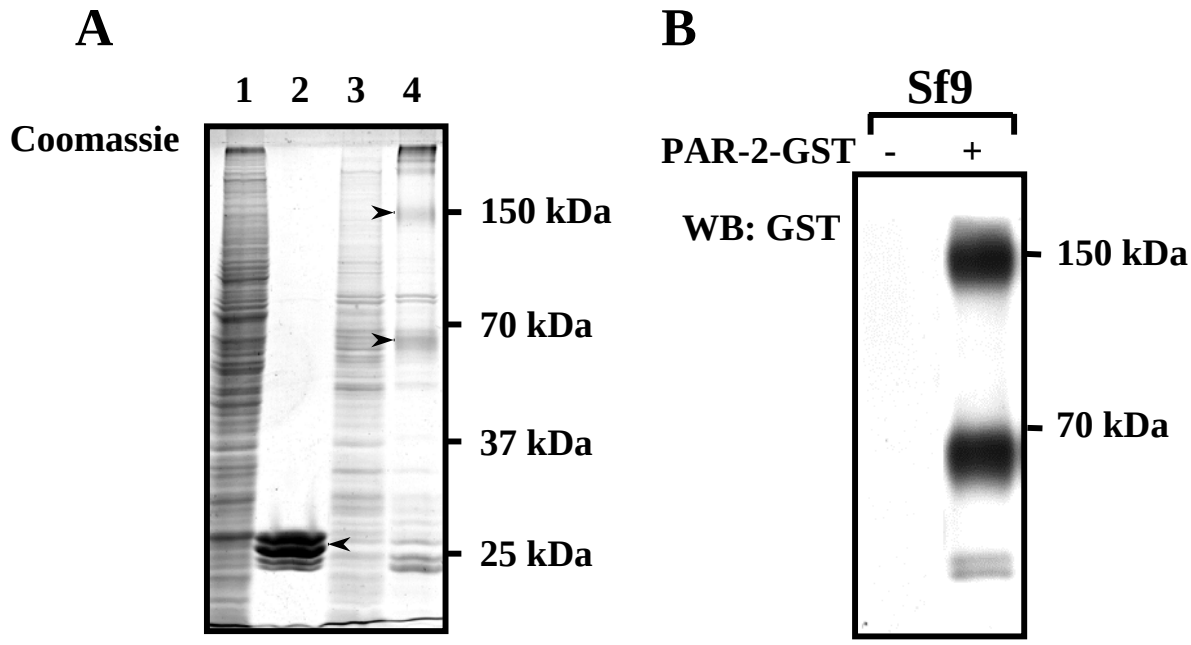

Fig. 3.2.1. The expression of PAR-2-GST in Sf9 cells. The cytosolic GST and membrane fraction of PAR-2-GST were extracted from infected Sf9 cells, purified by glutathione-Sepharose beads, and separated by 10% SDS-PAGE. (A). The expression of PAR-2-GST and GST were detected by Coomassie brilliant blue staining. The purified PAR-2-GST fusion protein (lane 4) was visible with two major bands (~60-70 kDa and ~140-160 kDa). The purified GST (lane 2) served as control. The respective cell lysates are also shown (lanes 1 and 3). (B). The expression of PAR-2-GST was determined by western blot analysis (WB). Cell lysates from uninfected (-) and PAR-2-GST-infected Sf9 cells (+) were immunoblotted by using a polyclonal anti-GST antibody. A representative blot from three independent experiments is given. The molecular mass marker is indicated on the right. Note: The band with higher molecular mass (~140-160 kDa) might represent the PAR-2 homodimer.

In order to map the domain of PAR-2 that is responsible for the interaction with candidate partners in the GST pull-down assay, we further constructed a series of truncated PAR-2-GST fusion proteins, which are given schematically in Figure 3.2.2, below the wild-type PAR-2-GST. As shown in Fig. 3.2.3 A, PAR-2Δ(246-397)-GST (lane 4) and PAR-2Δ(1-213)-GST (lane 6) purified by glutathione-Sepharose beads both were detectable by Coomassie blue staining. The purified GST served as control (lane 2, Fig. 3.2.3 A). In parallel, the expression of PAR-2EL2-GST (Fig. 3.2.3 B, lane 4), PAR-2IL1-GST (Fig. 3.2.3 C, lane 4), PAR-2IL2-GST (Fig. 3.2.3 C, lane 6), PAR-2IL3-GST (Fig. 3.2.3 C, lane 8) and PAR-2C-GST (Fig. 3.2.3 C, lane 10) was also observed after being purified by glutathione-Sepharose beads from Sf9 cells. The expression of truncated PAR-2-GST fusion proteins was confirmed by western blot with the anti-GST antibody (data not shown).

Interestingly, PAR-2Δ(246-397)-GST was present as a dimer in Sf9 cells (lane 4, Fig. 3.2.3 A), similar to the wild-type PAR-2-GST (Fig. 3.2.1). The receptor dimerization was eliminated by deletion mutants PAR-2IL1-GST (lane 4, Fig. 3.2.3 C), but not by PAR-2IL2-GST (lane 6, Fig. 3.2.3 C). Therefore, the transmembrane domains 3 and 4 and the intracellular loop 2 of PAR-2 contribute to receptor homodimer formation.

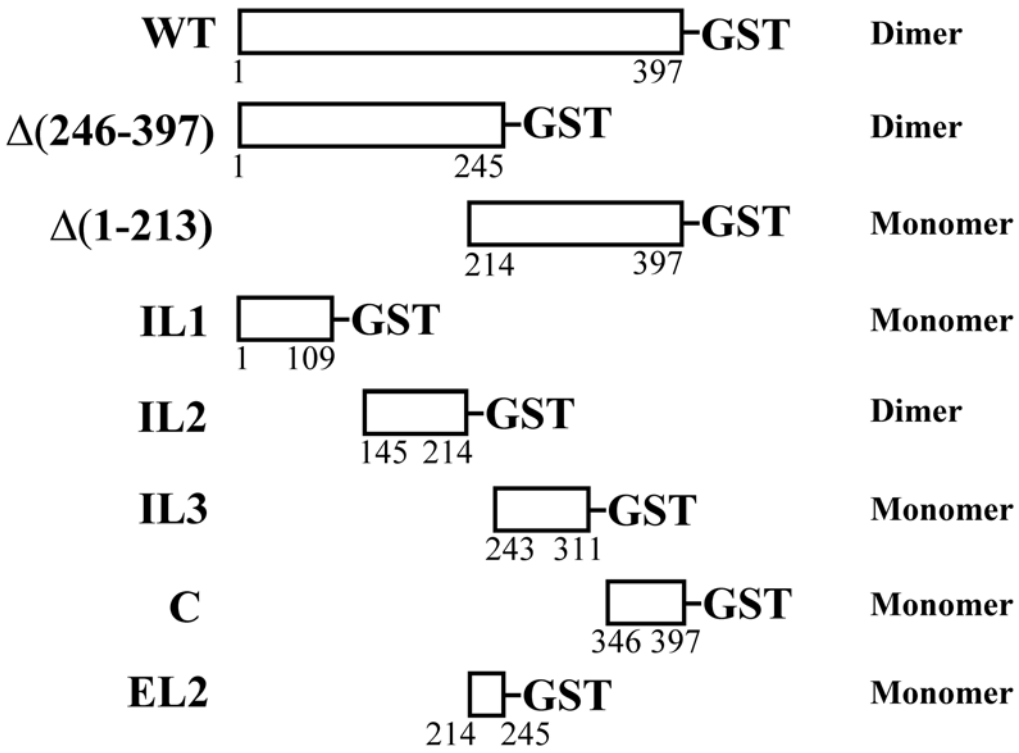

Fig. 3.2.2. Schematic representation of full-length PAR-2-GST and PAR-2 deletion GST constructs. The position of amino acids of PAR-2 are noted below constructs. The oligomeric state of fusion proteins is indicated on the right. WT, full-length PAR-2-GST; Δ(246-397), PAR-2Δ(246-397)-GST; Δ(1-213), PAR-2Δ(1-213)-GST; IL1, PAR-2IL1-GST; IL2, PAR-2IL2-GST; IL3, PAR-2IL3GST; C, PAR-2C-GST; EL2, PAR-2EL2-GST.

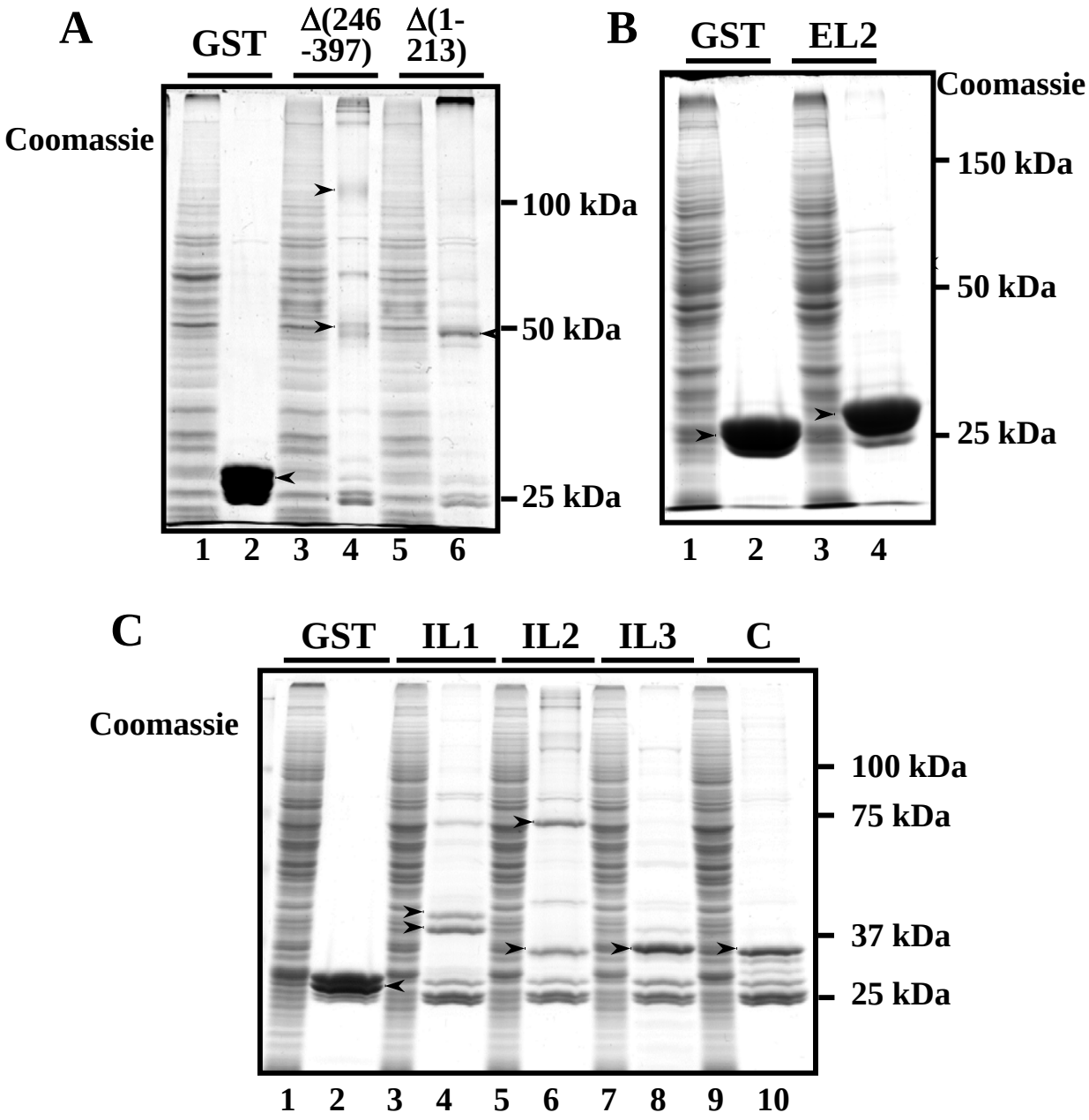

Fig. 3.2.3. The expression of truncated PAR-2 GST fusion proteins in Sf9 cells. (A). The cytosolic fraction of GST and the membrane fractions of PAR-2Δ(246-397)-GST (Δ(246-397)) and PAR-2Δ(1-213)-GST (Δ(1-213)) were extracted from infected Sf9 cells, purified by glutathione-Sepharose beads, and separated by 10% SDS-PAGE. The expression of PAR-2Δ(246-397)-GST, PAR-2Δ(1-213)-GST and GST was detected by Coomassie brilliant blue staining. The purified PAR-2Δ(246-397)-GST fusion protein (lane 4) was present as a homodimer (~50 kDa and ~100 kDa), whereas PAR-2Δ(1-213)-GST (lane 6) was a monomer (~50 kDa). The purified GST (lane 2) served as control. The respective cell lysates are also shown (lanes 1, 3 and 5). (B and C). The cytosolic fractions of GST, PAR-2EL2-GST (EL2, in B), PAR-2IL1-GST (IL1, in C), PAR-2IL2-GST (IL2, in C), PAR-2IL3-GST (IL3, in C) and PAR-2C-GST (C, in C) were extracted from infected Sf9 cells, purified by glutathione-Sepharose beads, separated by 10% SDS-PAGE, and detected by Coomassie brilliant blue staining. Similar to PAR-2-GST and PAR-2Δ(246-397)-GST, PAR-2IL2-GST (lane 6, in C) was also present as a homodimer. In contrast, PAR-2EL2-GST (EL2, in B), PAR-2IL1-GST (lane 4, in C), PAR-2IL3-GST (lane 8, in C) and PAR-2C-GST (lane 10, in C) were monomers. Interestingly, PAR-2IL1-GST (lane 4, in C) had two bands, suggesting that it might be *N*-glycosylated, since this protein contains the extracellular N-terminus of the receptor that possesses a *N*-glycosylation site. The purified GST (lane 2) served as control. The respective cell lysates are also shown (lanes 1, 3, 5, 7 and 9). Representative blots from at least three independent experiments are given. The molecular mass marker is indicated on the right.

3.2.2 PAR-2 overexpression in HEK293 cells

We constructed a mammalian expression vector pEAK10 inserted with the full-length PAR-2 cDNA fused with HA at the C-terminus. Therefore, PAR-2 protein would be easily detected by the anti-HA antibody. PAR-2-HA was stably expressed in HEK293 cells, to determine the protein-protein interaction in the mammalian system. As shown in Fig. 3.2.4 A, PAR-2-HA expression was detected in the whole cell lysates from HEK293-PAR-2-HA cells, by using an antibody against HA. PAR-2-HA protein appeared as a smear band (mainly at ~37-70 kDa), which is consistent with previous reports by others [46, 150]. It is known that human PAR-2 possesses two potential *N*-linked glycosylation sites [46]. Receptor glycosylation is important for PAR-2 expression and activation [46, 158]. To study whether the smear band of PAR-2 resulted from receptor *N*-glycosylation, the whole cell lysates from HEK293-PAR-2-HA were incubated with PNGase F. As shown in Fig. 3.2.4 B, PNGase F treatment significantly reduced the molecular mass of PAR-2-HA to ~32-44 kDa, suggesting that PAR-2-HA is a *N*-glycosylated glycoprotein. PAR-2 might also be *O*-glycosylated, because *N*-deglycosylated PAR-2 in Fig. 3.2.4 B still appeared as a smear band.

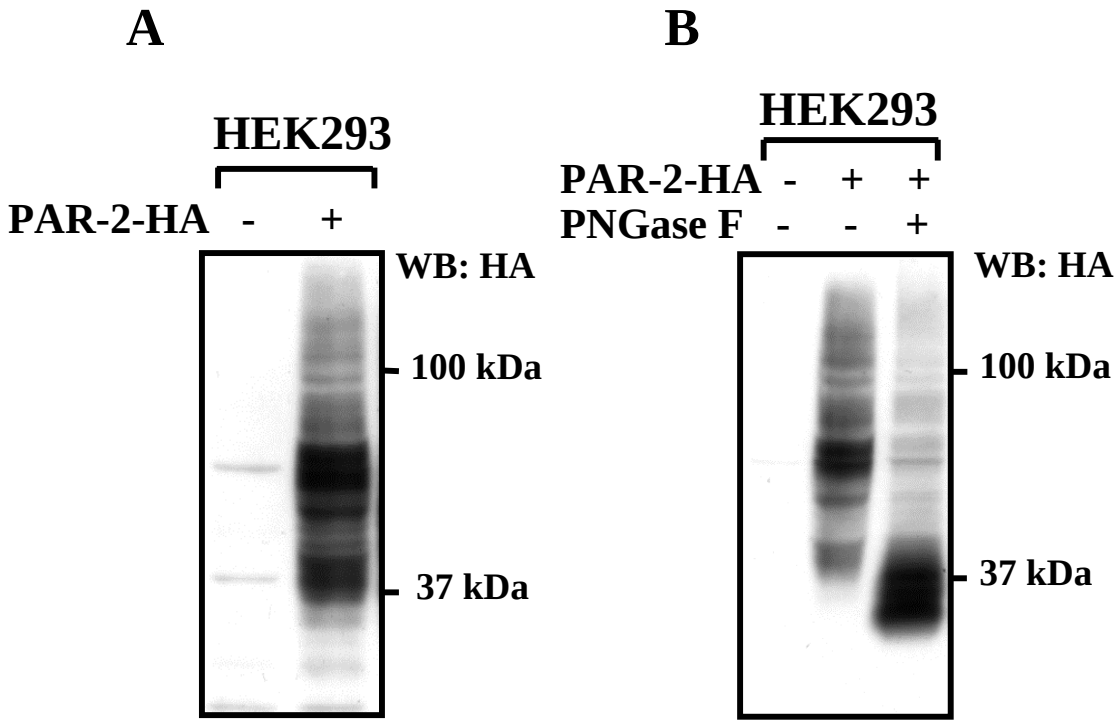

Fig. 3.2.4. The expression of PAR-2-HA in HEK293 cells. (A). The whole cell lysates from HEK293-PAR-2-HA cells were analyzed in 10% SDS-PAGE, and immunoblotted by using a monoclonal anti-HA (6E2) antibody. (B). The whole cell lysates (20 μg) from HEK293-PAR-2-HA cells were incubated overnight with peptide *N*-glycosidase F (PNGase F, 500 units/reaction) at 4^{o}C. Afterward, the reaction was stopped by dissolving in Laemmli buffer, electrophoresed, and immunoblotted by using a monoclonal anti-HA (6E2) antibody. Both experiments were repeated three times with comparable results. The molecular mass marker is indicated on the right. WB, western blot.

Next, we asked whether PAR-2-HA was functionally expressed in HEK293 cells. We stimulated transfected cells with PAR-2 agonists trypsin or PAR-2 AP, to investigate the receptor internalization by immunofluorescence staining using the antibody against HA. As shown in the left top panel of Fig. 3.2.5, PAR-2-HA was strongly expressed at the plasma membrane and in intracellular stores in unstimulated cells, which is consistent with other reports [139]. Wild-type HEK293 cells stained by anti-HA antibody and HEK293-PAR-2-HA cells without anti-HA antibody staining both served as negative control (Fig. 3.2.5, middle and right top panels). At 10 min after stimulation with either 100 nM trypsin or 100 μM PAR-2 AP, some of PAR-2 was internalized, and localized beneath the plasma membrane (Fig. 3.2.5, middle and bottom panels in the left column). After 30 min, the receptor was completely internalized (Fig. 3.2.5, middle and bottom panels in the center column). Similar results were also observed at 60 min incubation with PAR-2 agonists (Fig. 3.2.5, middle and bottom panels in the right column). Further experiments showed that PAR-2-HA was colocalized with the early endosome marker EEA1 at 15 min after trypsin stimulation (Fig. 3.2.6 A), suggesting that PAR-2 was rapidly internalized to early endosomes after activation. After 60 min, PAR-2-HA was detected in lysosomes, shown by colocalization with the lysosome marker LAMP1 (Fig. 3.2.6 B). These data support previous findings by others [139].

Taken together, our data above indicate that PAR-2-HA is functionally expressed in HEK293 cells. Moreover, the HA tag has no effect on the receptor expression and functions.

In addition, we investigated the expression of truncated PAR-2, PAR-2Δ(1-213)-HA and PAR-2Δ(246-397)-HA, in HEK293 cells as well. As shown in Fig. 3.2.7 A, PAR-2Δ(1-213)-HA was strongly expressed in transfected HEK293 cells. Immunofluorescence staining studies revealed that PAR-2Δ(1-213)-HA localized at the plasma membrane, and abundantly in the cytosol in HEK293-PAR-2Δ(1-213)-HA cells (Fig. 3.2.7 B). However, the expression of PAR-2Δ(246-397)-HA was very weak in HEK293 cells (data not shown).

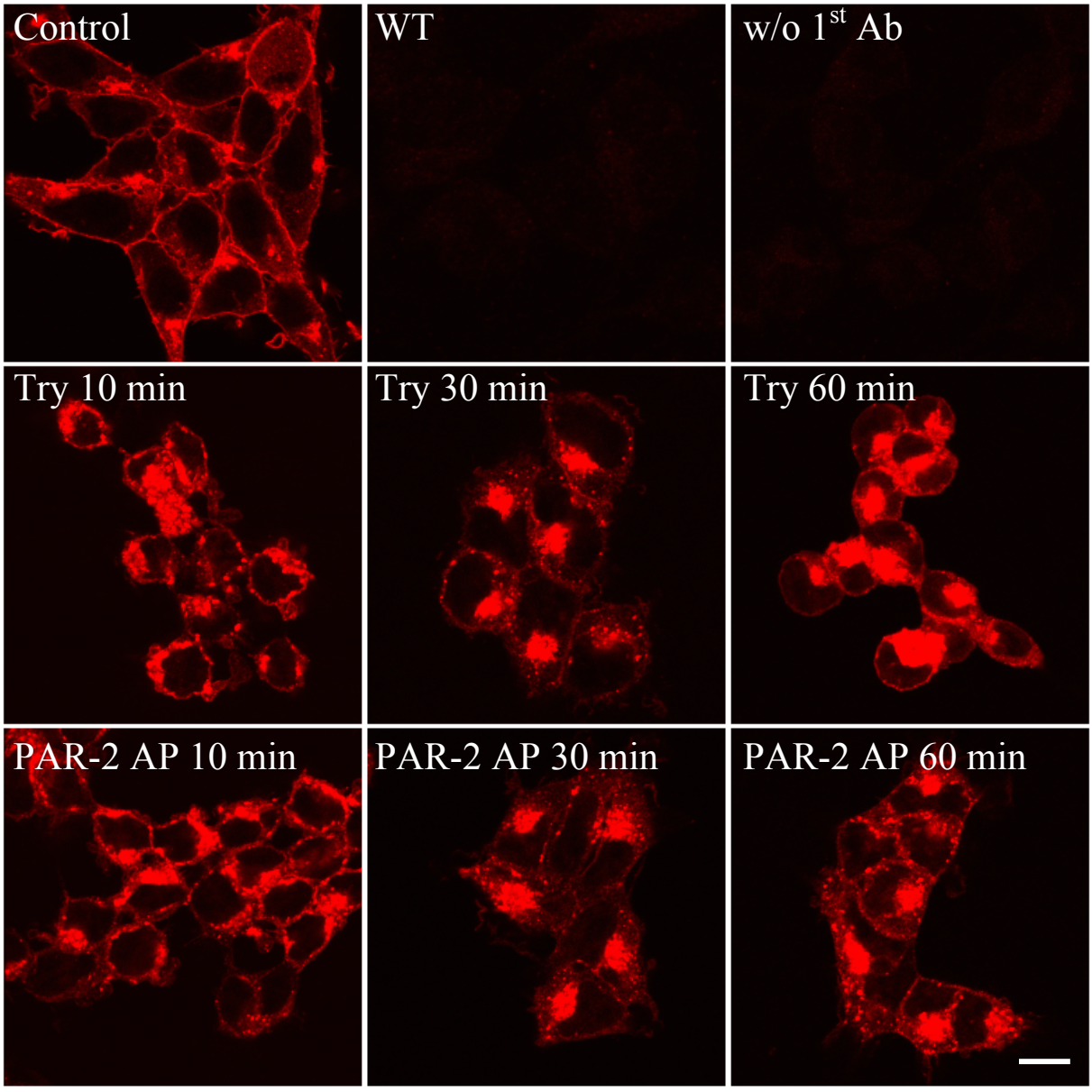

Fig. 3.2.5. Immunofluorescence staining of PAR-2-HA in transfected HEK293 cells. HEK293 cells stably expressed with PAR-2-HA were stimulated for indicated times with either 100 nM trypsin (Try) or 100 μM PAR-2 AP. Afterwards, cells were fixed, permeabilized, stained, and observed by a confocal microscope. PAR-2-HA was visualized by polyclonal anti-HA antibody and Alexa Fluor 568 goat anti-rabbit IgG. Wild-type HEK293 cells (WT) and HEK293-PAR-2-HA cells without anti-HA antibody (w/o 1st Ab) staining both served as negative control. All images are representative for three independent experiments. Scale bar, 10 μm.

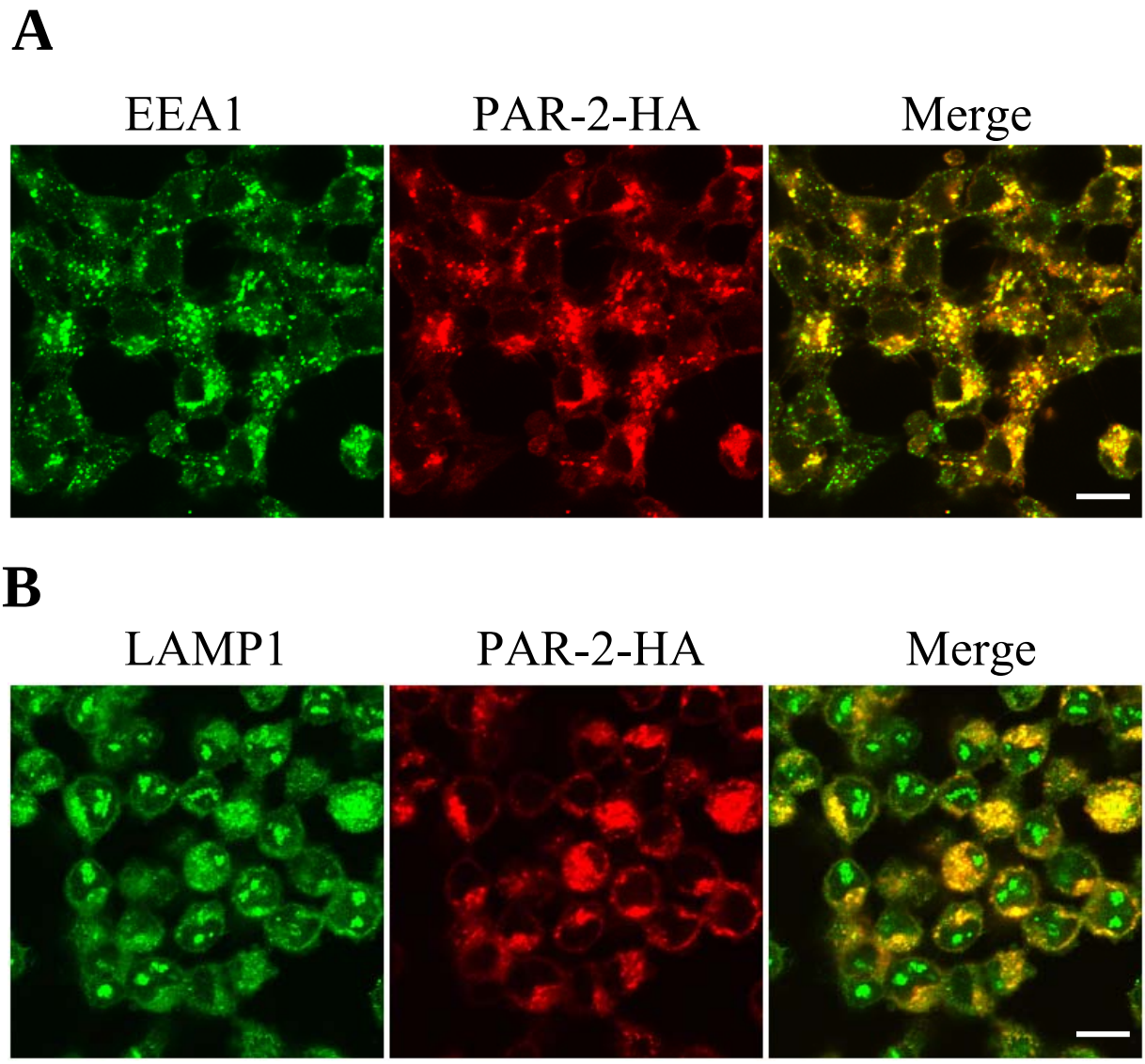

Fig. 3.2.6. PAR-2 was detected in both early endosomes and lysosomes after activation. HEK293 cells stably expressed with PAR-2-HA were incubated with 100 nM trypsin for either 15 min (A) or 60 min (B). Afterwards, cells were fixed, permeabilized, stained, and observed by a confocal microscope. EEA1 (green) was visualized by monoclonal anti-EEA1 antibody and Alexa Fluor 488 goat anti-mouse IgG (A). LAMP1 (green) was visualized by monoclonal anti-LAMP1 antibody and Alexa Fluor 488 goat anti-mouse IgG (B). PAR-2-HA (red) was visualized by polyclonal anti-HA antibody and Alexa Fluor 568 goat anti-rabbit IgG (A, B). The overlay image (Merge, yellow) revealed the colocalization of PAR-2 with either EEA1 or LAMP1. All images are representative for three independent experiments. Scale bar, 10 μm.

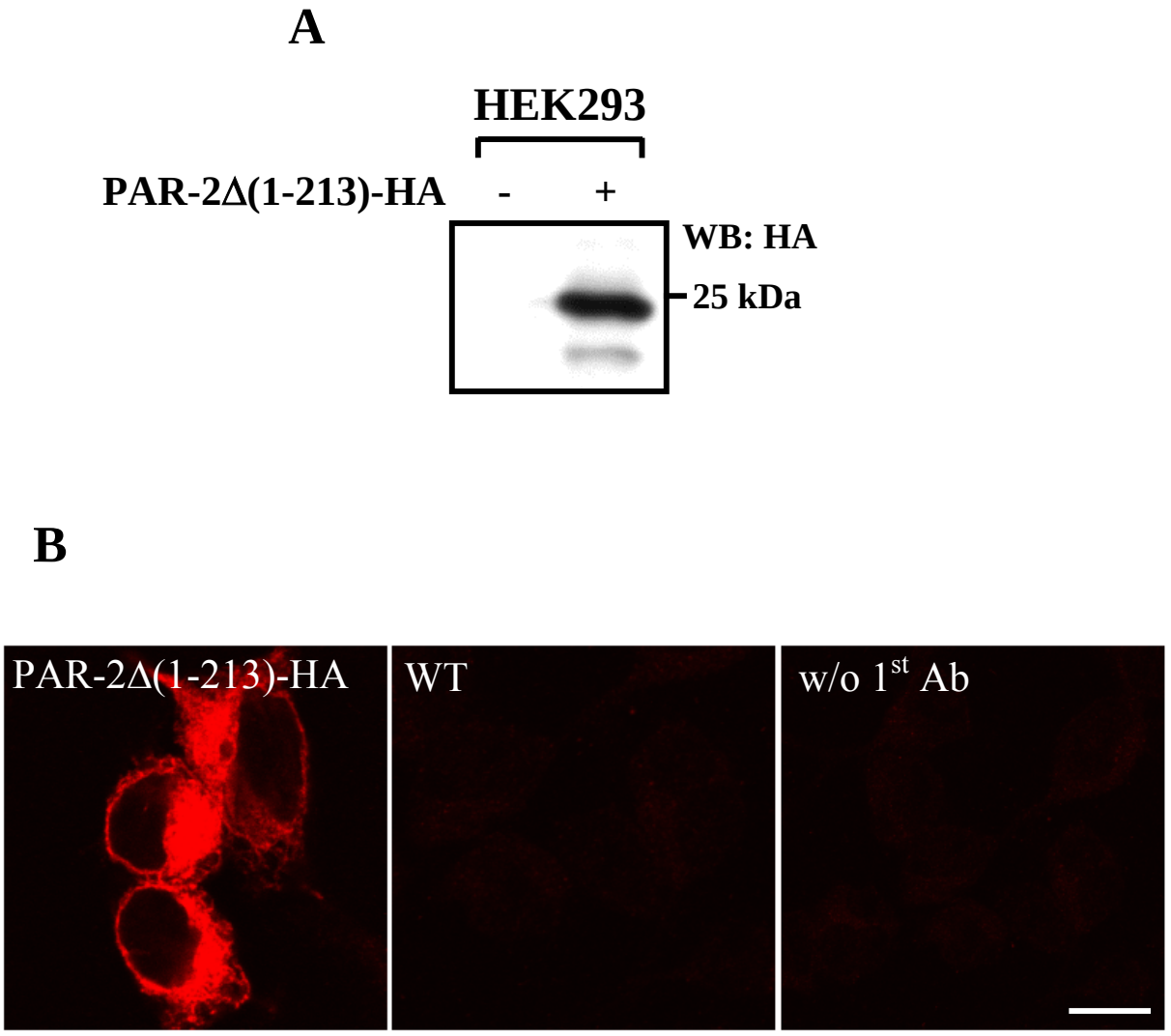

Fig. 3.2.7. The expression of PAR-2Δ(1-213)-HA in transfected HEK293 cells. (A). The whole cell lysates from HEK293-PAR-2Δ(1-213)-HA cells were analyzed in 10% SDS-PAGE, and immunoblotted by using a monoclonal anti-HA (6E2) antibody. The representative blot from at least three independent experiments is given. The molecular mass marker is indicated on the right. WB, Western blot. (B). HEK293 cells stably expressing PAR-2Δ(1-213)-HA were fixed, permeabilized, stained, and observed by a confocal microscope. PAR-2Δ(1-213)-HA was visualized by polyclonal anti-HA antibody and Alexa Fluor 568 goat anti-rabbit IgG. Wild-type HEK293 cells (WT) and HEK293-PAR-2Δ(1-213)-HA cells without anti-HA antibody staining (w/o 1st Ab) both served as negative control. All images are representative for three independent experiments. Scale bar, 10 μm.

Part III. Jun activation domain-binding protein 1 (Jab1) is involved in PAR-2-induced activation of AP-1

Jab1 was initially identified as a coactivator of c-Jun [167], and was later shown to be the fifth subunit of the COP9 signalosome complex [168]. The COP9 signalosome is a conserved multiprotein complex that has been found in plants, mammals, *Drosophila* and the fission yeast [169]. It consists of eight subunits, which exhibit significant similarity to the eight subunits of the lid of the 26S proteasome [169, 170]. Previous work has already demonstrated that a number of diverse proteins interact with the subunits of the COP9 signalosome, especially with Jab1. Using the yeast two-hybrid system, it was found that Jab1 binds to the N-terminal activation domain of c-Jun and thereby activates c-Jun [167]. Interestingly, Jab1 was shown to regulate the cell cycle by degrading the cyclin-dependent kinase inhibitor $p27^{Kip1}$ [171]. Recently, Jab1 was found to interact with the transmembrane protein integrin adhesion receptor LFA-1, and to mediate the activation of LFA-1-induced AP-1 [172]. It was also reported that Jab1 interacts with the transcription factor hypoxia-inducible factor-1 α (HIF-1 α), as well as the nuclear receptor progesterone receptor and the steroid receptor coactivator-1 (SRC-1), which control the transcription and expression of a number of genes [173, 174].

3.3.1. Multiple intracellular domains of PAR-2 are responsible for interaction with Jab1

We performed GST pull-down assays *in vitro*, to confirm the interaction between PAR-2 and Jab1 found in yeast. The PAR-2-GST fusion protein expressed in Sf9 cells was purified by glutathione-Sepharose beads. These beads with immobilized PAR-2-GST fusion protein were incubated overnight with the whole cell lysates from HEK293-Jab1myc cells to examine the interaction of PAR-2-GST with Jab1myc. The interaction was detected by western blot analysis using the anti-myc antibody. As shown in Fig. 3.3.1, Jab1 specifically interacted with the full-length PAR-2-GST fusion protein (lane 3). To exclude the possible interaction of Jab1 with the GST tag protein, we, in parallel, incubated GST protein on glutathione-Sepharose beads with the crude HEK293-Jab1myc cell lysates. Western blot analysis showed that Jab1 did not interact with GST protein alone (Fig. 3.3.1, lane 2). Aliquots from the HEK293-Jab1myc cell lysates, which were used for the pull-down assay served also as control for the western blot (Fig. 3.3.1, lane 1).

To map the domain of PAR-2 responsible for the interaction with Jab1, the truncated PAR-2-GST fusion proteins were tested similarly for their capacities to bind to Jab1 in the GST pull-down assay. As shown in Fig. 3.3.1, PAR-2Δ(246-397)-GST fusion protein (aa 1-

245 of PAR-2) weakly interacted with Jab1 (lane 4), but a stronger interaction occurred with the PAR-2Δ(1-213)-GST fusion protein (aa 214-397 of PAR-2) and Jab1 (lane 5), which was comparable to that between the full-length PAR-2-GST fusion protein and Jab1 (lane 3). These results suggest that the intracellular loop 3 and C-tail of PAR-2 were mainly responsible for the interaction with Jab1. Several previous studies have revealed that the C-tail of PAR-2 contributes to receptor trafficking and receptor-induced signal transduction [138, 175]. Interestingly, our studies here demonstrated that the PAR-2 C-tail alone (aa 346-397 of PAR-2) weakly interacted with Jab1 (Fig. 3.3.1, lane 7). The interaction of PAR-2IL3-GST fusion protein (aa 243-311 of PAR-2) with Jab1 (Fig. 3.3.1, lane 6) was notably weaker than that between PAR-2Δ(1-213)-GST fusion protein and Jab1 (Fig. 3.3.1, lane 5), although it seemed to be stronger than that between PAR-2C-GST fusion protein and Jab1 (Fig. 3.3.1, lane 7). Taken together, our GST pull-down findings imply that PAR-2 interacts with Jab1 through several intracellular domains.

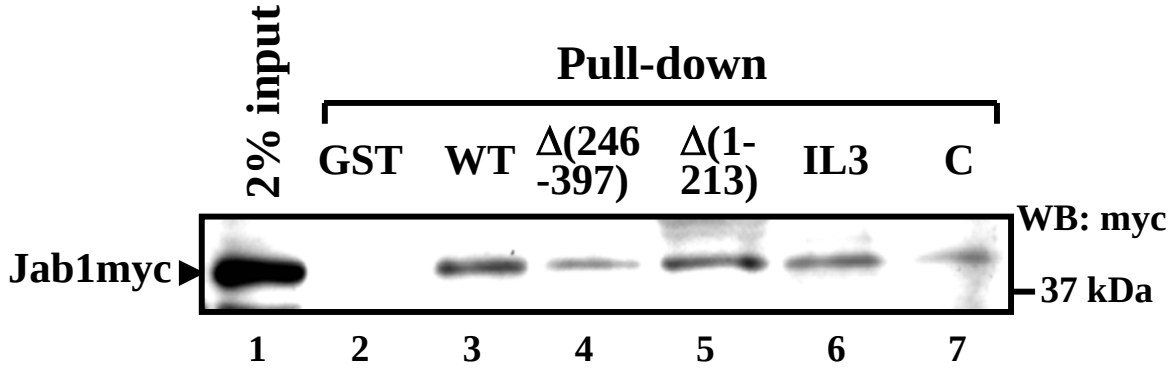

Fig. 3.3.1. Interaction of Jab1 with PAR-2 *in vitro*. The whole cell lysates from HEK293-Jab1myc cells were incubated overnight with GST protein alone or with full-length and truncated PAR-2-GST fusion proteins immobilized on glutathione beads followed by western blot analysis (WB) with the anti-myc antibody. Lysate shows 2% of HEK293-Jab1myc cell lysate used for the pull-down experiment. Experiments were repeated three times with similar results. The molecular mass marker is indicated on the right. WT, full-length PAR-2-GST; Δ(246-397), PAR-2Δ(246-397)-GST; Δ(1-213), PAR-2Δ(1-213)-GST; IL3, PAR-2IL3-GST; C, PAR-2C-GST.

3.3.2 Jab1 interacts with PAR-2 *in vivo*

To further determine whether Jab1 could interact with PAR-2 *in vivo*, we performed co-IP experiments. We generated a HEK293 cell line stably co-expressing PAR-2-HA and Jab1myc. Thus we had two different tags, the HA and the myc on the two proteins of interest. The whole cell lysates were immunoprecipitated by anti-HA antibody, and the interaction of PAR-2-HA with Jab1myc was examined by western blot analysis using the anti-myc

antibody. As shown in Fig. 3.3.2 A, Jab1 was specifically co-immunoprecipitated by PAR-2-HA in HEK293-PAR-2-HA+Jab1myc cells (lane 6), but not in the negative control wild-type HEK293 cells (lane 4) and HEK293-Jab1myc cells (lane 5). The same lysates from the respective cells which were used for the IP experiment, served as control for the western blot (lanes 1-3). The nitrocellulose membrane was reprobed with the anti-HA antibody to confirm the specificity of the co-immunoprecipitation of PAR-2-HA. These results suggest that Jab1 interacts with PAR-2 within cells.

We further asked whether interaction between endogenous Jab1 and native PAR-2 could occur. The western blot analysis using the anti-Jab1 antibody showed that endogenous Jab1 was specifically co-immunoprecipitated by anti-PAR-2 antibody from wild-type HEK293 cells (Fig. 3.3.2 B, lane 3), which are known to express endogenous PAR-2 [75], but not by the unrelated antibody against GST (Fig. 3.3.2 B, lane 2). The cell lysate for the IP experiment is shown in lane 1. The membrane reprobed with the anti-PAR-2 antibody confirmed the specificity of the co-immunoprecipitation of PAR-2 (data not shown). These data demonstrate that Jab1 interacts with PAR-2 *in vivo*.

Next, we tested whether Jab1 could be immunoprecipitated by PAR-2Δ(1-213)-HA *in vivo*. The whole cell lysates were immunoprecipitated by anti-HA antibody, and the interaction of PAR-2Δ(1-213)-HA with Jab1myc was examined by western blot analysis using the anti-myc antibody. As shown in Fig. 3.3.2 C, Jab1 specifically associated with PAR-2Δ(1-213)-HA in HEK293-PAR-2Δ(1-213)-HA+Jab1myc cells (lane 3), but not in the negative control wild-type HEK293 cells (lane 1) and HEK293-Jab1myc cells (lane 2). The same lysates from the respective cells which were taken for the IP experiment served as control (lanes 4-6). The membrane was reprobed with the anti-HA antibody to confirm the specificity of the co-immunoprecipitation of PAR-2Δ(1-213)-HA. These results confirm the GST pull-down data above in Figure 3.3.1 showing that Jab1 interacts with the intracellular loop 3 and the C-tail of PAR-2.

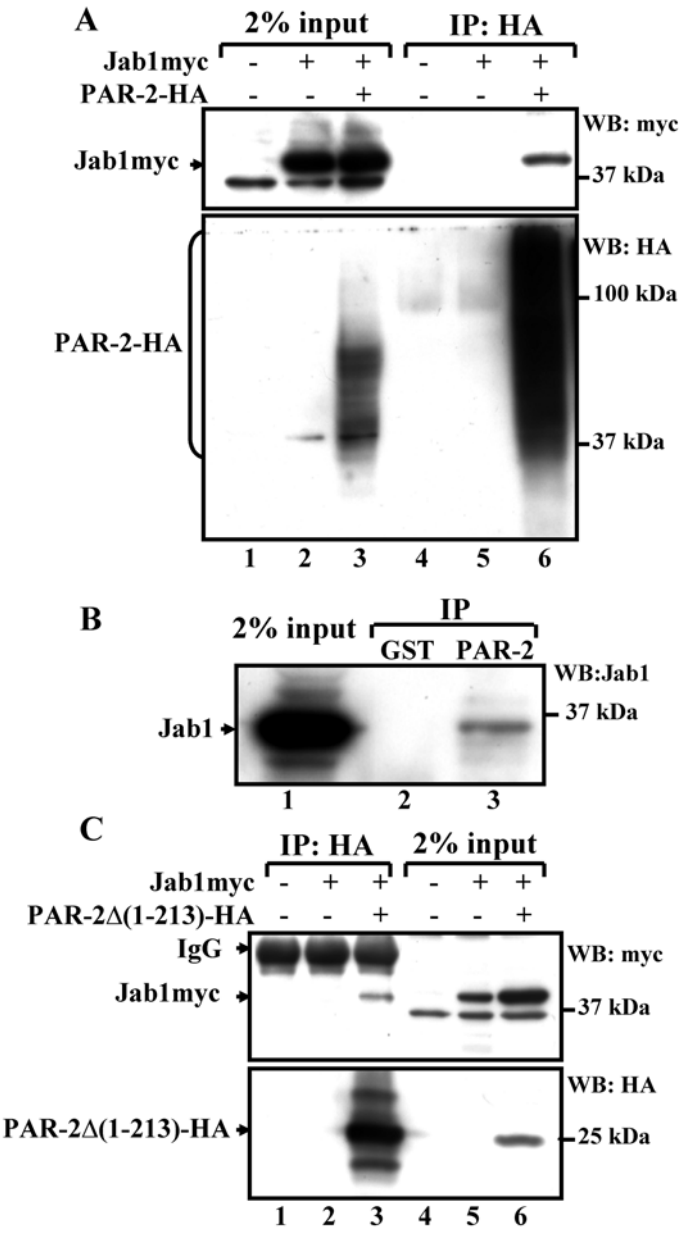

Fig. 3.3.2. Interaction of Jab1 with PAR-2 *in vivo*. (A). HEK293 cells were stably co-transfected with PAR-2-HA and Jab1myc or transfected with Jab1myc. The whole cell lysates from HEK293-PAR-2-HA+Jab1myc cells, as well as wild-type HEK293 cells (negative control) and HEK293-Jab1myc cells (negative control) were immunoprecipitated (IP) by anti-HA antibody in the presence of protein A Sepharose beads and the immunocomplex was detected by western blot (WB) using the anti-myc antibody. The immunoprecipitation was further confirmed by reprobing with the anti-HA antibody. (B). The whole cell lysates from wild-type HEK293 cells were immunoprecipitated by anti-PAR-2 (C-17) antibody or by the unrelated antibody against GST (negative control) in the presence of protein G agarose beads and the immunocomplex was detected by WB with the anti-Jab1 antibody. (C). HEK293 cells were stably co-transfected with PAR-2Δ(1-213)-HA and Jab1myc or transfected with Jab1myc. The whole cell lysates from HEK293-PAR-2Δ(1-213)-HA+Jab1myc cells, as well as wild-type HEK293 cells (negative control) and HEK293-Jab1myc cells (negative control) were immunoprecipitated by anti-HA antibody in the presence of protein A Sepharose beads and the immunocomplex was detected by WB using the anti-myc antibody. The immunoprecipitation was further confirmed by reprobing with the anti-HA antibody. All experiments were repeated at least three times with identical results. The molecular mass marker is indicated on the right. Note: Lower bands in the myc blot are unspecific staining by the myc antibody.

3.3.3 Colocalization of Jab1 with PAR-2 *in vivo*

We next examined whether the interaction of Jab1 with PAR-2 is reflected by colocalization of the two proteins *in vivo* using double immunofluorescence staining. HEK293 cells were transiently co-transfected with pEAK10-PAR-2-HA and pcDNA-Jab1myc plasmids. 24 h after transfection, Jab1myc was shown to be diffusely distributed in the cytosol and in the nucleus, and was also detected at the plasma membrane (Fig. 3.3.3 A, left top panel). PAR-2-HA, on the other side, was predominantly localized at the plasma membrane and in intracellular stores (Fig. 3.3.3 A, middle top panel), where it colocalized with Jab1myc, as given by the merge in the right top panel of Figure 3.3.3 A. In parallel, we co-stained wild-type HEK293 cells as negative control (Fig. 3.3.3 A, lower panels).

We further asked whether the endogenous Jab1 protein could colocalize with PAR-2-HA. As shown in Fig. 3.3.3 B, the endogenous Jab1 (left panel) was shown to have the same distribution pattern as the transfected protein (Fig. 3.3.3 A, left top panel). Endogenous Jab1 was clearly colocalized with PAR-2-HA at the plasma membrane and in intracellular stores in HEK293-PAR-2-HA cells (Fig. 3.3.3 B, right panel).

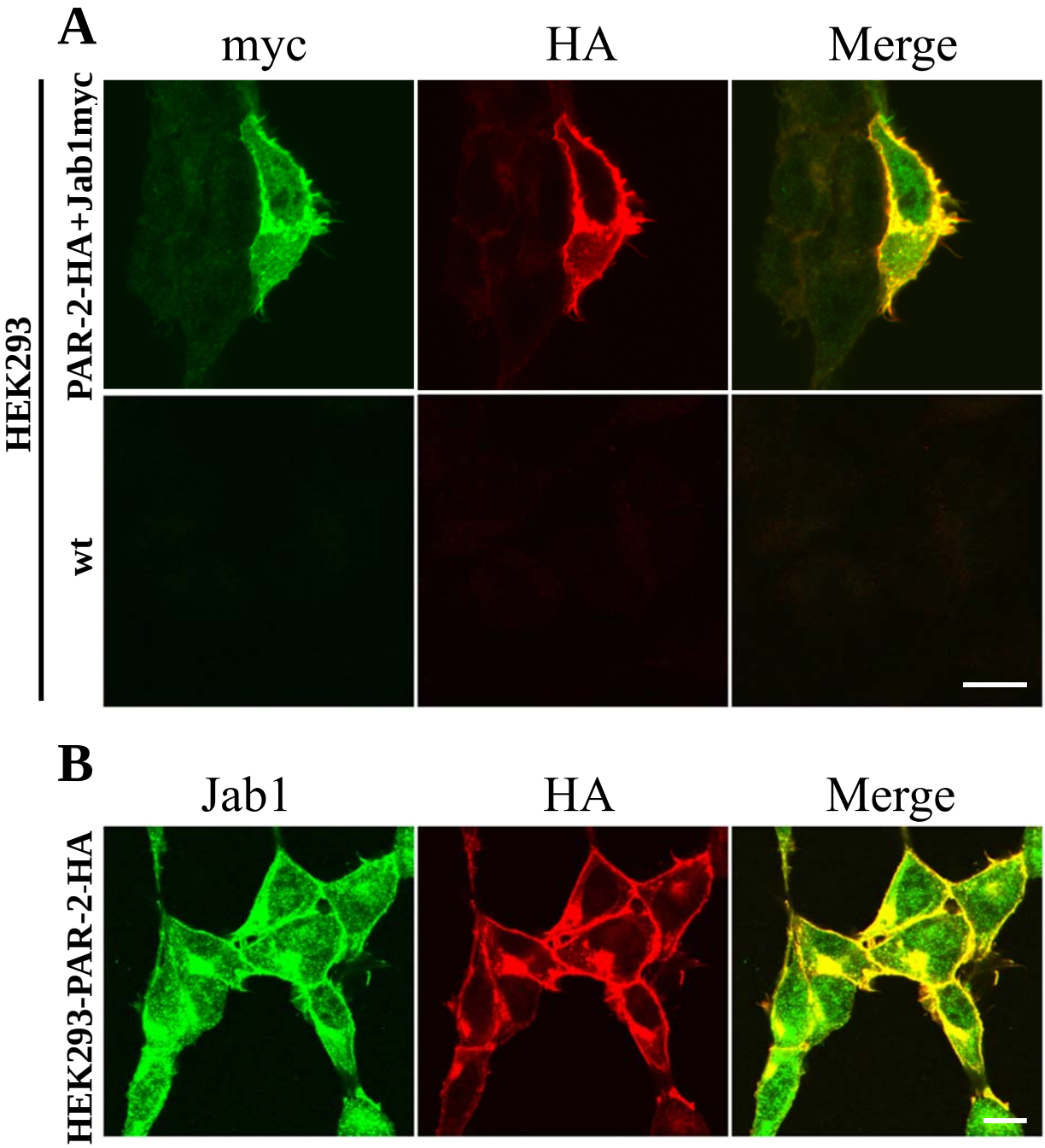

Fig. 3.3.3. Colocalization of Jab1 with PAR-2 *in vivo*. HEK293 cells transiently co-transfected with pEAK10-PAR-2-HA and pcDNA-Jab1myc plasmids (A, upper panel), wild-type HEK293 cells (A, lower panel, wt), and HEK293 cells stably transfected with pEAK10-PAR-2-HA plasmids (B) were fixed, permeabilized, stained, and observed by a confocal microscope. Jab1 (green) was visualized by monoclonal anti-myc antibody (A) or by monoclonal anti-Jab1 antibody (B) and Alexa Fluor 488 goat anti-mouse IgG. PAR-2-HA (red) was visualized by polyclonal anti-HA antibody and Alexa Fluor 568 goat anti-rabbit IgG (A, B). The overlay image (Merge, yellow) revealed the colocalization of Jab1 with PAR-2. Wild-type HEK293 cells served as negative control. All images are representative for three independent experiments. Scale bar, 10 μm.

3.3.4 Jab1 interacts with PAR-2 in normal primary human astrocytes

We asked to test the interaction of PAR-2 with Jab1 in neural cells. Normal human astrocytes (NHA) were chosen as cell model here, because astrocytes represent a critical cell type in the brain and it has been shown that PARs mediate important functions in astrocytes [13, 108, 111]. Data from RT-PCR shown in Fig. 3.3.4 A demonstrated that NHA cells abundantly express PAR-1 (lane 3) and PAR-2 (lane 4), and to a lower extent PAR-3 (lane 5), but not PAR-4 (lane 6). Glyceraldehyde-3-phosphate dehydrogenase (GAPDH) served as an internal control (lane 2, Fig. 3.3.4 A) To assure that NHA cells functionally express PAR-2, we measured $[Ca^{2+}]_i$ in response to PAR-2 agonists trypsin or PAR-2 AP. As shown in Fig. 3.3.4 B and C, both trypsin (100 nM) and PAR-2 AP (100 μM) induced a transient $[Ca^{2+}]_i$ rise, which rapidly declined to the basal level. These results indicate that PAR-2 is functionally expressed in normal primary human astrocytes.

Next, we performed the immunoprecipitation experiment to detect the interaction of Jab1 with PAR-2 in NHA cells. The astrocyte lysates were immunoprecipitated by anti-PAR-2 antibody in the presence of protein G agarose beads. The subsequent western blot analysis (Fig. 3.3.5 A) using the anti-Jab1 antibody demonstrated that Jab1 was specifically immunoprecipitated by anti-PAR-2 antibody (lane 2), but not by the antibody against GST (lane 3), indicating that Jab1 associates with PAR-2 in normal primary human astrocytes. The membrane reprobed with the anti-PAR-2 antibody confirmed the specificity of the co-immunoprecipitation of PAR-2 (data not shown).

We further studied the colocalization of Jab1 with PAR-2 in NHA cells. NHA cells were transiently transfected with pEAK10-PAR-2-HA plasmids. At 24 h after transfection, cells were stained to detect the Jab1 and PAR-2-HA proteins by double immunofluorescence staining. As shown in Fig. 3.3.5 B, Jab1 was mainly localized in the cytosol, as well as at the plasma membrane in NHA cells (left panel). PAR-2-HA, on the other side, was predominantly localized at the plasma membrane (middle panel), where it colocalized with Jab1, as shown by the merge in the right panel of Figure 3.3.5 B. Therefore, these data demonstrate that PAR-2 interacts with Jab1 in normal primary human astrocytes.

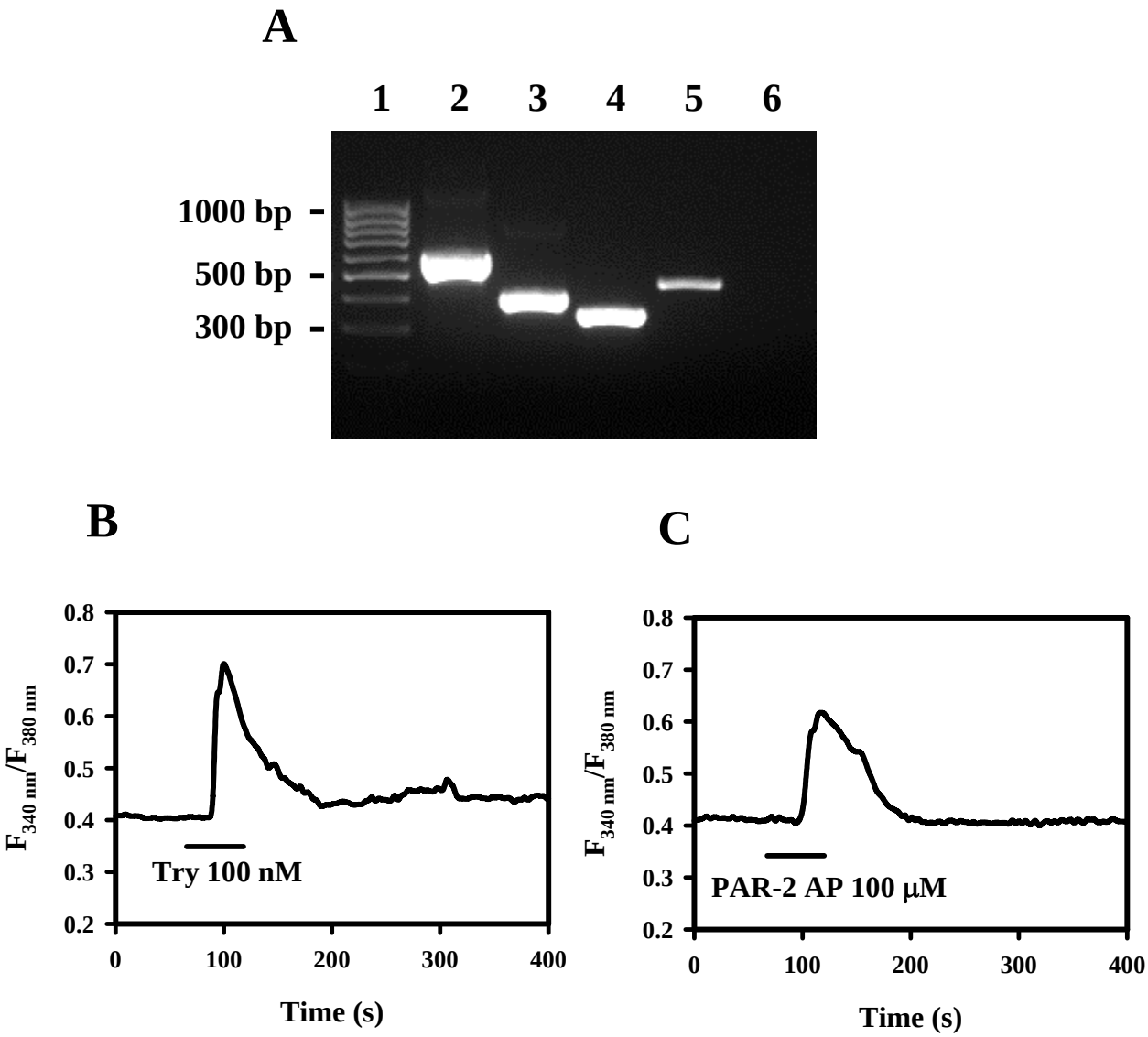

Fig. 3.3.4. The functional expression of PAR-2 in normal primary human astrocytes (NHA). (A). Determination of four types of PAR mRNA by RT-PCR in NHA cells. Fragments were amplified by RT-PCR with specific primers, separated on 2% agarose gel, and stained with ethidium bromide. PAR-1 (415 bp, lane 3), PAR-2 (341 bp, lane 4) and PAR-3 (452 bp, lane 5) mRNAs but no PAR-4 (424 bp, lane 6) mRNA, are detected in astrocytes. GAPDH (600 bp, lane 2) served as an internal control. Lane 1 represents 100-bp DNA standard. Data are representative of three independent experiments. (B-C) Determination of functional expression of PAR-2 by calcium measurements in NHA cells. Cells were loaded with Fura-2 AM to measure the changes of the intracellular free calcium concentration indicated by the change in the fluorescence ratio ($F_{340\ nm}$ /$F_{380\ nm}$). The time periods of application of 100 nM trypsin (B) and 100 μM PAR-2 AP (C) are indicated by the respective bars. The traces are the mean responses from at least 10 single cells measured in a single experiment. Experiments were repeated three times with comparable data.

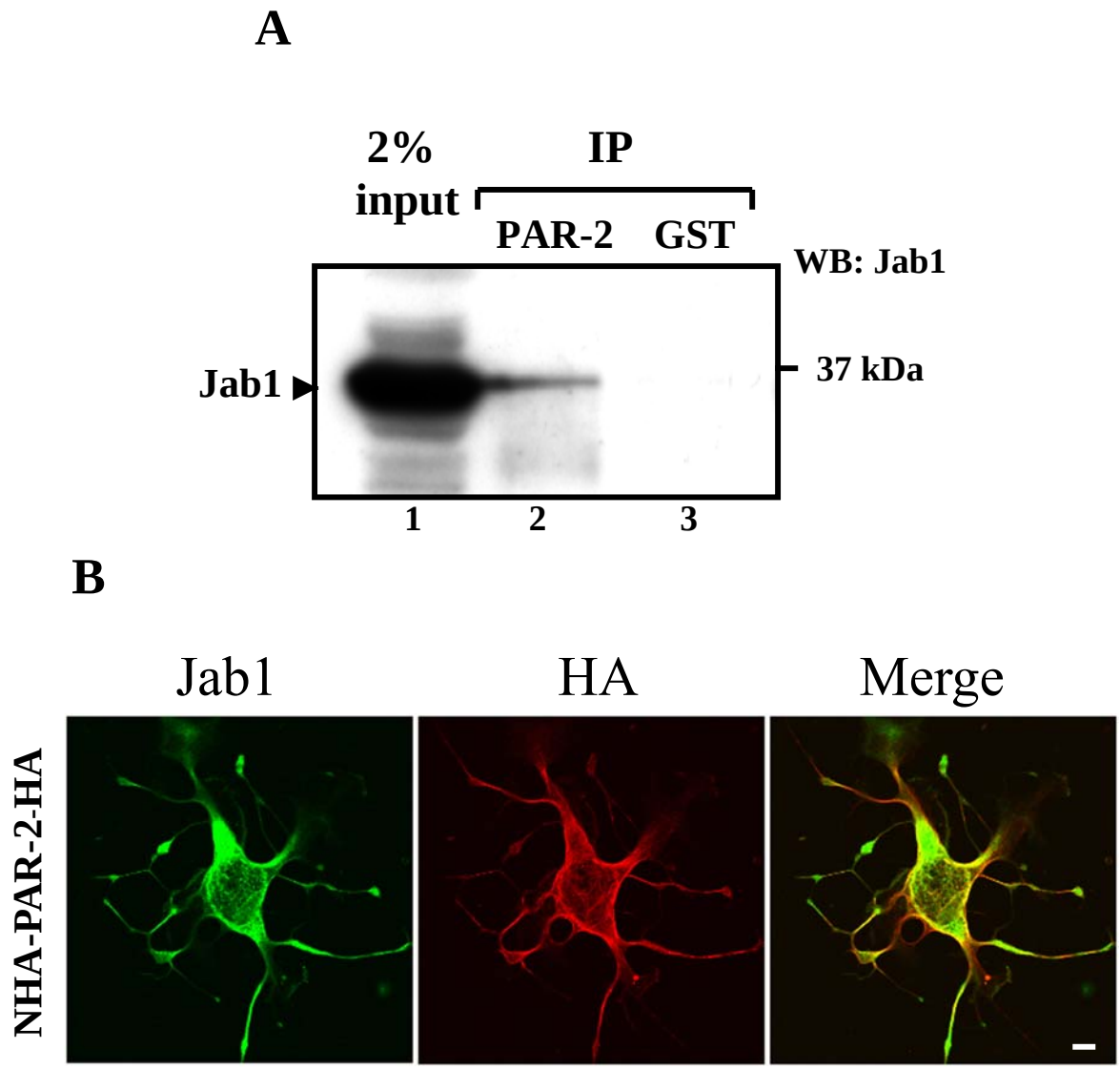

Fig. 3.3.5. The interaction of Jab1 with PAR-2 in normal primary human astrocytes. (A). The whole cell lysates from normal primary human astrocytes were immunoprecipitated (IP) by anti-PAR-2 (C-17) antibody or by the unrelated antibody against GST (negative control) in the presence of protein G agarose beads and the immunocomplex was detected by western blot (WB) with the anti-Jab1 antibody. Typical blot from three independent experiments is given. The molecular mass marker is indicated on the right. (B) Primary human astrocytes (NHA) were transiently transfected with pEAK10-PAR-2-HA plasmids. 24 h after transfection, cells were fixed, permeabilized, stained, and observed by a confocal microscope. Jab1 (green) was visualized by monoclonal anti-Jab1 antibody and Alexa Fluor 488 goat anti-mouse IgG. PAR-2-HA (red) was visualized by polyclonal anti-HA antibody and Alexa Fluor 568 goat anti-rabbit IgG. The overlay image (Merge, yellow) revealed the colocalization of Jab1 with PAR-2. All images are representative for three independent experiments. Scale bar, 10 μm.

3.3.5 PAR-2 activation reduces interaction with Jab1

To evaluate whether activation of PAR-2 affects the interaction with Jab1, HEK293-PAR-2-HA+Jab1myc cells were treated with 100 nM trypsin for 2 and 30 min in serum-free medium. The whole cell lysates were immunoprecipitated by anti-HA antibody, and the immunocomplex was detected by western blot analysis using the anti-myc antibody. As shown in Fig. 3.3.6 A, the co-immunoprecipitation of Jab1 was slightly reduced at 2 min stimulation, compared to that in unstimulated cells (0 min). However, very little Jab1 protein was co-immunoprecipitated by PAR-2-HA at 30 min after stimulation, indicating that the interaction of Jab1 with PAR-2 was disrupted. The membrane reprobed with HA antibody revealed the specificity of the co-immunoprecipitation. To rule out any unspecific proteolytic activity of trypsin and to determine the specific activation of PAR-2, we treated the cells with the specific PAR-2 peptide agonist PAR-2 AP (100 μM), which has been shown to specifically activate PAR-2 [17]. PAR-2 activation by PAR-2 AP similarly reduced the interaction between Jab1 and PAR-2 at 2 min and abolished it at 30 min after stimulation (Fig. 3.3.6 B). The time course was similar to that observed with trypsin stimulation (Fig. 3.3.6 A). These data obviously demonstrate that PAR-2 interacts with Jab1 in an agonist-dependent manner.

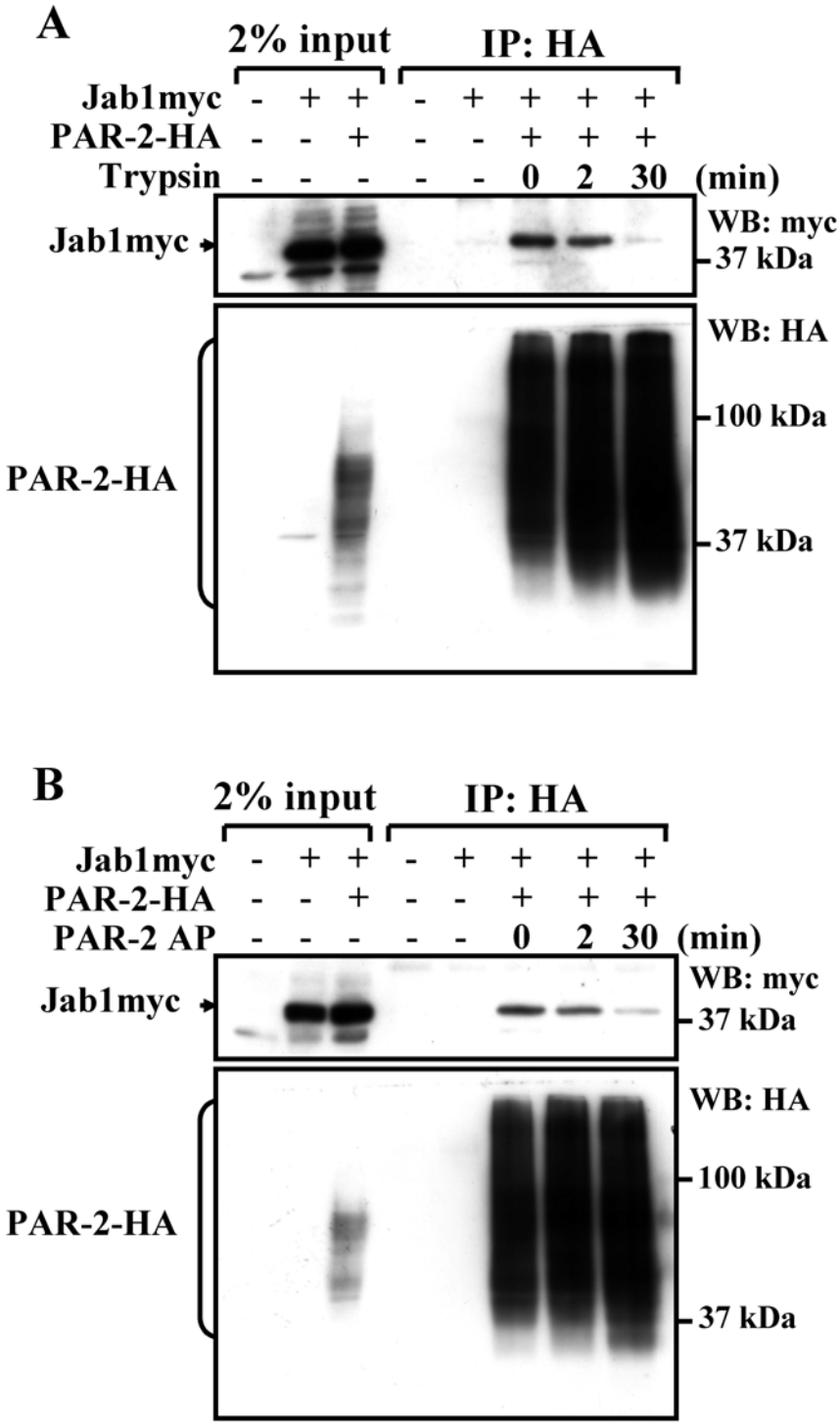

Fig. 3.3.6. Agonist-dependent dynamic interaction of Jab1 with PAR-2. HEK293-PAR-2-HA+Jab1myc cells were treated with 100 nM trypsin (A) or 100 μM PAR-2 AP (B) for 0, 2 and 30 min in serum-free medium. The whole cell lysates from HEK293-PAR-2-HA+Jab1myc cells, as well as wild-type HEK293 cells (negative control) and HEK293-Jab1myc cells (negative control) were immunoprecipitated (IP) by anti-HA antibody in the presence of protein A Sepharose beads, and the immunocomplex was detected by western blot (WB) using the anti-myc antibody. The immunoprecipitation was further confirmed by reprobing with the anti-HA antibody. Experiments were repeated at least three times with comparable results. The molecular mass marker is indicated on the right. Note: Lower bands in the myc blot are unspecific staining by the myc antibody.

The activated PAR-2 is rapidly internalized, and predominantly sorted into lysosomes for degradation [132]. To clarify whether the reduction of the interaction between Jab1 and PAR-2 results from protein dissociation or from PAR-2 degradation, we pretreated HEK293-PAR-2-HA+Jab1myc cells for 30 min with the lysosomal protease inhibitor ZPAD (100 μM) [150] followed by 100 μM PAR-2 AP stimulation for another 30 min. As shown in Fig. 3.3.7 A, also in this case PAR-2 AP stimulation significantly reduced the interaction of PAR-2 with Jab1. However, ZPAD did not block the reduction of the interaction induced by PAR-2 activation. The data summarized in Fig. 3.3.7 B demonstrate that activation of PAR-2 induced a 64±2% loss of interaction of PAR-2 with Jab1 at 30 min after PAR-2 AP stimulation ($p < 0.001$), and ZPAD had no significant effect on this reduction ($p > 0.05$). The inhibitory effect of ZPAD was confirmed, as shown in Fig. 3.3.7 C. Long-term stimulation (3 h and 5 h) by PAR-2 AP time-dependently led to PAR-2 degradation in the presence of the protein synthesis inhibitor cycloheximide (70 μM). This apparently was prevented by the lysosomal protease inhibitor ZPAD (100 μM). These results indicate that protein dissociation, but not PAR-2 degradation, leads to a loss of the interaction at 30 min after PAR-2 activation.

On the other side, we treated cells for 15 min with the inhibitor of receptor endocytosis PAO (80 μM) [132] prior to PAR-2 AP stimulation. Interestingly, PAO partially inhibited the PAR-2-induced reduction of the interaction at 30 min (Fig, 3.3.7 D). The summarized data demonstrate that activation of PAR-2 led to only 33±3% loss of interaction of PAR-2 with Jab1 after the pretreatment with PAO, and the reduction of the interaction was much less than that induced by PAR-2 AP alone ($p < 0.001$, Fig, 3.3.7 E). Therefore, the dynamic interaction between PAR-2 and Jab1 is dependent on agonist stimulation and receptor endocytosis.

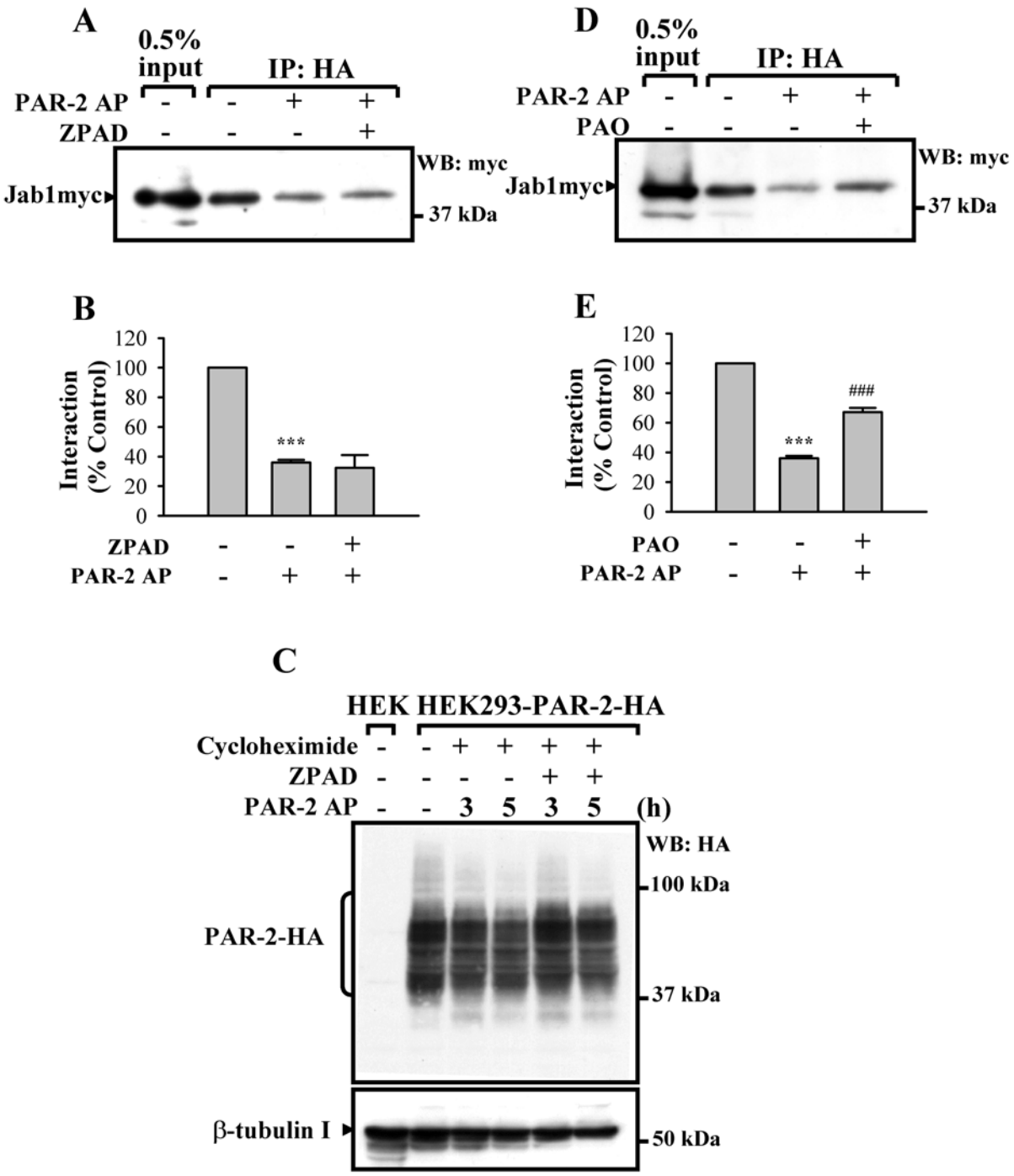

Fig. 3.3.7. Agonist-dependent reduction of interaction is prevented by the inhibitor of receptor endocytosis PAO, but not by lysosomal protease inhibitor ZPAD. HEK293-PAR-2-HA+Jab1myc cells were preincubated with 100 μM ZPAD for 30 min (A) or with 80 μM PAO for 15 min (D) prior to a 30 min-PAR-2 AP stimulation (100 μM). The whole cell lysates were immunoprecipitated (IP) by anti-HA antibody in the presence of protein A Sepharose beads, and the immunocomplex was detected by western blot (WB) using the anti-myc antibody. (A and D). Representative blots from three independent experiments. The molecular mass marker is indicated on the right. (B and E). The signal for the interaction was quantitated by analyzing the density by Quantity One software (Bio-Rad), and values were normalized to that in control cells. Mean ± SEM, $^{***}p < 0.001$, compared to control; $^{###}p < 0.001$, compared to PAR-2 AP stimulation alone. (C). The inhibitory effect of ZPAD on PAR-2 degradation. HEK293-PAR-2-HA cells were preincubated with cycloheximide (70 μM) alone or together with ZPAD (100 μM) for 30 min, followed by PAR-2 AP stimulation for 3 h and 5 h. PAR-2-HA expression was determined by western blot analysis. Representative blots from three independent experiments are given. β-tubulin I detection served as loading control. HEK, wild-type HEK293 cells. The molecular mass marker is indicated on the right.

3.3.6 The effect of PAR-2 activation on Jab1 distribution and expression

We further studied the effect of PAR-2 activation on the distribution of endogenous Jab1 in HEK293-PAR-2-HA cells by immunofluorescence staining. As shown in Fig. 3.3.8, the endogenous Jab1 was localized in the cytosol and nucleus, as well as at the plasma membrane in unstimulated cells. After 10 min incubation with 100 nM trypsin or with 100 μM PAR-2 AP, Jab1 was detected beneath the plasma membrane. After 30 min, Jab1 was accumulated in the cytosol and was not detected at the plasma membrane. Therefore, activation of PAR-2 induces the rapid redistribution of endogenous Jab1.

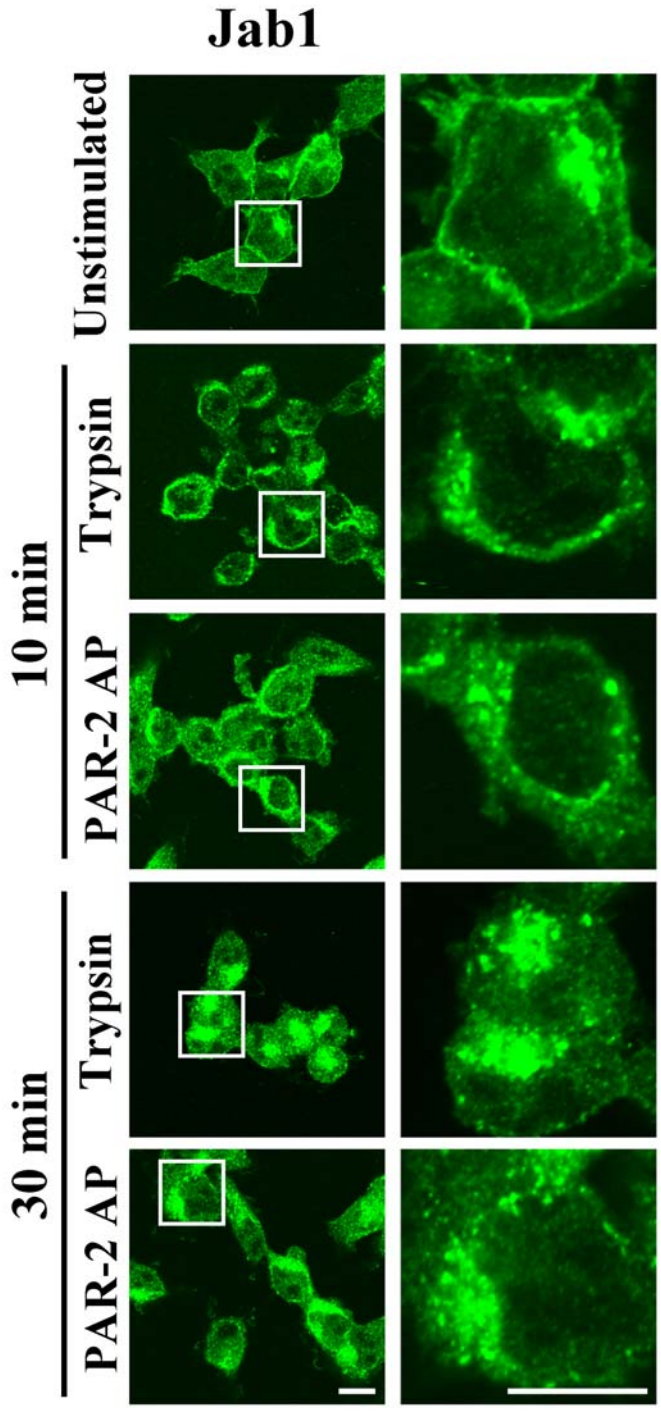

Fig. 3.3.8. The effect of PAR-2 agonists on the distribution of endogenous Jab1 in HEK293-PAR-2-HA cells. HEK293-PAR-2-HA cells were treated with 100 nM trypsin or with 100 μM PAR-2 AP for 0, 10 and 30 min in serum-free medium. The endogenous Jab1 was stained using the monoclonal antibody against Jab1, and visualized with the Alexa Fluor 488 goat anti-mouse IgG by a confocal microscope. Areas marked by a square are enlarged and shown on the right. The endogenous Jab1 was translocated to beneath the plasma membrane at 10 min after PAR-2 agonist treatment, and was redistributed to the cytosol at 30 min. All images are representative for three independent experiments. Scale bar, 10 μm.

We also examined whether Jab1 expression was upregulated by PAR-2 activation. HEK293-Jab1myc cells were treated with 100 nM trypsin for 0-120 min in serum-free medium. Western blot analysis using the anti-Jab1 antibody demonstrated that the transfected (upper bands) and endogenous (lower bands) Jab1 expression are both not influenced by PAR-2 activation. The membrane was reprobed with β-tubulin I to confirm the comparable loading for all lanes (Fig. 3.3.9).

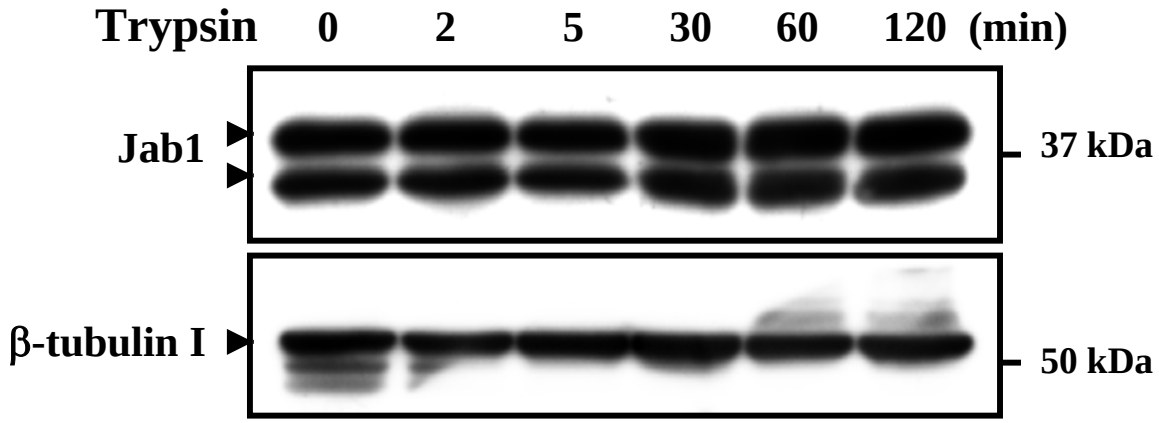

Fig. 3.3.9. The effect of trypsin on Jab1 expression in HEK293-Jab1myc cells. HEK293-Jab1myc cells were treated with 100 nM trypsin for 0-2 h in serum-free medium. Western blot analysis showed that trypsin stimulation did not influence the Jab1 expression in HEK293-Jab1myc cells. The upper bands represent the transfected Jab1myc protein, whereas the lower bands represent the endogenous Jab1 protein. β-tubulin I served as loading control. Experiments were repeated three times with identical results. The molecular mass marker is indicated on the right.

3.3.7 Jab1 mediates PAR-2-induced c-Jun activation

Because Jab1 is known as a coactivator of c-Jun [167], here we studied whether activation of PAR-2 increases endogenous c-Jun phosphorylation in HEK293-Jab1myc cells. HEK293-Jab1myc cells and wild-type HEK293 cells were rinsed with Hank's solution, and treated with 100 μM PAR-2 AP for 0-2 h in serum-free medium. As shown in Fig. 3.3.10 A and B, PAR-2 AP stimulation time-dependently increased c-Jun phosphorylation in HEK293-Jab1myc cells. The peak was obtained at 5 min, then the phosphorylation decreased gradually during 30 min. Further studies demonstrated that the increase in c-Jun phosphorylation induced by PAR-2 activation was significantly higher at 10 min in HEK293-Jab1myc cells than that in wild-type HEK293 cells ($p < 0.01$, Fig. 3.3.10 C), although c-Jun was also activated by PAR-2 AP at 10 min in wild-type HEK293 cells (Fig. 3.3.10 A and C).

Our recent observations demonstrated that activation of PAR-1 could significantly upregulate total c-Jun, besides c-Jun phosphorylation [110]. Therefore, here we investigated whether activation of PAR-2 could also regulate total c-Jun concentration via interaction with Jab1. As shown in Fig. 3.3.10 A, D and E, a similar pattern was observed. Total c-Jun was slightly increased in a time-dependent manner by PAR-2 AP (100 μM) stimulation in HEK293-Jab1myc cells, but not in wild-type HEK293 cells. Moreover, total c-Jun was significantly upregulated at 10 min upon PAR-2 activation in HEK293-Jab1myc cells, compared to that in wild-type HEK293 cells ($p < 0.05$). These results suggest that the interaction of PAR-2 with Jab1 results in activation of c-Jun.

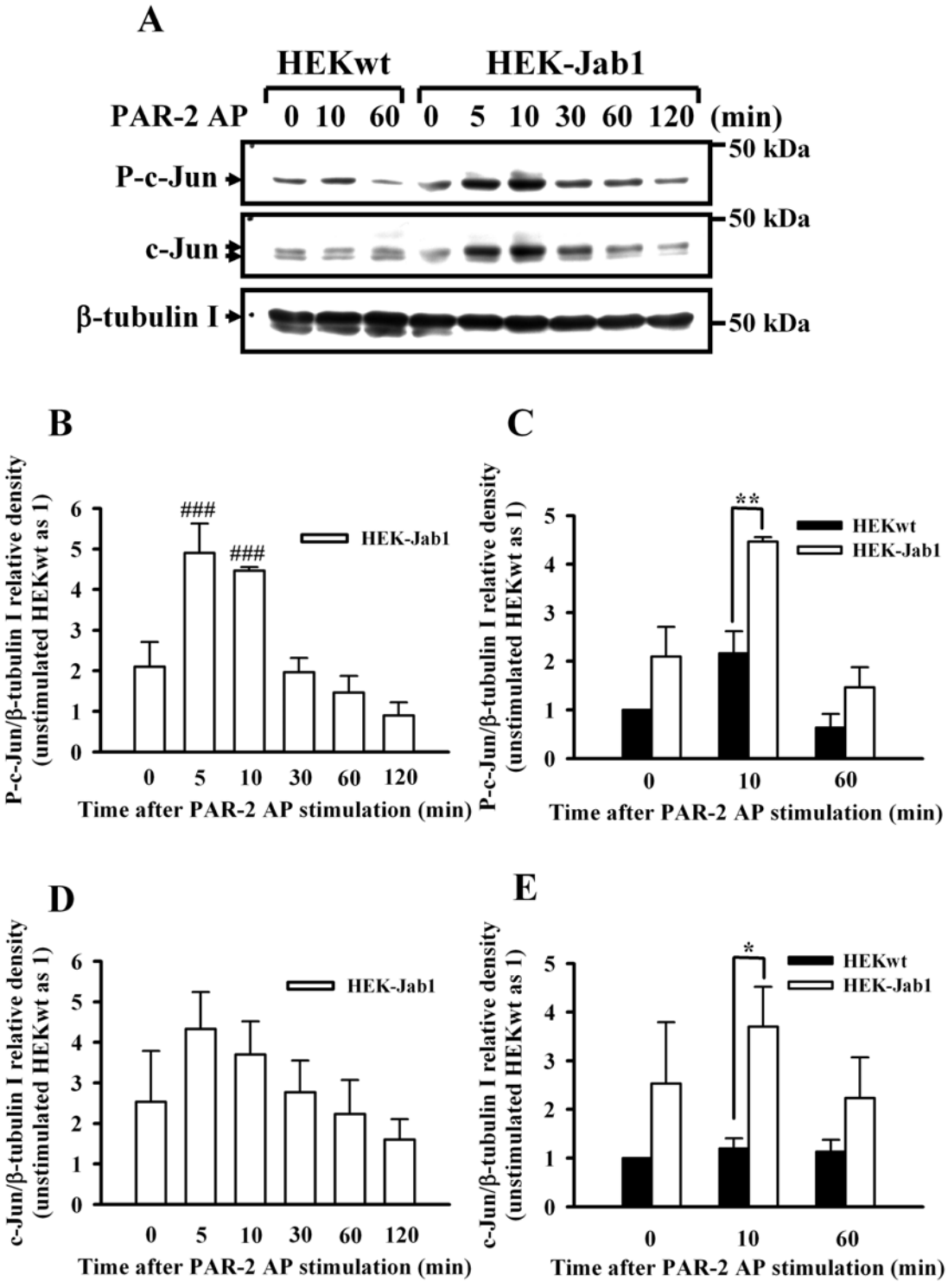

Fig. 3.3.10. Jab1 mediates PAR-2-induced c-Jun activation. Wild-type HEK293 cells (HEKwt) and HEK293-Jab1myc cells (HEK-Jab1) were treated with 100 μM PAR-2 AP for the indicated times in serum-free medium. The c-Jun phosphorylation was determined by western blot analysis. (A). Representative blots from three independent experiments. The molecular mass marker is indicated on the right. (B-E). Data from three independent experiments were quantitated by Quantity One software (Bio-Rad). Densities of phospho-c-Jun (P-c-Jun)/β-tubulin I and c-Jun/β-tubulin I were normalized to the unstimulated HEKwt cells. Mean ± SEM, $^{*}p < 0.05$; $^{**}p < 0.01$; $^{###}p < 0.001$, compared to unstimulated HEK-Jab1 cells. P-c-Jun and c-Jun were time-dependently increased upon 100 μM PAR-2 AP stimulation in HEK-Jab1 cells. Moreover, the increase was significant in HEK-Jab1 cells, compared to that in HEKwt cells at 10 min after PAR-2 AP stimulation. β-tubulin I served as loading control.

3.3.8 Jab1 potentiates PAR-2-induced AP-1 activation

The activated c-Jun translocates into the nucleus, and interacts with Fos and other Jun proteins to generate a dimer called the AP-1 complex. This AP-1 complex binds to a conserved DNA motif to regulate gene transcription and expression [115]. Therefore, here we studied whether activation of PAR-2 further regulated AP-1 activity via interaction with Jab1, by using an AP-1-driven CAT reporter gene. HEK293-Jab1myc cells and wild-type HEK293 cells were transiently transfected with pBL AP-1-CAT2 plasmids as well as the negative control pBL CAT2 plasmids. We treated these cells for 48 h with 100 μM PAR-2 AP at 6 h after transfection. The CAT activity in cell lysates was measured by CAT ELISA. As shown in Fig. 3.3.11, PAR-2 AP stimulation significantly increased the CAT activity by 36% in HEK293-Jab1myc cells ($p < 0.05$; middle columns in Fig. 3.3.11), indicating that activation of PAR-2 increased the AP-1 activity in HEK293-Jab1myc cells. The CAT activity itself was not influenced by PAR-2 activation which was shown in cells transfected with control pBL CAT2 plasmid ($p > 0.05$). However, activation of PAR-2 stimulated by PAR-2 AP did not induce AP-1 activation in wild-type HEK293 cells (left columns in Fig. 3.3.11). Therefore, these results suggest the existence of a physiological interaction between PAR-2 and Jab1. We then asked whether AP-1 activity could be further upregulated in HEK293-Jab1myc cells transfected with PAR-2. As shown in the right columns in Fig. 3.3.11, the PAR-2-induced AP-1 activity was dramatically enhanced by 93% in HEK293-PAR-2-HA+Jab1myc cells ($p < 0.001$). Taken together, these findings clearly demonstrate that Jab1 mediates PAR-2-induced activation of AP-1.

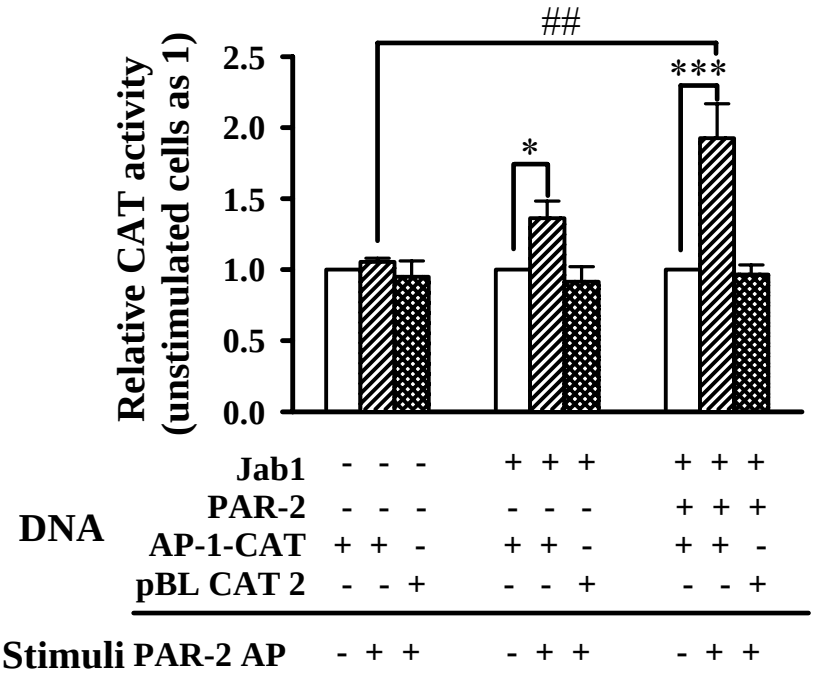

Fig. 3.3.11. Jab1 potentiates PAR-2-induced AP-1 activation. Wild-type HEK293 cells, HEK293-Jab1myc cells, and HEK293-PAR-2-HA+Jab1myc cells, all transiently transfected with either pBL AP-1-CAT2 plasmids or negative control pBL CAT2 plasmids, were treated with 100 μM PAR-2 AP for 48 h. The CAT activity in cell lysates was determined by CAT ELISA. The relative CAT activity was normalized to the unstimulated control. $^{*}p < 0.05$; $^{\#\#}p < 0.01$; $^{***}p < 0.001$. PAR-2 AP stimulation significantly increased the AP-1 activity in HEK293-Jab1myc cells. The AP-1 activity was further strongly enhanced in HEK293-PAR-2-HA+Jab1myc cells upon PAR-2 AP stimulation.

To further confirm the specific function of Jab1 in PAR-2-induced AP-1 activation, we knocked down the endogenous Jab1 using Jab1 siRNA. Transfection of Jab1 siRNA (100 nM) significantly reduced the endogenous Jab1 expression at both mRNA and protein levels in HEK293-PAR-2-HA cells (Fig. 3.3.12 A and B). Scrambled siRNA did not affect Jab1 expression (Fig. 12 A and B), confirming the specificity of Jab1 siRNA. Next, we transfected HEK293-PAR-2-HA cells with Jab1 siRNA, followed after 24 h by transfection with AP-1-driven CAT reporter plasmid. As shown in Fig. 3.3.12 C, activation of PAR-2 by PAR-2 AP significantly enhanced AP-1 activity by 67% in HEK293-PAR-2-HA cells. This stimulation was blocked by Jab1 siRNA, but not affected by scrambled siRNA transfection.

To determine the specificity of Jab1 in the PAR-2 signaling events, we stimulated HEK293-Jab1myc cells with the specific PAR-1 agonist TRag (10 μM) [74] to examine AP-1 activity. Activation of PAR-1 failed to increase the AP-1 activity in HEK293-Jab1myc cells (data not shown). These results suggest that Jab1 is specifically involved in PAR-2-induced activation of AP-1.

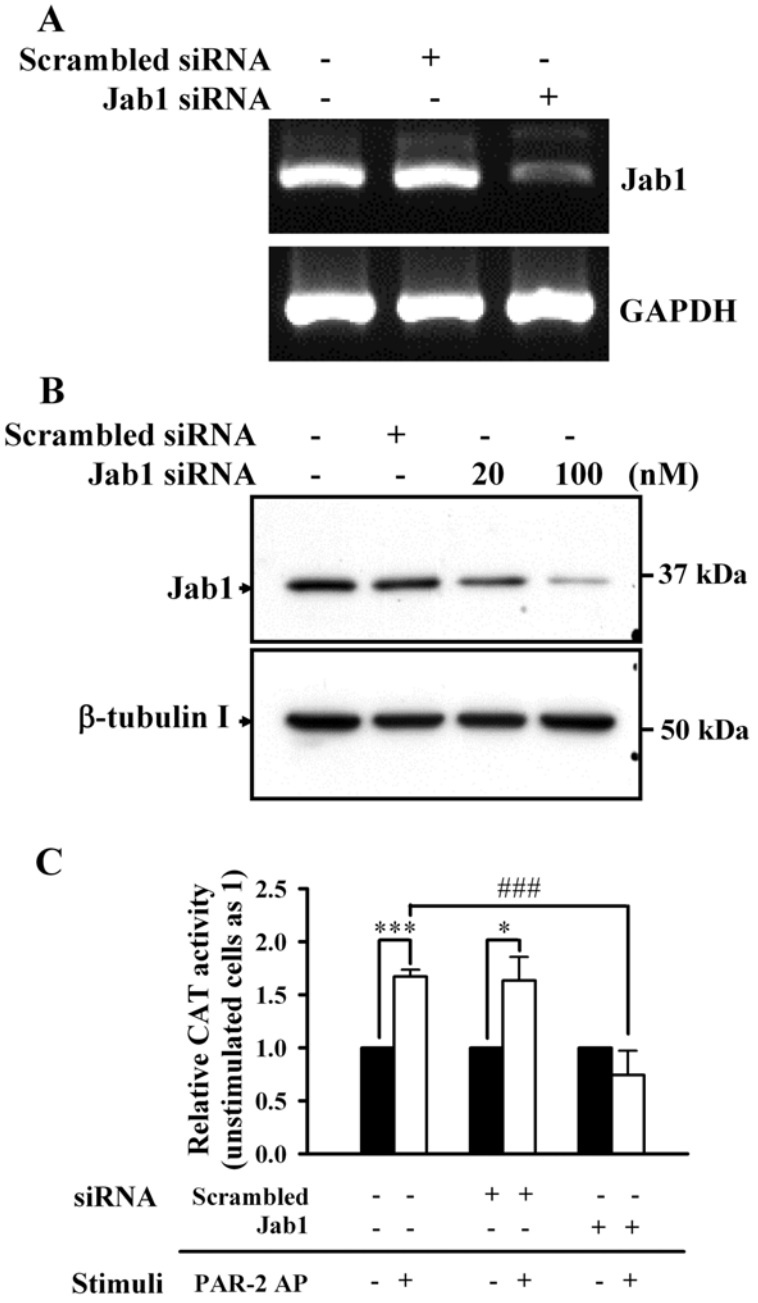

Fig. 3.3.12. Jab1 siRNA inhibits PAR-2-induced AP-1 activation. HEK293-PAR-2-HA cells were transfected with either scrambled siRNA (control siRNA) or Jab1 siRNA. At 48 h after transfection, Jab1 knockdown was determined by RT-PCR (A) and western blot analysis (B). Representative data from three independent experiments are given. GAPDH served as an internal control for PCR (A), and β-tubulin I served as loading control for western blot (B). The molecular mass marker is indicated on the right. (C). Blockade of AP-1 activation by Jab1 siRNA in HEK293-PAR-2-HA cells. Cells were transfected with either Jab1 siRNA (100 nM) or scrambled siRNA (100 nM), followed after 24 h by AP-1-driven CAT reporter plasmid transfection. Then cells were treated with PAR-2 AP (100 μM) for 48 h. The CAT activity in cell lysates was determined by CAT ELISA. The relative CAT activity was normalized to the unstimulated control. $^{*}p < 0.05$; $^{***}p < 0.001$; $^{###}p < 0.001$.

Part IV. p24A binds to the intracellular PAR-2, and might regulate resensitization of PAR-2.

The mammalian p24A was initially isolated from Golgi-derived coatomer-coated vesicles in CHO cells [176]. Human p24A was cloned later from a human brain cDNA library, by using the rat sequence as a probe [177]. Based on aa sequence homology, p24A belongs to coat protein (COP) I-coated vesicle membrane protein p24 family, which was supposed to act as cargo receptors and mediate protein trafficking between the ER and the Golgi apparatus and within the Golgi apparatus [176, 178-181].

p24A is a type I transmembrane protein, which was shown to localize in membranes of the intermediate compartment and the *cis*-Golgi network, with a large N-terminus at the Golgi lumen and a highly conserved short cytoplasmic tail at the cytosol (Fig. 3.4.1) [177, 181, 182]. The GOLD (Golgi dynamics) domain, which is found in several eukaryotic Golgi and lipid-traffic proteins, has been identified at the N-terminal lumen of p24A by computational sequence analysis [183], and is predicted to bind to cargo proteins. However, no specific cargo proteins have been demonstrated so far. The N-terminal lumen near the transmembrane domain contains the heptad repeats of hydrophobic residues suggestive of a capability to participate in coiled-coil interactions. This coiled-coil domain is likely to mediate the hetero- and homo-oligomeric complex formation within members of the p24 family [184, 185]. It has been shown that the cytoplasmic tail of p24A is able to bind to COPI and COPII subunits [179, 182, 186], ADP-ribosylation factor 1 (ARF1) [187], as well as Golgi matrix proteins [188]. Therefore, p24A might be involved in the vesicle biogenesis and subsequent cargo protein transport in the early secretory pathway [189].

Interestingly, data from the *Caenorhabditis elegans* demonstrate that loss-of-function of p24A regulates the transport to the cell surface of mutant LIN-12 and GLP-1 that would otherwise accumulate within cells, suggesting that p24A functions as quality control in the early secretory pathway, and then p24A might not mediate cargo protein sorting directly [190]. Similar results were also observed in yeast cells that lack all members of the p24 family [191]. p24 gene deletions do not cause a significant defect in protein transport in the early secretory pathway in yeast [191]. Therefore, the precise functions of p24A are still a puzzle.

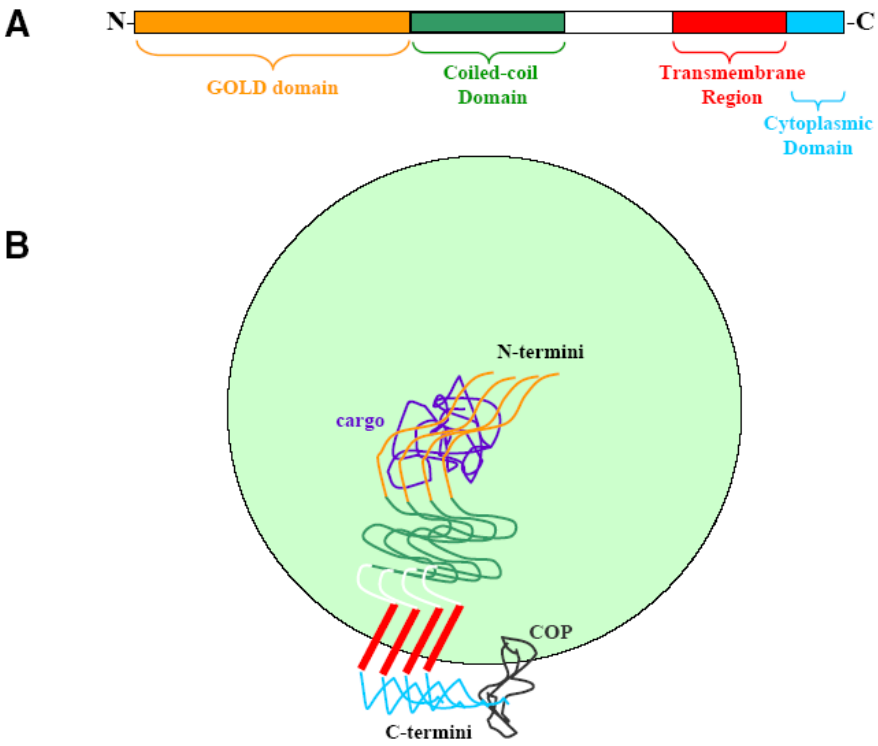

Fig. 3.4.1. Schematic representation of p24A domains and localization. (A). p24A has a GOLD domain (orange) and a coiled-coil domain (green) at the large N-terminus, a transmembrane domain (red), and a short C-terminal domain (blue). (B). p24A locates at membranes of the intermediate compartment and the *cis*-Golgi network. The oligomeric complex formation is mediated by the coiled-coil domain. The GOLD domain at the Golgi lumen is predicted to bind to cargo proteins; whereas the C-terminus that is exposed to the cytosol interacts with COPI and/or COPII (189).

3.4.1. PAR-2 interacts with p24A *in vitro*

To confirm the finding in yeast, we tested the interaction of PAR-2 with p24A by *in vitro* GST pull-down assays. HEK293-p24Amyc cell lysates were incubated overnight with either purified GST or purified PAR-2-GST fusion proteins bound on glutathione-Sepharose beads. Western blot analysis using the anti-myc antibody demonstrated that p24A specifically interacted with the full-length PAR-2-GST fusion protein (Fig. 3.4.2 A, lane 3), but not with GST alone (Fig. 3.4.2 A, lane 2). Subsequent experiments revealed that p24A also interacted with both PAR-2Δ(246-397)-GST (1- 245 aa of PAR-2, Fig. 3.4.2 A, lane 4) and PAR-2Δ(1-213)-GST (214-397 aa of PAR-2, Fig. 3.4.2 A, lane 5). Interestingly, their binding capacities were comparable to that of the full-length PAR-2-GST. Since p24A is an intracellular protein, it is generally thought that the intracellular loops and C-tail of the receptor would be required for the interaction. Therefore, we further tested the interaction of p24A with the intracellular loops and C-tail of PAR-2 in the GST pull-down assay. Interestingly, the intracellular loops and C-tail of PAR-2 failed to interact with p24A (Fig. 3.4.2 B). Instead, we found that the second extracellular loop of PAR-2 (EL2, 214-245 aa of PAR-2) strongly interacted with p24A (Fig. 3.4.2 C, lane 3).

Next, we generated a series of truncated p24A-GFP fusion proteins in HEK293 cells (Fig. 3.4.3 A), to map the domain of p24A that is responsible for the interaction with PAR-2. The wild-type and truncated p24A-GFP fusion proteins in HEK293 cell lysates were incubated overnight with the full-length PAR-2-GST immobilized on glutathione-Sepharose beads in the GST pull-down assay. Western blot analysis using the anti-GFP antibody demonstrated that deletion of the N-terminal lumen of p24A (ΔN) completely abolished the interaction with PAR-2-GST (Fig. 3.4.3 B, lane 8). However, C-terminal deletions (ΔC, Fig. 3.4.3 B, lane 9) and deletions of the transmembrane domain and C-terminal domain (ΔCT, Fig. 3.4.3 B, lane 10) both efficiently interacted with PAR-2-GST. GFP alone served as negative control (Fig. 3.4.3 B, lane 6). These data strongly suggest that the N-terminus of p24A is required for the interaction with PAR-2.

The GOLD domain located at the N-terminus of p24A is supposed to bind to cargo proteins [183]. Thus, we further tested whether the GOLD domain is involved in the interaction with PAR-2 in the GST pull-down assay. As expected, p24AΔGOLD-GFP (ΔG) failed to interact with PAR-2 (Fig. 3.4.3 C, lane 10), suggesting that the GOLD domain is required for the interaction with PAR-2. However, the single GOLD domain (G) only weakly bound to PAR-2 (Fig. 3.4.3 C, lane 8). Therefore, the GOLD domain is necessary, but not sufficient to interact with PAR-2. Further experiments indicated that p24AGL-GFP (GL)

which contains the GOLD domain and a neighboring linker indeed strongly interacted with PAR-2 (Fig. 3.4.3 C, lane 9). These results clearly demonstrate that p24AGL (residues 1-125) is responsible for the interaction with PAR-2.

Taken together, our data show that the N-terminal region of p24A (residues 1-125) specifically interacts with the second extracellular loop (EL2) of PAR-2.

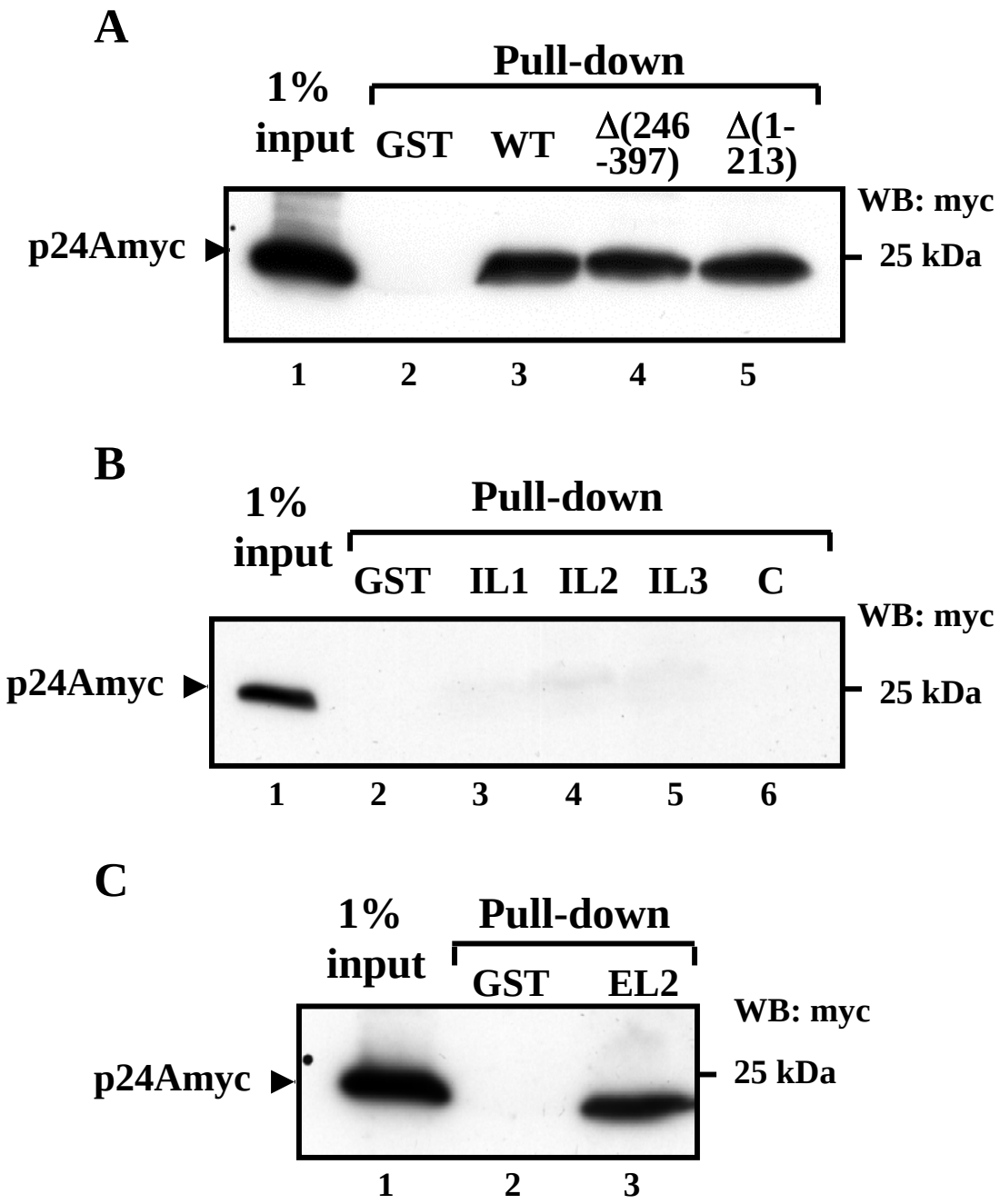

Fig. 3.4.2. Interaction of p24A with PAR-2 *in vitro*. The whole cell lysates from HEK293-p24Amyc cells were incubated overnight with GST protein alone or full-length and truncated PAR-2-GST fusion proteins immobilized on glutathione beads followed by western blot analysis (WB) with the anti-myc antibody. Experiments were repeated at least three times with similar results. The molecular mass marker is indicated on the right. WT, full-length PAR-2-GST; Δ(246-397), PAR-2Δ(246-397)-GST; Δ(1-213), PAR-2Δ(1-213)-GST; IL1, PAR-2IL1-GST; IL2, PAR-2IL2-GST; IL3, PAR-2IL3-GST; C, PAR-2C-GST; EL2, PAR-2EL2-GST.

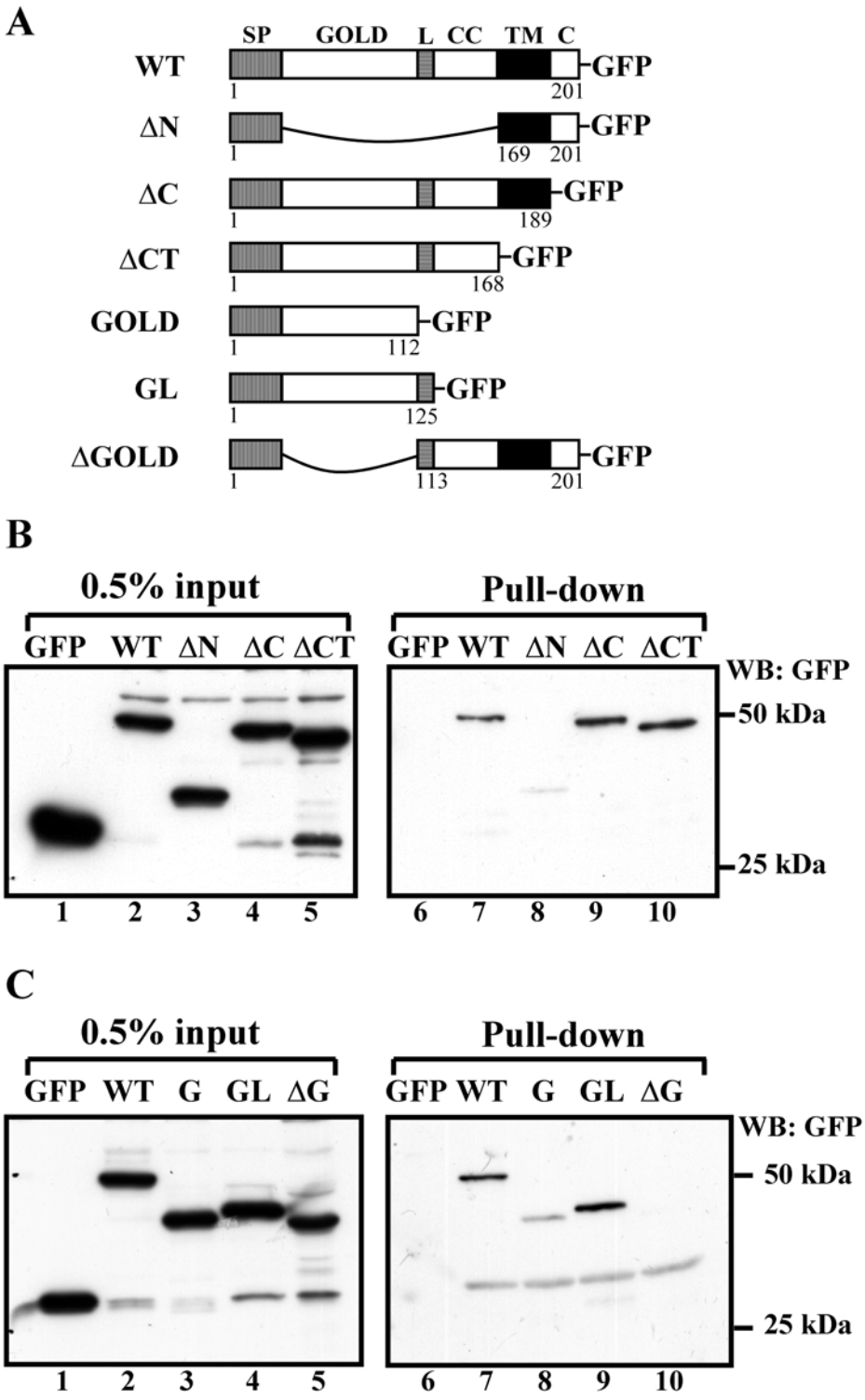

Fig. 3.4.3. Domains of p24A required for the interaction with PAR-2 *in vitro*. (A). Schematic representation of wild-type p24A-GFP (WT) and truncated p24A-GFP constructs. The position of amino acids of p24A is noted below constructs. SP, signal peptide. GOLD, GOLD domain. L, the linker between the GOLD domain and the coiled-coil domain. CC, coiled-coil domain. TM, transmembrane domain. C, C-tail. (B-C). The whole cell lysates from HEK293 cells transfected with different WT, truncated p24A-GFP or empty GFP plasmids were incubated overnight with the full-length PAR-2-GST fusion protein immobilized on glutathione beads followed by western blot analysis (WB) with the anti-GFP antibody. Experiments were repeated three times with identical results. The molecular mass marker is indicated on the right. ΔN, p24AΔN-GFP; ΔC, p24AΔC-GFP; ΔCT, p24AΔCT-GFP; G/GOLD, p24AGOLD-GFP; GL, p24AGL-GFP; ΔG/ΔGOLD, p24AΔGOLD-GFP.

3.4.2. PAR-2 interacts with p24A *in vivo*

We next performed the co-IP assay, to confirm the interaction of PAR-2 with p24A under physiological conditions. HEK293 cells co-expressing PAR-2-HA and p24Amyc were generated as cell model. The whole cell lysates were immunoprecipitated with anti-HA antibody, and the interaction of PAR-2-HA with p24Amyc was examined by western blot analysis using the anti-myc antibody. As shown in Fig. 3.4.4 A, p24A was specifically co-immunoprecipitated by PAR-2-HA in HEK293-PAR-2-HA+p24Amyc cells (lane 6), but not in the negative control wild-type HEK293 cells (lane 4) and HEK293-p24Amyc cells (lane 5). The same lysates from the respective cells which were used for the IP experiment, served as control for the western blot (Fig. 3.4.4 A, lanes 1-3). The nitrocellulose membrane was reprobed with the anti-HA antibody to confirm the specificity of the co-immunoprecipitation of PAR-2-HA. These results suggest that p24A interacts with PAR-2 within cells.

We found that p24A bound to PAR-2Δ(1-213)-GST in the GST pull-down assay (Fig. 3.4.2 A, lane 5). To further confirm this interaction *in vivo*, similar co-IP experiments were performed in HEK293-PAR-2Δ(1-213)-HA+p24Amyc cells. Western blot analysis using the anti-myc antibody demonstrated that p24A was also immunoprecipitated by anti-HA antibody in HEK293-PAR-2Δ(1-213)-HA+p24Amyc cells (Fig. 3.4.4 B, lane 6), but not in the negative control wild-type HEK293 cells (Fig. 3.4.4 B, lane 4) and HEK293-p24Amyc cells (Fig. 3.4.4 B, lane 5), suggesting that PAR-2Δ(1-213) was involved in the interaction with p24A within cells.

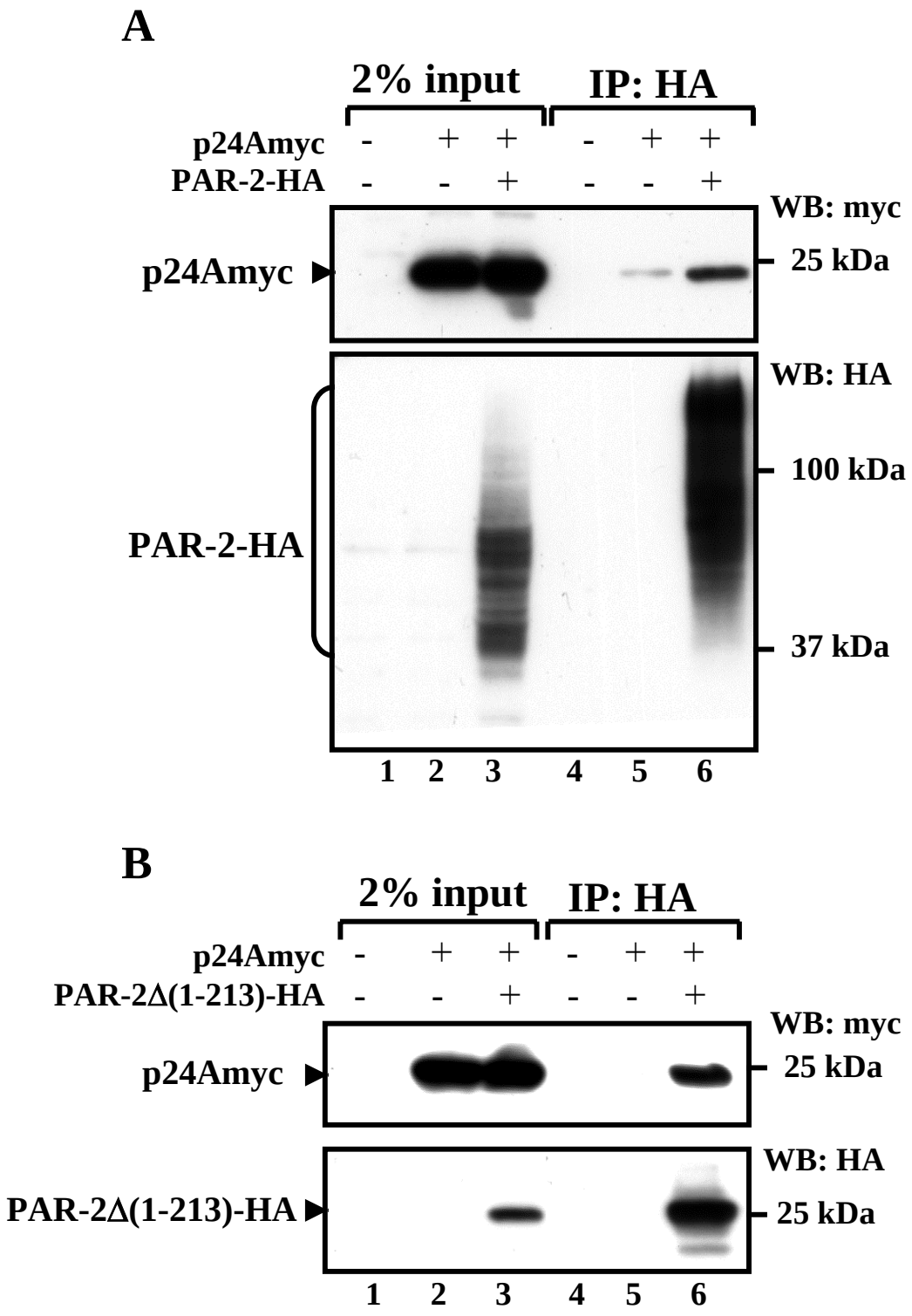

Fig. 3.4.4. Interaction of p24A with PAR-2 *in vivo*. The whole cell lysates from HEK293-PAR-2-HA+p24Amyc cells (A), or HEK293-PAR-2Δ(1-213)-HA+p24Amyc cells (B), together with wild-type HEK293 cells (negative control) and HEK293-p24Amyc cells (negative control) were immunoprecipitated (IP) by anti-HA antibody in the presence of protein A Sepharose beads and the immunocomplex was detected by western blot (WB) using the anti-myc antibody. The immunoprecipitation was further confirmed by reprobing with the anti-HA antibody. All experiments were repeated at least three times with identical results. The molecular mass marker is indicated on the right.

Next, we asked whether the interaction of PAR-2 with p24A could occur in a relevant physiological system and whether this interaction was species-specific. We performed immunoprecipitation experiments with anti-p24A antibody in rat primary astrocytes, and the interaction between PAR-2 and p24A was determined by western blot using anti-PAR-2 antibody. As shown in Fig. 3.4.5, the anti-p24A antibody strongly immunoprecipitated PAR-2 from rat astrocytes (lane 2), whereas the control antibody (IgG) did not (lane 1). Immunoprecipitation by anti-PAR-2 antibody from rat astrocyte lysates served as control (Fig. 3.4.5, lane 3). These results indicate that there is endogenous interaction between PAR-2 and p24A in the native system. Moreover, this interaction is not restricted to human proteins.

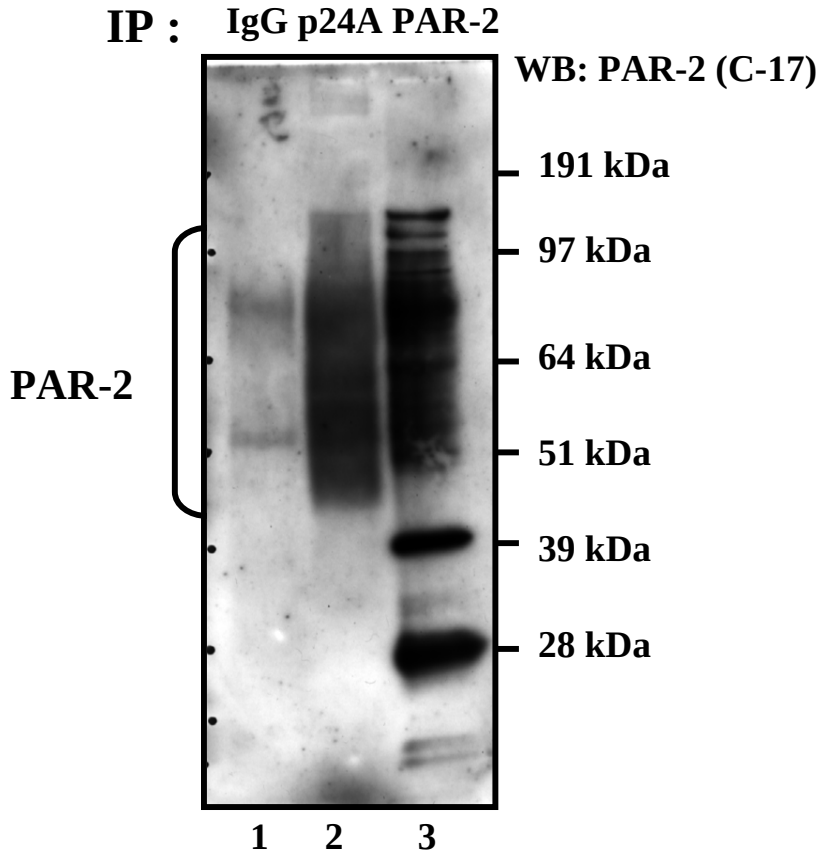

Fig. 3.4.5. The interaction of PAR-2 with p24A in rat primary astrocytes. The whole cell lysates from rat primary astrocytes were immunoprecipitated (IP) by the control antibody (IgG), or by anti-p24A antibody in the presence of protein G agarose beads, and the immunocomplex was detected by western blot (WB) with the anti-PAR-2 (C-17) antibody. Immunoprecipitation by anti-PAR-2 antibody from rat astrocyte lysates served as control. A typical blot from three independent experiments is given. The molecular mass marker is indicated on the right. Note: The lowest band in lane 3 is IgG.

3.4.3 Colocalization of PAR-2 with p24A *in vivo*

We next examined whether the interaction of p24A with PAR-2 is reflected by colocalization of the two proteins *in vivo* using double immunofluorescence staining. HEK293-PAR-2-HA+p24Amyc cells were stained with anti-HA antibody to detect PAR-2-HA and with anti-myc antibody to detect p24Amyc. As shown in Fig. 3.4.6 A, p24Amyc was distributed beneath the plasma membrane and mainly accumulated in the cytosol. On the other side, PAR-2-HA was predominantly localized at the plasma membrane and in intracellular stores in HEK293-PAR-2-HA+p24Amyc cells (Fig. 3.4.6 B). From the merge in Figure 3.4.6 C, we found that p24A predominantly colocalizes with the intracellular PAR-2, but not with the cell surface receptor in unstimulated cells. In parallel, we co-stained wild-type HEK293 cells as negative control (Fig. 3.4.6 D-F).

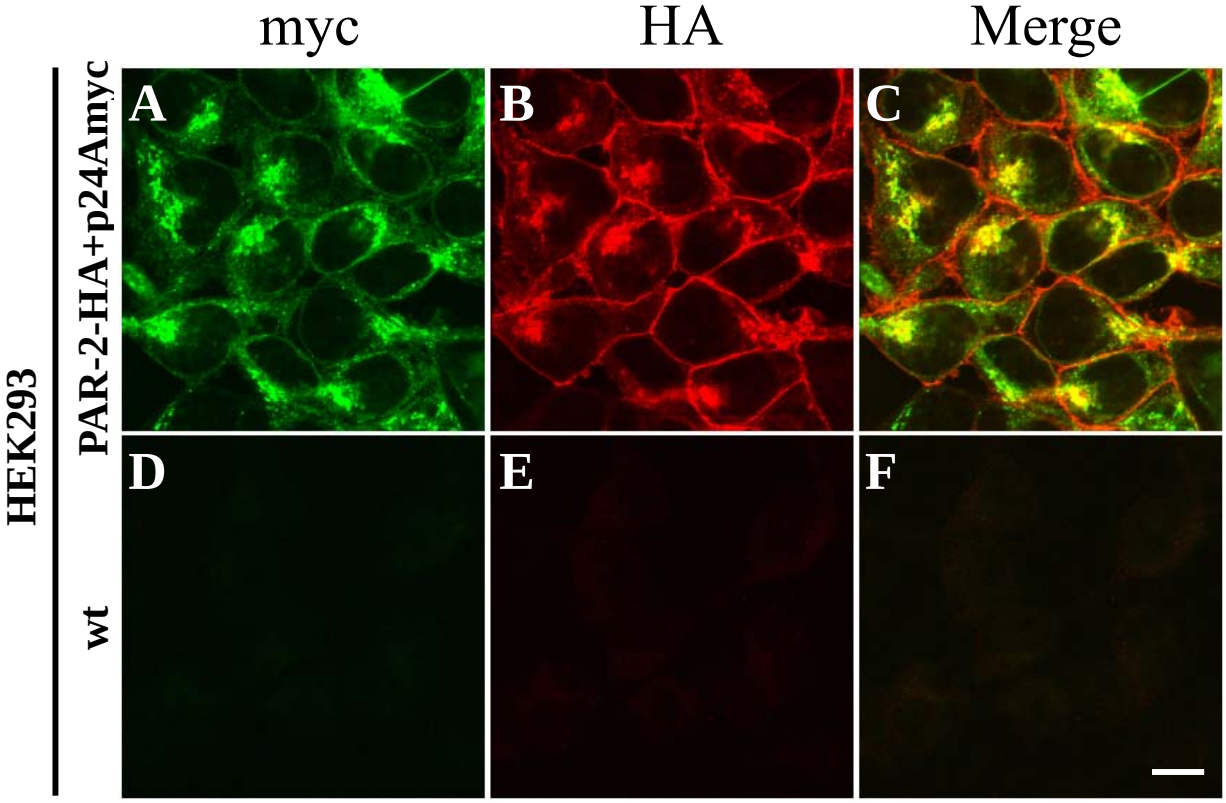

Fig. 3.4.6. Colocalization of p24A with PAR-2 *in vivo*. HEK293 cells stably co-expressing PAR-2-HA and p24Amyc (A-C), and wild-type HEK293 cells (D-F, wt) were fixed, permeabilized, stained, and observed by a confocal microscope. p24A (green, A) was visualized by monoclonal anti-myc antibody and Alexa Fluor 488 goat anti-mouse IgG. PAR-2-HA (red, B) was visualized by polyclonal anti-HA antibody and Alexa Fluor 568 goat anti-rabbit IgG. The overlay image (yellow, C) revealed the colocalization of p24A with PAR-2. Wild-type HEK293 cells served as negative control (D-F). All images are representative for three independent experiments. Scale bar, 10 µm.

It has been known that the intracellular PAR-2 locates at the Golgi stores [132]. p24A is also shown to be a Golgi protein [181]. To test whether the colocalization of PAR-2 with p24A occurs at the Golgi apparatus, HEK293-PAR-2-HA cells were transiently transfected with pEGFP-p24A plasmids. At 24 h after transfection, cells were fixed, and co-stained with the anti-HA antibody and the anti-GM130 antibody, a Golgi apparatus marker. As shown in Fig. 3.4.7 A-C, the intracellular PAR-2 predominantly colocalized with the Golgi marker GM130, suggesting that the intracellular PAR-2 stores are present at the Golgi apparatus. We further found that p24A in p24A-GFP-overexpressing HEK293-PAR-2-HA cells strongly colocalized with the intracellular PAR-2, as well as with the GM130 (Fig. 3.4.7 E). Cells without staining of primary antibodies served as negative control (Fig. 3.4.7 F). Therefore, these data clearly indicate that PAR-2 interacts with p24A at the Golgi apparatus.

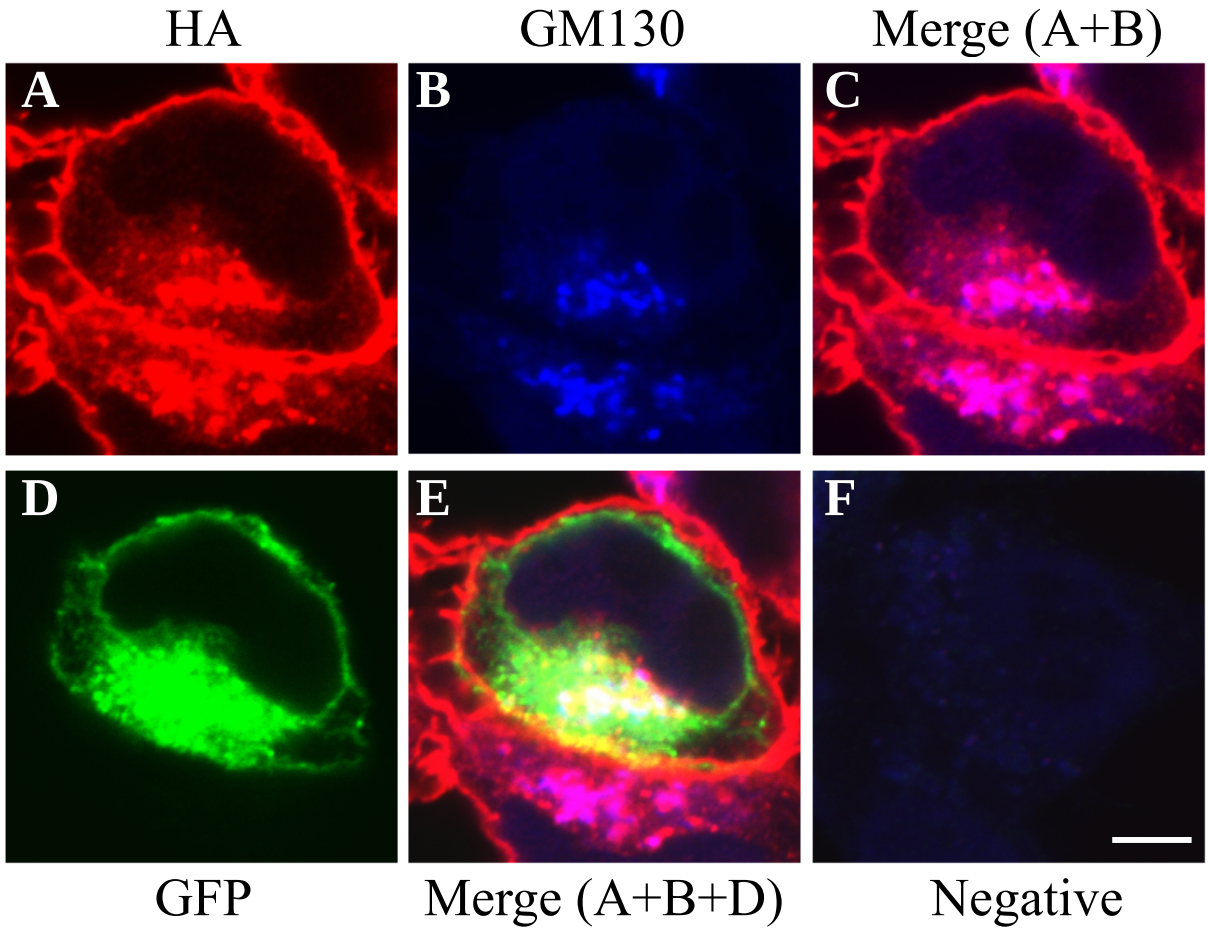

Fig. 3.4.7. PAR-2 interacts with p24A at the Golgi apparatus. HEK293-PAR-2-HA cells were transiently transfected with pEGFP-p24A plasmids. At 24 h after transfection, cells were fixed, permeabilized, stained, and observed by a confocal microscope. PAR-2-HA (red, A) was visualized by polyclonal anti-HA antibody and Alexa Fluor 568 goat anti-rabbit IgG. The Golgi marker GM130 (blue, B) was visualized by monoclonal anti-GM130 antibody and Alexa Fluor 633 goat anti-mouse IgG. p24A (green, D) was visualized by the fluorescent GFP. The merge image (pink, C) reveals that the intracellular PAR-2 is present at the Golgi apparatus. While the combined image (white, E) clearly demonstrates that the interaction of PAR-2 with p24A occurs at the Golgi apparatus in transfected cells. HEK293-PAR-2-HA cells without staining of primary antibodies served as negative control (F). All images are representative for three independent experiments. Scale bar, 5 μm.

3.4.4 PAR-2 interacts with p23, another member of the p24 family

The mammalian p24 family is divided into p25 (α), p24A (β), p23 (γ) and p26 (δ) subfamilies [182]. It is well known that p24A and p23 form a hetero-oligomer. Interaction is mediated by the coiled-coil domain at the N-terminal lumen [184, 185, 192]. Therefore, here we also investigated the interaction of PAR-2 with p23 by co-IP. The whole cell lysates from HEK293-PAR-2-HA+p23myc cells were immunoprecipitated with anti-HA antibody, and the interaction of PAR-2-HA with p23myc was examined by western blot analysis using the anti-myc antibody. As shown in Fig. 3.4.8, p23 was specifically co-immunoprecipitated by PAR-2-HA in HEK293-PAR-2-HA+p23myc cells (lane 6), but not in the negative control wild-type HEK293 cells (lane 4) and HEK293-p23myc cells (lane 5). The same lysates from the respective cells which were used for the IP experiment, served as control for the western blot (Fig. 3.4.8, lanes 1-3). The nitrocellulose membrane was reprobed with the anti-HA antibody to confirm the specificity of the co-immunoprecipitation of PAR-2-HA. These results suggest that PAR-2 interacts with p23 within cells.

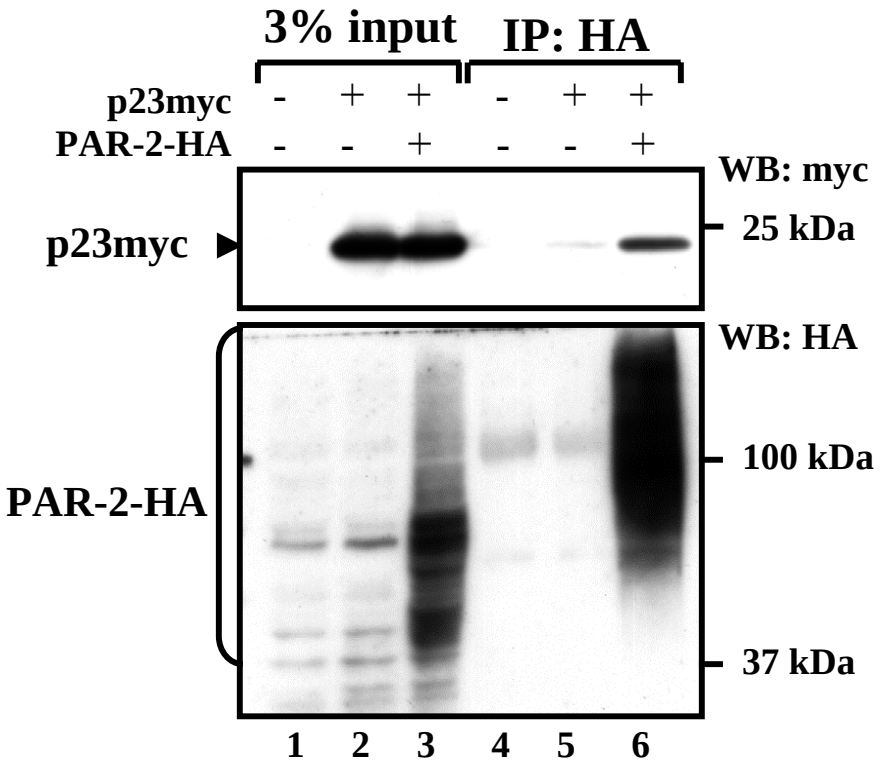

Fig. 3.4.8. Interaction of PAR-2 with p23 *in vivo*. HEK293 cells were stably co-transfected with PAR-2-HA and p23myc or transfected with p23myc. The whole cell lysates from HEK293-PAR-2-HA+p23myc cells, as well as wild-type HEK293 cells (negative control) and HEK293-p23myc cells (negative control) were immunoprecipitated (IP) by anti-HA antibody in the presence of protein A Sepharose beads and the immunocomplex was detected by western blot (WB) using the anti-myc antibody. The immunoprecipitation was further confirmed by reprobing with the anti-HA antibody. Experiments were repeated at least three times with identical results. The molecular mass marker is indicated on the right.

3.4.5 p24A interacts with further receptors: PAR-1 and $P2Y_1$ receptor

Since PAR-1 and PAR-2 both belong to the PAR family, and they share similar structure and functions [21], it is of interest to test whether PAR-1 is also capable of interacting with p24A. To this end, we generated a stable HEK293 cell line co-expressing PAR-1-HA and p24Amyc. The interaction between PAR-1-HA and p24Amyc within cells was determined by co-IP. As shown in Fig. 3.4.9, p24Amyc was strongly immunoprecipitated by PAR-1-HA with the anti-HA antibody (lane 3), but not by the control antibody (IgG, lane 2) in HEK293-PAR-1-HA+p24Amyc cells. The nitrocellulose membrane was reprobed with the anti-HA antibody to confirm the specificity of the co-immunoprecipitation of PAR-1-HA. These data clearly reveal that PAR-1 also interacts with p24A within cells.

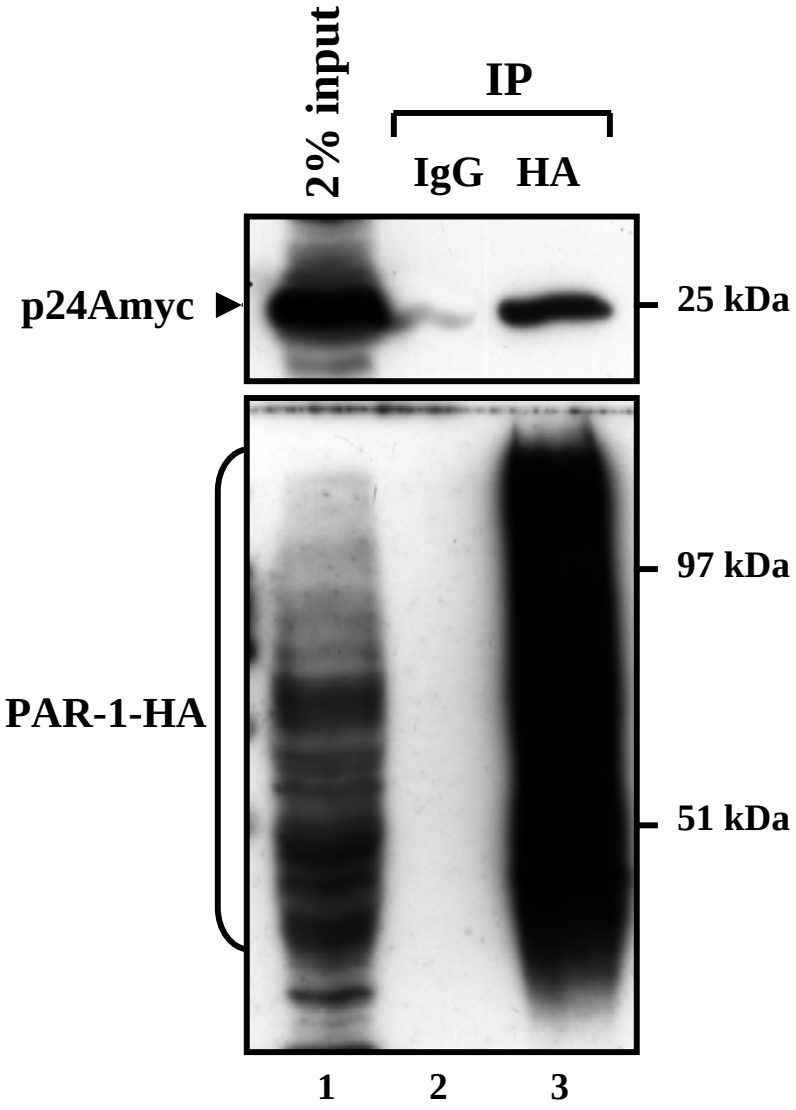

Fig. 3.4.9. Interaction of PAR-1 with p24A *in vivo*. A HEK293 cell line stably co-expressing PAR-1-HA and p24Amyc was generated. The whole cell lysates from HEK293-PAR-1-HA+p24Amyc cells were immunoprecipitated (IP) by anti-HA antibody or by control antibody (IgG) in the presence of protein A Sepharose beads, and the immunocomplex was detected by western blot (WB) using the anti-myc antibody. The immunoprecipitation was further confirmed by reprobing with the anti-HA antibody. Experiments were repeated at least three times with identical results. The molecular mass marker is indicated on the right.

PARs belong to the class I family of the GPCR [193]. To know whether other GPCRs within the class I family can also interact with p24A, we tested the possible interaction of p24A with a purinergic receptor, the $P2Y_1$ receptor ($P2Y_1R$). To this aim, HEK293 cells were transiently co-transfected with pEGFP-$P2Y_1R$ and pcDNA-p24Amyc plasmids. At 24 h after transfection, the whole cell lysates were immunoprecipitated with the anti-GFP antibody, and the interaction of $P2Y_1$-GFP receptor with p24Amyc was examined by western blot analysis using the anti-myc antibody. In parallel, HEK293-GFP+p24Amyc cells were also generated, as negative control. As shown in Fig. 3.4.10, the GFP antibody specifically immunoprecipitated p24Amyc in HEK293-$P2Y_1R$-GFP+p24Amyc cells, but not in HEK293-GFP+p24Amyc cells, suggesting that the $P2Y_1$ receptor also interacts with p24A within cells.

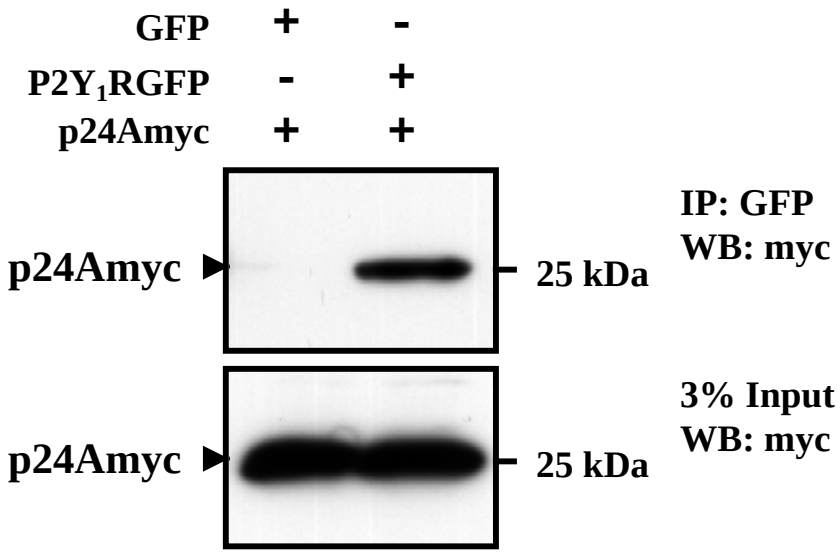

Fig. 3.4.10. Interaction of $P2Y_1$ receptor with p24A *in vivo*. HEK293 cells were transiently co-transfected with pEGFP-$P2Y_1$ and pcDNA-p24Amyc plasmids or with pEGFP and pcDNA-p24Amyc plasmids for 24 h. The whole cell lysates from HEK293-$P2Y_1R$-GFP+p24Amyc cells, as well as from HEK293-GFP+p24Amyc cells were immunoprecipitated (IP) by anti-GFP antibody in the presence of protein A Sepharose beads, and the immunocomplex was detected by western blot (WB) using the anti-myc antibody. A representative blot from three independent experiments is given. The molecular mass marker is indicated on the right.

3.4.6 PAR-2 activation disrupts the interaction with p24A and p23

To evaluate whether activation of PAR-2 affects the interaction with p24A, HEK293-PAR-2-HA+p24Amyc cells were treated with the specific PAR-2 agonist PAR-2 AP (100 μM) for 30 and 60 min in serum-free medium. The whole cell lysates were immunoprecipitated by anti-HA antibody, and the immunocomplex was detected by western blot analysis using the anti-myc antibody. As shown in Fig. 3.4.11 A, the co-immunoprecipitation of p24A was significantly reduced at 30 min after stimulation with PAR-2 AP, compared to that in unstimulated cells (0 min). The reduction in interaction was also observed at 60 min after receptor activation (Fig. 3.4.11 A). The summarized data in Fig. 3.4.11 B demonstrate that activation of PAR-2 significantly reduced the interaction with p24A. It was decreased by 64% at 30 min, and by 57% at 60 min, respectively (Fig. 3.4.11 B). The membrane reprobed with anti-HA antibody revealed the specificity of the co-immunoprecipitation. Similar results were also observed in trypsin-treated HEK293-PAR-2-HA+p24Amyc cells (data not shown). Therefore, these data indicate that the interaction of p24A with PAR-2 is disrupted by receptor activation.

Next, we also tested the effect of PAR-2 activation on the interaction between PAR-2 and p23. HEK293-PAR-2-HA+p23myc cells were treated with the specific PAR-2 agonist PAR-2 AP (100 μM) for 30 and 60 min in serum-free medium, and the whole cell lysates were used for co-IP. Interestingly, activation of PAR-2 resulted in the reduction of interaction with p23 by 26% at 30 min (Fig. 3.4.11 C and D). However, p23 was dramatically dissociated from PAR-2 by 65% at 60 min after stimulation with PAR-2 AP (Fig. 3.4.11 C and D). The membrane reprobed with anti-HA antibody revealed the specificity of the co-immunoprecipitation. Therefore, activation of PAR-2 also reduces the interaction with p23, but in a different pattern.

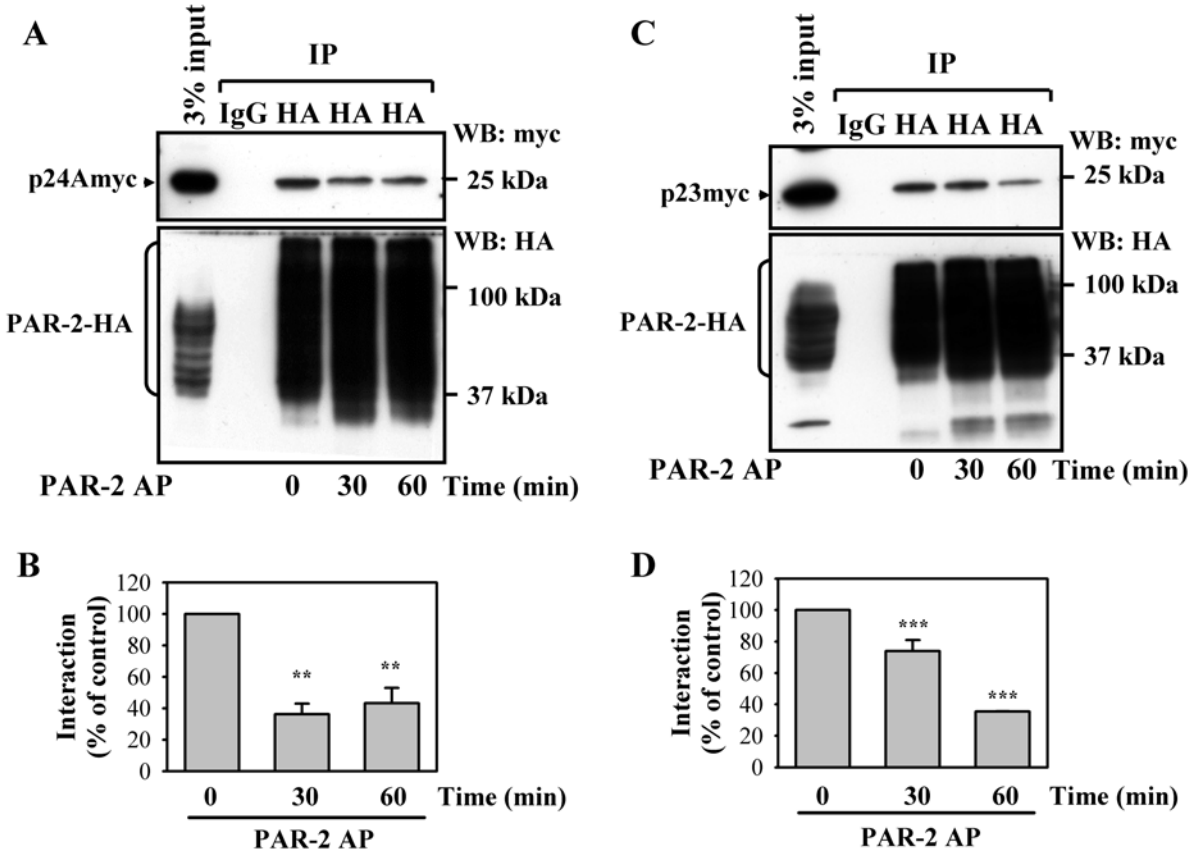

Fig. 3.4.11. Agonist-dependent dynamic interaction of PAR-2 with p24A and p23. HEK293-PAR-2-HA+p24Amyc cells (A and B) and HEK293-PAR-2-HA+p23myc cells (C and D) were treated with 100 μM PAR-2 AP for 0, 30 and 60 min in serum-free medium. (A and C). The whole cell lysates were immunoprecipitated (IP) by anti-HA antibody or control antibody (IgG) in the presence of protein A Sepharose beads, and the immunocomplex was detected by western blot (WB) using the anti-myc antibody. The immunoprecipitation was further confirmed by reprobing with the anti-HA antibody. Typical blots from three independent experiments are shown. The molecular mass marker is indicated on the right. (B and D). The intensity of the interaction was quantitated by Quantity One software (Bio-Rad), and the values were normalized to that in control cells (0 min). Mean ± SEM, $^{**}p < 0.01$, $^{***}p < 0.001$, compared to control.

We then asked mechanisms underlying protein dissociation of p24A from PAR-2 after receptor activation. HEK293-PAR-2-HA+p24Amyc cells were pretreated with brefeldin A, followed by human PAR-2 AP stimulation. As shown by co-IP in Fig. 3.4.12, we found that brefeldin A completely prevented protein dissociation of p24A from PAR-2 after PAR-2 activation, both at 30 and 60 min.

The intracellular PAR-2 would be triggered to be sorted to the plasma membrane for resensitization, once the cell surface receptor is activated and internalized. Brefeldin A has been previously shown to inhibit PAR-2 resensitization [132]. Therefore, our data suggest that protein dissociation between PAR-2 and p24A might be required for PAR-2 resensitization.

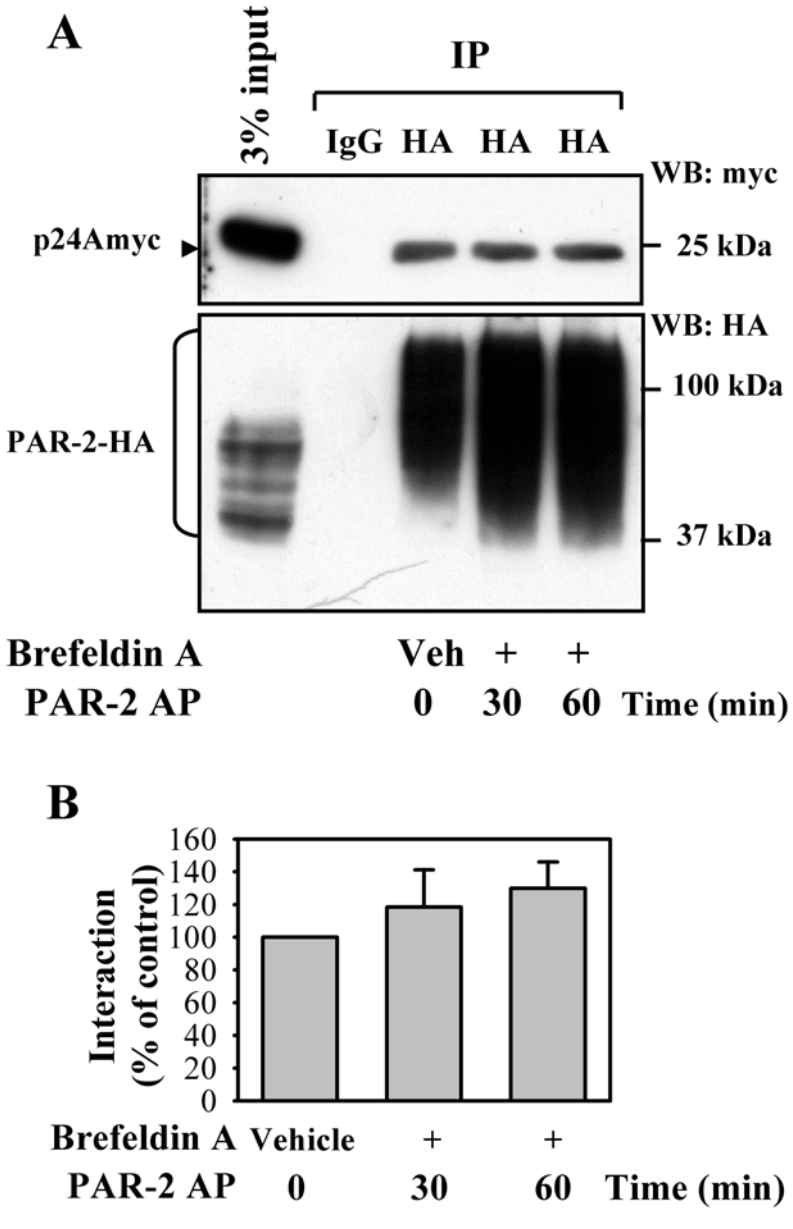

Fig. 3.4.12. The inhibitory effect of brefeldin A on protein dissociation. (A). HEK293-PAR-2-HA+p24Amyc cells were pretreated with 10 μg/ml brefeldin A for 30 min, followed by 100 μM PAR-2 AP stimulation for another 30 and 60 min in serum-free medium. The control cells were treated with vehicle (Veh, ethanol). The whole cell lysates were immunoprecipitated (IP) by anti-HA antibody or control antibody (IgG) in the presence of protein A Sepharose beads, and the immunocomplex was detected by western blot (WB) using the anti-myc antibody. The immunoprecipitation was further confirmed by reprobing with the anti-HA antibody. Typical blots from three independent experiments are given. The molecular mass marker is indicated on the right. (B). The intensity of the interaction was quantitated by Quantity One software (Bio-Rad), and the values were normalized to that in control cells (0 min). Mean ± SEM.

4. DISCUSSION

4.1 General background and scenario for assessing the significance of the present findings

It is well accepted that protein–protein interactions play crucial roles not only in structural but also in the functional organization of the cell. The formation of cellular structures such as the cytoskeleton, the nuclear scaffold and the 26S proteasome results from multiple protein-protein interactions. Protein–protein interactions also regulate signalling within cells. Kinases, phosphatases and transferases bind to their protein substrates to exert the enzymatic function. Protein scaffolds and adaptors interact with kinases, or with activated membrane receptors to transmit signals. Furthermore, the protein interaction has been shown to be a key determinant to initiate the transcriptional and translational machineries. Therefore, uncovering of protein interactions often sheds light on molecular mechanisms underlying biological processes. Since the completion of the human genome project enables us to predict novel proteins, it is of special interest to discover the biological functions of such proteins in nature. For such novel proteins, interactions with known proteins serve as invaluable clues to their biological roles. On the other hand, the study of protein-protein interactions could also give insight into functions of known proteins.

PAR-2, a seven-transmembrane domain GPCR, was identified as the second member of the PAR family in 1994. Accumulating evidence has demonstrated that PAR-2 relays signals from extracellular serine proteases trypsin, tryptase and others to intracellular targets, and exerts important physiological and pathological functions in multiple systems. Studies on the biochemical properties of PAR-2 have demonstrated that PAR-2, upon activation, is rapidly desensitized. At the same time, the activated receptors are recruited to clathrin-coated pits for internalization, like the classic GPCRs. However, the internalized PAR-2 is predominantly sorted into lysosomes where it is degraded by lysosomal proteases. Therefore, cellular receptor resensitization depends on the intracellular presynthesized PAR-2 that is stored at the Golgi apparatus and the newly synthesized receptor.

In the present study, we identified 12 candidate interacting partner proteins of the human PAR-2 by the yeast two-hybrid screening. These PAR-2 partner proteins range from cell surface proteins to intracellular proteins, functioning differently in protein degradation, protein transport, gene expression, apoptosis, and cell growth. For some partner proteins, such as p24A, COP9S4, and HUEL, the biological functions are largely unclear so far. Therefore, our data would provide important clues to investigate PAR-2 properties and functions. As a result, we could improve understanding of receptor functions.

Most importantly, in the part III of results, we demonstrate that one of the partners, Jab1, was confirmed to interact with the PAR-2 within cells. We further found that Jab1 regulated PAR-2-mediated activation of AP-1 via interaction with the plasma membrane receptor under physiological conditions. In the part IV of results, we show the interaction of PAR-2 with p24A *in vitro* and *in vivo*. Our functional studies imply that p24A regulates resensitization of PAR-2.

4.2 Jab1 as a signal messenger mediates the signalling of extracellular proteases trypsin, tryptase and others to the nucleus

Here, we for the first time show that Jab1 directly interacts with the human PAR-2 and potentiates PAR-2-induced c-Jun/AP-1 activation. GST pull-down findings clearly demonstrate that Jab1 mainly bound to the intracellular loop 3 and the C-tail of PAR-2. However, the isolated intracellular loop 3 alone and the PAR-2 C-tail alone both weakly interacted with Jab1. This indicates that several domains of PAR-2 are required to promote a synergistic interaction with Jab1. The intracellular loops and the C-tail of PAR-2 are essential for the interaction with heterotrimeric G proteins and other signal effectors [40, 101-103], as well as for receptor desensitization, internalization and degradation [39, 132, 150], which lead to initiation or termination of PAR-2-mediated signal transduction. Therefore, Jab1 may be an important signal effector to mediate PAR-2-induced signal transduction. Several reports already demonstrated that the MPN (Mpr1p and Pad1p N-terminal) domain (aa 54-190), the conserved functional domain of Jab1, mediated the interaction of Jab1 with DNA topoisomerase IIα [194], or with macrophage migration inhibitory factor (MIF) [195]. In our work, the truncated Jab1 proteins isolated from yeast (aa 31-334 and aa 49-334) include this MPN domain, suggesting that the MPN domain might be responsible for the interaction between Jab1 and PAR-2.

Here, we found that only a part of the amount of Jab1 present in cells interacts with PAR-2. To date, apart from the interaction with other subunits of the COP9 signalosome [170], many diverse proteins were found to interact with Jab1, e.g., c-Jun, HIF-1 α, progesterone receptor, SRC-1, Bcl-3, $p27^{Kip1}$, MIF, LFA-1, p53, Smad4 and Smad7 [167, 169, 171-174, 196, 197]. Therefore, PAR-2 might bind to Jab1 competitively with other Jab1-interacting partners.

The activated PAR-2 is rapidly internalized, translocated to endosomes, and then predominantly sorted into lysosomes. Our data and others [139] demonstrated that the internalized PAR-2 was localized in endosomes, and partially in lysosomes at 30 min after

agonist stimulation. Here, we found that PAR-2 was almost completely dissociated from Jab1 at this time. However, the lysosomal protease inhibitor ZPAD did not prevent protein dissociation of PAR-2 from Jab1. In contrast, the inhibitor of receptor endocytosis PAO clearly inhibited the reduction of protein interaction. Furthermore, immunofluorescence staining studies demonstrated that Jab1 was redistributed from the plasma membrane to the cytosol after PAR-2 activation. Therefore, our data support a model, which is given in Fig. 4.1. Jab1 constitutively interacts with PAR-2 in the steady state (Fig. 4.1 A). After PAR-2 activation, the receptor is internalized, which promotes dissociation of Jab1 from PAR-2 (Fig. 4.1 B-C). The internalized receptor is translocated to early endosomes, where Jab1 is completely dissociated from PAR-2 (Fig. 4.1 D). Subsequently, PAR-2 is further sorted into lysosomes for degradation. On the other hand, the dissociated Jab1 acting as a signal messenger mediates the PAR-2 signaling to activate downstream factors (Fig. 4.1 E).

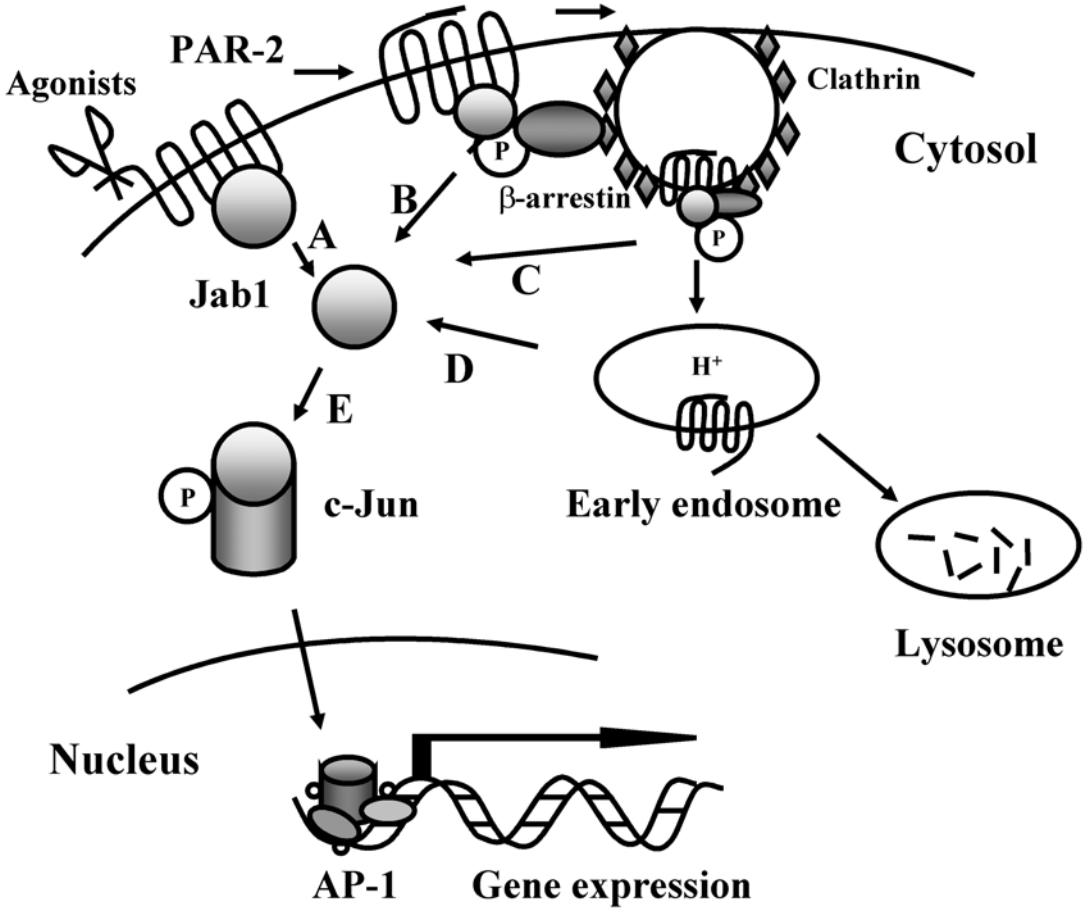

Fig. 4.1. Model for Jab1-mediated signaling pathway for PAR-2. Jab1 constitutively interacts with PAR-2 in the steady state (A). After PAR-2 activation, the receptor is phosphorylated, and internalized in a clathrin-dependent manner, which promotes dissociation of Jab1 from PAR-2 (B and C). The internalized receptor is translocated to early endosomes, where Jab1 is completely dissociated from PAR-2 (D). Subsequently, PAR-2 is further sorted into lysosomes for degradation. On the other hand, the dissociated Jab1 binds to c-Jun and thereby activates it (E). The activated c-Jun then translocates to the nucleus, and binds to AP-1 motif to initiate gene expression.

Furthermore, we found that activation of PAR-2 induced c-Jun phosphorylation, and subsequently activated the transcription factor AP-1. Importantly, here we provide new insights that Jab1, as a protein partner of PAR-2, mediated PAR-2-induced c-Jun/AP-1 activation. It is well known that JNK as a major protein kinase mediates c-Jun phosphorylation [113]. Previous work already demonstrated that tryptase, acting on PAR-2, induced IL-6 and IL-8 release by activation of MAPK/AP-1 in human peripheral blood eosinophils, which may result in inflammatory responses [124]. Recently, it has been shown that Jab1 is also able to phosphorylate c-Jun and to increase AP-1 activation [167, 197]. Jab1 is the fifth subunit of the COP9 signalosome, and all eight subunits of the COP9 signalosome form a complex to exert the biological functions in mammals [169]. It was reported that the COP9 signalosome possesses the protein kinase activity, which is able to phosphorylate c-Jun, IκBα, and p105 [198]. In addition, other studies also demonstrated that the COP9 signalosome associates with protein kinase CK2 and protein kinase D, which phosphorylate c-Jun and p53 [199]. However, COP9 signalosome-induced c-Jun phosphorylation is independent of JNK [200]. Therefore, our data here demonstrate that Jab1-induced c-Jun/AP-1 activation might be a novel alternative signal transduction pathway for PAR-2, suggesting that Jab1 regulates the signalling of extracellular proteases trypsin, tryptase and others to the nucleus.

Loss-of-function studies using specific Jab1 siRNA confirmed that Jab1 was involved in this novel signalling transduction pathway. This pathway put forward by us here might explain mechanisms of gene regulation by proteases, neurotransmitters or hormones through their cognate GPCRs.

Interestingly, a previous report has shown that Jab1 is able to interact with an intracellular membrane protein, the precursor of lutropin/choriogonadotropin receptor (LHR), but not with the mature cell surface LHR [201]. That study further found that Jab1 failed to potentiate the activity of AP-1 in the presence of overexpressed LHR. The explanation given by the authors was that the precursor of LHR competitively interacts with Jab1 to prevent the binding of c-Jun to Jab1. The precursor of LHR is different from the mature receptor, and it is impossible for the precursor of LHR to interact with receptor ligands and to further exert the physiological actions, as does the mature LHR [202]. Therefore, it is not surprising that Jab1 functions differently in both cases interaction with PAR-2 on the one side and with LHR precursor on the other side.

Here, the reporter gene assay demonstrated that Jab1 specifically potentiated PAR-2-induced AP-1 activation. However, Jab1 failed to increase AP-1 activity induced by the PAR-

1 agonist TRag, although it has been reported that thrombin, through PAR-1, could induce AP-1-mediated gene expression in 1321N1 astrocytoma cells [116]. Therefore, other effectors, rather than Jab1, are involved in PAR-1-induced gene expression mediated by activated AP-1.

It is well known that PAR-2 is involved in inflammatory processes, since the proteases tryptase and trypsin are released during inflammation [203, 204], and PAR-2 expression is upregulated upon stimulation by some proinflammatory factors [205]. Moreover, PAR-2 agonists caused an increase in IL-1β, IL-6, IL-8, nitric oxide, prostaglandin E_2, matrix metalloproteinase-9, and tumor necrosis factor-α (TNF-α) productions *in vivo* and *in vitro*, which mediate the inflammatory reactions [55, 124, 206, 207]. It has been reported that AP-1 regulates the gene transcription and expression of several proinflammatory factors, such as IL-1β, IL-6, IL-8, and TNF-α [208]. Therefore, our findings imply that Jab1 might mediate PAR-2-dependent inflammatory responses by regulating the release of proinflammatory factors.

4.3 p24A interacts with intracellular PAR-2: possible functions of p24A-PAR-2 interaction

Here, we identified the interaction of PAR-2 with p24A, by using different biochemical and cell biological methods. This is the first report that PAR-2 directly interacts with vesicle proteins. We have discovered that several intracellular domains of PAR-2 were responsible for the interaction with Jab1. However, here we found that the intracellular loops, C-tail and transmembrane domains of PAR-2 failed to interact with p24A. Instead, we observed a strong interaction between the second extracellular loop of PAR-2 and p24A in the GST pull-down assay. Data from immunostaining demonstrated that p24A colocalized with the intracellular PAR-2 at the Golgi stores, but not with the cell surface receptor. Therefore, these findings strongly support our *in vitro* binding data showing that p24A specifically interacts with the second extracellular loop of PAR-2.

By computational sequence analysis, it was found that the N-terminal lumenal region of p24A contains a GOLD domain that was postulated to interact with cargo proteins [183]. However, our mutagenesis studies clearly revealed that the aa sequence 1-125 of p24A was required for the interaction with PAR-2. The GOLD domain is necessary, but not sufficient to interact with PAR-2.

Altogether, our findings concerning p24A protein clearly demonstrated that p24A, via its N-terminus, interacts with the second extracellular loop of PAR-2 at the lumen of the

Golgi apparatus. The second extracellular loop of PAR-2 is critical for receptor activation, since the tethered ligand domain at the extracellular N-terminus of the receptor binds intramolecularly to the second extracellular loop to activate the receptor. Therefore, our data suggest that novel receptor agonists or antagonists could be developed based on the N-terminal aa sequence of p24A.

It has been demonstrated that the short conserved C-tail of p24A binds to COPI and COPII [179, 182, 186]. COPI and COPII are involved in bi-directional protein transport between the Golgi apparatus and the ER and within the Golgi network [209]. Therefore, p24A was suggested, as the cargo receptor, to mediate protein transport in the early secretory pathway [189]. However, no specific cargo proteins have been found so far. Significantly, here we discovered PAR-2 as the first cargo protein of the p24A. In addition, we reported that PAR-1 and $P2Y_1$ receptor also specifically interacted with p24A. One possible hypothesis is that these three receptors interact with each other, since most GPCRs exist as homo- or hetero-dimers [210]. By aa sequence analysis [211], we found that the second extracellular loop of PAR-1 has very high homology (~64%) with that of PAR-2 (Fig. 4.2). A significantly homologous extracellular loop 2 is also present in the $P2Y_1$ receptor (~27%, Fig. 4.2). Therefore, the second extracellular loop of these receptors would be a general binding motif for p24A, and such receptors that contain a domain homologous to the second extracellular loop of PAR-2 might be cargo proteins specifically that are selected by p24A.

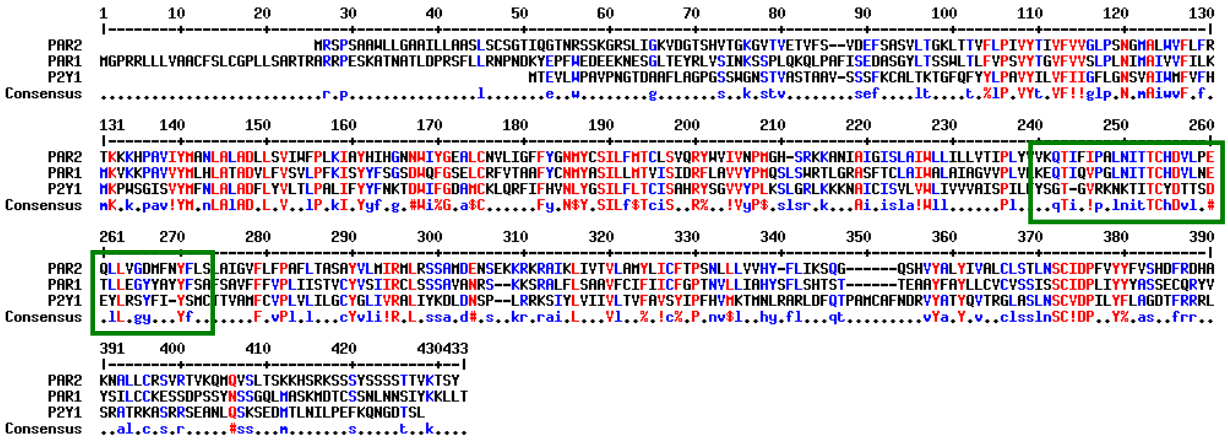

Fig. 4.2. The aa sequence alignment of PAR-1, PAR-2 and $P2Y_1$ receptor. The alignment is performed by multalin on the Internet (http://prodes.toulouse.inra.fr/multalin/multalin.html). The consensus sequence is also shown. The second extracellular loop of receptors is marked by the green box. Red color indicates that the aa is highly conserved, whereas blue color indicates that the aa is low conserved.

We have shown that Jab1 interacted with PAR-2, and relayed PAR-2 signalling to the c-Jun/AP-1 complex, which could further regulate gene expression [125]. Therefore, Jab1 regulates functions of the PAR-2 at the plasma membrane, although Jab1 also interacts with the intracellular PAR-2. On the other side, we found that p24A interacted with the intracellular PAR-2 only, but not with the plasma membrane receptor, indicating that p24A mainly regulates functions of the intracellular PAR-2 at the Golgi apparatus. Furthermore, we distinguished the PAR-2 domain that is responsible for the interaction with both Jab1 and p24A. Several intracellular domains of PAR-2 were involved in the interaction with Jab1 [125]. In contrast, p24A specially bound to the second extracellular loop of PAR-2, but not to intracellular domains. This difference in interaction domain implies that both Jab1 and p24A have equal chances to interact with the same intracellular PAR-2 in the cytosol.

We furthermore found that PAR-2 also associated with the member of p24 family p23, besides p24A. Interestingly, p24A and p23 display a different pattern in the interaction with PAR-2 after PAR-2 activation. Activation of PAR-2 dramatically dissociated p24A from PAR-2 both at 30 min and 60 min. In contrast, p23 still strongly interacted with PAR-2 at 30 min after PAR-2 activation, but was dissociated from PAR-2 at 60 min. It has been shown that PAR-2 was completely resensitized at 30-60 min after agonist stimulation [132]. Moreover, the intracellular presynthesized PAR-2 contributes to receptor resensitization [132]. Therefore, our data suggest that the dissociation between PAR-2 and p24A enables the intracellular PAR-2 sorting to the plasma membrane. Based on our findings above, we speculate that both p23 and p24A trap PAR-2 at the Golgi apparatus in unstimulated cells, to exclude the receptor from transport vesicles that are operated in the secretory pathway. As a result, the intracellular PAR-2 pool is formed at the Golgi apparatus, as depicted in Figure 4.3. Upon PAR-2 activation, p24A loses its ability to interact with the intracellular PAR-2 at the Golgi apparatus. This facilitates PAR-2 to be incorporated into transport vesicles. Then PAR-2 can be further sorted to the plasma membrane for resensitization (Fig. 4.3). On the other side, p23 is synergistically incorporated into transport vesicles with PAR-2. However, p23 seems to dissociate from PAR-2 after the receptor is fused to the plasma membrane.

Interestingly, we found that brefeldin A completely prevented the protein dissociation between PAR-2 and p24A induced by PAR-2 AP. Previous data have shown that brefeldin A is able to attenuate resensitization of PAR-2 [132]. Therefore, these data support our hypothesis that p24A and p23 regulate the post-Golgi transport of PAR-2. It is also known that brefeldin A is an inhibitor of the guanine nucleotide exchange factors (GEFs) specific for ARF1, and can prevent ARF1 activation within cells [212]. Thus, our finding also suggests

that ARF1 might regulate the interaction of PAR-2 with p24A. Recently, it has been shown that p23, possibly p24A as well, recruit inactive ARF1-GDP to the Golgi membrane, which is a pre-requisite for conversion of ARF1-GDP to ARF1-GTP catalyzed by the GEF [213]. On the other side, the activated ARF1-GTP is likely to induce the dissociation of p23 from p24A [214], which are present as hetero-oligomeric complexes in resting conditions, essential for correct localization and stability [185, 192, 215]. Eventually, the homo-oligomeric complex of p23 or p24A is generated to assist the vesicle assembly and budding [189, 213, 214]. Therefore, we hypothesize that activation of PAR-2 leads to ARF1 activation, which in turn disrupts the interaction of p23 with p24A. As a consequence, the intracellular PAR-2 is released from p24A, and sorted to the plasma membrane for resensitization under the assistance of p23 (Fig. 4.3).

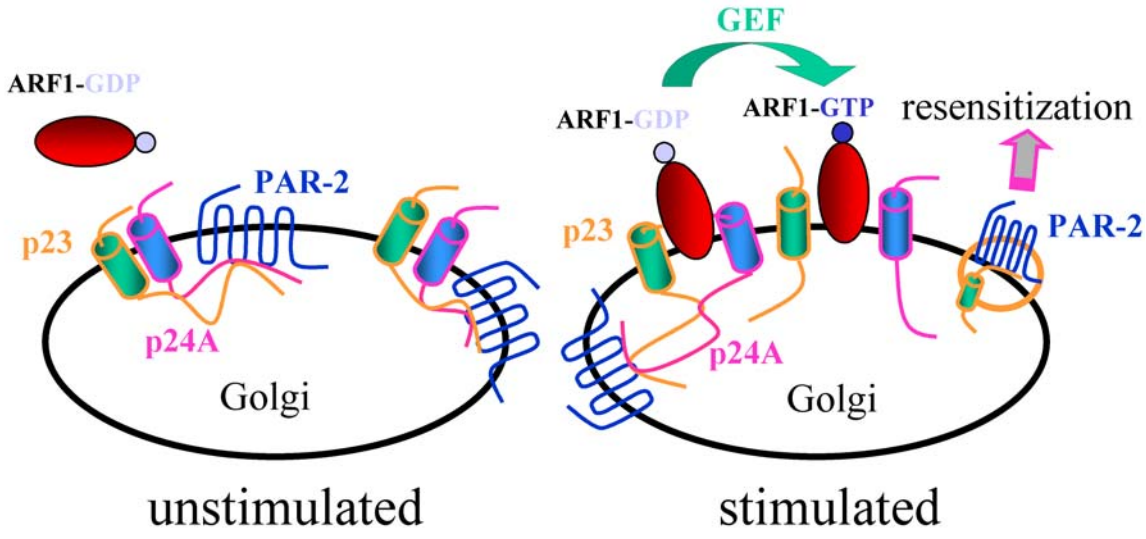

Fig. 4.3. The hypothesis for p23 and p24A functions in the PAR-2 signalling. Both p23 and p24A trap PAR-2 at the Golgi apparatus, to exclude it from transport vesicles in unstimulated cells. As a result, the intracellular PAR-2 pool is formed at the Golgi apparatus. Upon PAR-2 activation, ARF1 is recruited to the Golgi membrane and activated by the GEF, which results in the dissociation of p23 from p24A. Subsequently, the intracellular PAR-2 is released from p24A, and sorted to the plasma membrane for resensitization under the assistance of p23.

4.4 Conclusion

Here, we identified 12 interacting partner proteins of the human PAR-2 by the yeast two-hybrid screening. These PAR-2 partner proteins regulate diverse biological functions within cells, such as protein degradation, protein transport, gene expression, apoptosis, and cell growth. For some partner proteins such as p24A, COP9S4, and HUEL, the biological

functions are largely unclear so far. Therefore, these findings suggest many novel aspects of PAR-2 properties and functions.

Importantly, we confirmed that Jab1 physically interacts with human PAR-2 in the native system. Moreover, several intracellular domains of PAR-2 are required for the interaction with Jab1. Activation of PAR-2 induces the redistribution of Jab1 from the plasma membrane to the cytosol. Meanwhile, the internalization of the activated receptor promotes the dissociation of PAR-2 from Jab1. As a result, PAR-2 and Jab1 are finally dissociated in the endosomes. Upon PAR-2 activation, Jab1 acting as a signal messenger potentiates PAR-2-induced c-Jun/AP-1 activation, which might mediate the release of proinflammatory factors and trigger PAR-2-dependent inflammatory responses (Fig. 4.1). These data demonstrate a novel alternative signal transduction pathway for PAR-2-dependent gene expression [125].

In the next part, we for the first time report that PAR-2 physically interacts with the coated-vesicle protein p24A. *In vitro* biochemical binding data and *in vivo* immunostaining studies clearly reveal that the aa sequence 1-125 of p24A at its N-terminus binds to the second extracellular loop of the intracellular PAR-2 at the Golgi apparatus. We also observed a comparable interaction between PAR-2 and p23, another member of the p24 family. Interestingly, activation of PAR-2 dramatically dissociates p24A from PAR-2 at the time, when the intracellular receptor is sorted to the plasma membrane for resensitization. The dissociation is completely prevented by the GEF inhibitor brefeldin A, which has been known to attenuate resensitization of PAR-2. In contrast, p23 is dissociated from PAR-2 at 60 min after agonist stimulation, when PAR-2 is already completely resensitized. Therefore, we speculate that both p23 and p24A trap the PAR-2 at the Golgi apparatus. This interaction is essential for the formation of the intracellular PAR-2 pool. Upon PAR-2 activation, p24A releases the trapped receptors and further regulates receptor resensitization. On the other side, p23 assists PAR-2 sorting to the plasma membrane (Fig. 4.3). This model has wide implications for GPCR physiology. It could possibly also explain the molecular mechanism underlying post-Golgi sorting of PAR-1 and $P2Y_1$ receptor, as well as other GPCRs, since we found that both PAR-1 and $P2Y_1$ receptor strongly interact with p24A.

5. ABSTRACT

5.1 Search for novel signalling proteins interacting with PAR-2

Protease-activated receptor-2 (PAR-2), a seven-transmembrane domain G protein-coupled receptor (GPCR), relays signals from extracellular serine proteases, like trypsin, tryptase and others, to intracellular targets. PAR-2 has been shown to exert important physiological and pathological functions in multiple systems. However, the role of PAR-2 in the central nervous system (CNS) is largely unknown. The PAR-2-mediated intracellular signal transduction pathways are also not yet understood. To improve our understanding of PAR-2 functions in the CNS, we used full-length human PAR-2 as bait to search for PAR-2-interacting partner proteins in the yeast two-hybrid system. We screened 1.6×10^6 clones of a human brain cDNA library. From there, 308 colonies were found positive for the selection markers histidine, adenine and LacZ. Subsequent sequencing and BLAST analysis revealed that the cDNAs from 34 colonies encoded 19 potential PAR-2-interacting proteins. The further yeast two-hybrid tests confirmed that 12 candidate proteins were truly positive in yeast.

5.2 Jab1 regulates PAR-2-dependent gene expression

Importantly, here we demonstrate the functional interaction of PAR-2 with Jab1, a interacting protein found in yeast. Jab1 was initially identified as a coactivator of c-Jun, and was later shown to be the fifth subunit of COP9 signalosome. Our data from *in vitro* glutathione *S*-transferase (GST) pull-down assays and *in vivo* co-immunoprecipitation assays clearly revealed that Jab1 physically interacted with PAR-2 within cells. Moreover, several intracellular domains of PAR-2 are required for the interaction with Jab1. Jab1 was also shown to be colocalized with PAR-2 both in transfected HEK293 cells and in normal primary human astrocytes by double immunofluorescence staining. We then showed that stimulation with PAR-2 agonists (trypsin or specific PAR-2-activating peptide) dissociated Jab1 from PAR-2 in a time-dependent manner. This dissociation could be prevented by the inhibitor of receptor endocytosis phenylarsine oxide, but not by the lysosomal protease inhibitor ZPAD. Interestingly, we found that activation of PAR-2 induced the redistribution of Jab1 from the plasma membrane to the cytosol, but had no effect on expression of Jab1. Furthermore, Jab1 mediated PAR-2-induced c-Jun activation, which was followed by increased activation of activator protein-1 (AP-1). Loss-of-function studies, using Jab1 small interfering RNA, demonstrated that Jab1 knockdown significantly blocked PAR-2-induced AP-1 activation. Therefore, these data demonstrate that Jab1 is an important effector that mediates a novel signal transduction pathway for PAR-2-dependent gene expression.

5.3 p24A might regulate post-Golgi sorting of PAR-2 to the plasma membrane

Furthermore, we characterized another PAR-2-interacting protein, p24A, as also found in the yeast screening. p24A belongs to the p24 family of coated vesicle membrane proteins. Binding studies by *in vitro* GST pull-down assays clearly demonstrate that the second extracellular loop of PAR-2 strongly bound to the aa 1-125 of p24A at its N-terminus. However, the intracellular domains and transmembrane domains of PAR-2 failed to interact with p24A. The physical interaction of PAR-2 with p24A was further confirmed by co-immunoprecipitation assays *in vivo*. Interestingly, p24A was shown by double immunofluorescence staining to be colocalized with the intracellular PAR-2 at the Golgi stores, but not with cell surface receptors in double transfected HEK293 cells. We then demonstrate the interaction of PAR-2 with p23, another member of p24 family, by co-immunoprecipitation assays *in vivo*. When we studied the functional significance of the PAR-2-p24A interaction, we found that activation of PAR-2 resulted in protein dissociation of p24A from PAR-2 at the time, when the intracellular receptor was sorted to the plasma membrane for resensitization. In contrast, p23 was dissociated from PAR-2 later only at 60 min after agonist stimulation, when PAR-2 is completely resensitized. The dissociation between PAR-2 and p24A was completely inhibited by brefeldin A, which has been known to attenuate resensitization of PAR-2. Brefeldin A is an inhibitor of guanine nucleotide exchange factor that was known to prevent conversion of inactive ADP-ribosylation factor 1 (ARF1)-GDP to active ARF1-GTP. Activation of ARF1 results in the dissociation of hetero-oligomeric complexes of p24A and p23. Therefore, our data imply that p23 and p24A trap the PAR-2 at the Golgi apparatus, which is essential for the intracellular PAR-2 pool formation. Upon PAR-2 activation, p24A releases the PAR-2 and regulates receptor resensitization. On the other side, p23 assists PAR-2 sorting to the plasma membrane. Here, we also demonstrate that p24A strongly interacted with PAR-1 and $P2Y_1$ receptor, suggesting that our model might explain the molecular mechanism underlying post-Golgi transport of certain GPCRs to the plasma membrane.

6. ZUSAMMENFASSUNG

6.1 Suche nach unbekannten, mit PAR-2 interagierenden Proteinen

Der Protease-aktivierte Rezeptor-2 (PAR-2) ist ein 7-TMD (Siebentransmembrandomänen) G-Protein-gekoppelter Rezeptor. PAR-2 vermittelt Signale von extrazellulären Serinproteasen, wie Trypsin, Tryptase, an intrazelluläre Ziele. PAR-2 hat in verschiedenen Systemen wichtige physiologische und pathologische Funktionen. Die Funktion von PAR-2 im zentralen Nervensystem (CNS) ist noch weitgehend unbekannt. Auch die PAR-2-vermittelten intrazellulären Signaltransduktionswege sind kaum klar. Um unser Verständnis der PAR-2 Funktionen im CNS zu erweitern, suchten wir nach Partnerproteinen. Dazu verwendeten wir die vollständige humane PAR-2 cDNA-Sequenz als Köder, um in einem Hefe Two-Hybrid System die mit PAR-2 interagierenden Proteine zu identifizieren. Unter den gefundenen Kandidaten bestätigten die Kontrolltests im Hefe Two-Hybrid-System 12 Proteine als wirklich positiv. Davon studierten wir im Detail die Proteine Jab1 und p24A.

6.2 Funktion des als PAR-2 Interaktionsprotein identifizierten Jab1: Regulation der PAR-2 abhängigen Genexpression

Wir konnten die funktionelle Wechselwirkung von PAR-2 mit Jab1 zeigen. Jab1 wurde ursprünglich als Koaktivator für c-Jun beschrieben. Später wurde gezeigt, dass Jab1 außerdem die fünfte Untereinheit des COP9-Signalosoms darstellt. Die Ergebnisse der in-vitro Glutathion-S-Transferase (GST) Pull-down Assays und der in-vivo Coimmunpräzipitationen bestätigten, dass Jab1 biochemisch mit PAR-2 in Zellen interagiert. Für die Wechselwirkung mit Jab1 sind mehrere intrazelluläre Domänen von PAR-2 notwendig. Für Jab1 konnte durch Doppelimmunfluoreszenzfärbung eine Kolokalisation mit PAR-2 in transfizierten HEK293-Zellen, aber auch in humanen Astrozyten-Primärkulturen nachgewiesen werden. Weiter zeigten wir, dass nach Stimulierung mit PAR-2-Agonisten (Trypsin oder das spezifische PAR-2-aktivierende Peptid) das interagierende Jab1 zeitabhängig von PAR-2 abdissoziiert. Diese Dissoziation konnte durch einen Inhibitor der Rezeptorendozytose, aber nicht durch einen Inhibitor lysosomaler Proteasen, verhindert werden. Interessanterweise fanden wir, dass die Aktivierung von PAR-2 eine Umverteilung von Jab1 von der Plasmamembran ins Cytosol induzierte, aber keinen Effekt auf die Expression von Jab1 hatte. Weiter vermittelte Jab1 die PAR-2-induzierte c-Jun-Aktivierung, welcher die Aktivierung des Transkriptionsfaktors Aktivator-Protein-1 (AP-1) verstärkte. Funktionelle Hemmung durch Einsatz von kleinen, mit der Jab1-Expression interferierenden RNA (siRNA) ergab, dass die PAR-2-induzierte AP-1-Aktivierung signifikant blockiert war. Diese Ergebnisse beweisen, dass Jab1 ein wichtiger Effektor für einen neuen Signaltransduktionsweg der PAR-2-abhängigen Genexpression ist.

6.3 Das „coated vesicle“-Membranprotein p24A reguliert als PAR-2 Interaktionsprotein die Post-Golgi-Sortierung von PAR-2 zur Plasmamembran

Als zweites charakterisierten wir p24A, ein weiteres mit PAR-2 interagierendes Protein. Auch dieses wurde von uns im Hefe-Two-Hybrid Screening als positiv identifiziert. p24A gehört zur p24-Familie der 'coated vesicle'-Membranproteine. Bindungsstudien mittels in-vitro GST Pull-down Assays ergeben, dass die extrazelluläre Schleife Nr. 2 (loop-2) von PAR-2 stark an die Aminosäuren 1 bis 125 am N-Terminus von p24A bindet. Die intrazellulären Domänen und die Transmembrandomänen von PAR-2 zeigten keine Interaktion mit p24A. Die in-vivo Wechselwirkung von PAR-2 mit p24A wurde durch Coimmunpräzipitation bestätigt. Interessanterweise ergab sich bei der Doppelimmunfluoreszenzfärbung an doppeltransfizierten HEK293-Zellen, dass p24A mit intrazellulärem PAR-2 am Golgi-Apparat und nicht mit zellmembranständigen Rezeptoren kolokalisiert war. Auch mit p23, einem weiteren Mitglied der p24-Familie fanden wir durch Coimmunpräzipitation eine in-vivo Wechselwirkung von PAR-2. Bei der Untersuchung der funktionellen Bedeutung der PAR-2-p24A Wechselwirkung entdeckten wir, dass nach Aktivierung von PAR-2 die Abdissoziation von p24A vom PAR-2 zu jenem Zeitpunkt erfolgte, wenn bei der Resensitisierung die Sortierung der intrazellulären Rezeptoren zur Plasmamembran stattfindet. Im Gegensatz dazu dissoziierte p23 vom PAR-2-Rezeptor erst 60 min nach der Stimulation mit dem Agonisten ab. Dann PAR-2 war vollständig resensitisiert. Die Dissoziation von p24A vom PAR-2 wurde durch Brefeldin A vollständig gehemmt. Brefeldin A ist ein Inhibitor für Guaninnukleotid-Austauschfaktoren, und Brefeldin A verhindert die Umwandlung von inaktivem ADP-Ribosylierungsfaktor 1 (ARF1)-GDP in aktives ARF1-GTP. Die Aktivierung von ARF1 führt zur Dissoziation der hetero-oligomeren Komplexe aus p24A und p23. Daher legen unsere Ergebnisse nahe, dass p23 und p24A den PAR-2 im Golgi-Apparat zurückhalten. Dies ist für die Bildung eines intrazellulären PAR-2-Pools fundamental. Nach PAR-2-Aktivierung gibt p24A PAR-2 frei, und reguliert so die Rezeptorresensitisierung, während p23 an der Sortierung von PAR-2 zur Plasmamembran beteiligt ist. In weiteren Untersuchungen konnten wir zeigen, dass p24A auch stark mit anderen Rezeptoren, nämlich PAR-1 und $P2Y_1$ Rezeptor interagiert. Dies legt nahe, dass unser Modell den molekularen Mechanismus erklärt, der dem Post-Golgi-Transport von bestimmten G-Protein-gekoppelten Rezeptoren zur Plasmamembran zugrunde liegt. Damit identifizieren wir eine molekulare Komponente, die für einen grundlegenden Prozess der Rezeptorphysiologie verantwortlich ist, nämlich die Resensitisierung nach Rezeptorinternationalisierung.

7. REFERENCE

1 Barrett, A. J., Rawlings, N. D. and Woessner, J. F. (1998) Handbook of proteolytic enzymes. Academic Press, London

2 Hedstrom, L. (2002) Serine protease mechanism and specificity. Chem Rev **102**, 4501-4524

3 Xi, G., Reiser, G. and Keep, R. F. (2003) The role of thrombin and thrombin receptors in ischemic, hemorrhagic and traumatic brain injury: deleterious or protective? J Neurochem **84**, 3-9

4 Sheehan, J. J. and Tsirka, S. E. (2005) Fibrin-modifying serine proteases thrombin, tPA, and plasmin in ischemic stroke: a review. Glia **50**, 340-350

5 Striggow, F., Riek, M., Breder, J., Henrich-Noack, P., Reymann, K. G. and Reiser, G. (2000) The protease thrombin is an endogenous mediator of hippocampal neuroprotection against ischemia at low concentrations but causes degeneration at high concentrations. Proc Natl Acad Sci U S A **97**, 2264-2269

6 Madani, R., Hulo, S., Toni, N., Madani, H., Steimer, T., Muller, D. and Vassalli, J. D. (1999) Enhanced hippocampal long-term potentiation and learning by increased neuronal expression of tissue-type plasminogen activator in transgenic mice. Embo J **18**, 3007-3012

7 Qureshi, N. (1996) Tissue plasminogen activator for acute ischemic stroke. N Engl J Med **334**, 1406

8 Xu, W. F., Andersen, H., Whitmore, T. E., Presnell, S. R., Yee, D. P., Ching, A., Gilbert, T., Davie, E. W. and Foster, D. C. (1998) Cloning and characterization of human protease-activated receptor 4. Proc Natl Acad Sci U S A **95**, 6642-6646

9 Vu, T. K., Hung, D. T., Wheaton, V. I. and Coughlin, S. R. (1991) Molecular cloning of a functional thrombin receptor reveals a novel proteolytic mechanism of receptor activation. Cell **64**, 1057-1068

10 Nystedt, S., Emilsson, K., Wahlestedt, C. and Sundelin, J. (1994) Molecular cloning of a potential proteinase activated receptor. Proc Natl Acad Sci U S A **91**, 9208-9212

11 Ishihara, H., Connolly, A. J., Zeng, D., Kahn, M. L., Zheng, Y. W., Timmons, C., Tram, T. and Coughlin, S. R. (1997) Protease-activated receptor 3 is a second thrombin receptor in humans. Nature **386**, 502-506

12 Luo, W., Wang, Y. and Reiser, G. (2005) Two types of protease-activated receptors (PAR-1 and PAR-2) mediate calcium signaling in rat retinal ganglion cells RGC-5. Brain Res **1047**, 159-167

13 Wang, H., Ubl, J. J. and Reiser, G. (2002) Four subtypes of protease-activated receptors, co-expressed in rat astrocytes, evoke different physiological signaling. Glia **37**, 53-63

14 Wang, Y., Richter-Landsberg, C. and Reiser, G. (2004) Expression of protease-activated receptors (PARs) in OLN-93 oligodendroglial cells and mechanism of PAR-1-induced calcium signaling. Neuroscience **126**, 69-82

15 Balcaitis, S., Xie, Y., Weinstein, J. R., Andersen, H., Hanisch, U. K., Ransom, B. R. and Moller, T. (2003) Expression of proteinase-activated receptors in mouse microglial cells. Neuroreport **14**, 2373-2377

16 Oshiro, A., Otani, H., Yagi, Y., Fukuhara, S. and Inagaki, C. (2002) Protease-activated receptor-2-mediated Ca2+ signaling in guinea pig tracheal epithelial cells. Life Sci **71**, 547-558

17 Sokolova, E., Grishina, Z., Buhling, F., Welte, T. and Reiser, G. (2005) Protease-activated receptor-1 in human lung fibroblasts mediates a negative feedback downregulation via prostaglandin E2. Am J Physiol Lung Cell Mol Physiol **288**, L793-802

18 Schmidlin, F., Amadesi, S., Vidil, R., Trevisani, M., Martinet, N., Caughey, G., Tognetto, M., Cavallesco, G., Mapp, C., Geppetti, P. and Bunnett, N. W. (2001) Expression and function of proteinase-activated receptor 2 in human bronchial smooth muscle. Am J Respir Crit Care Med **164**, 1276-1281
19 Santulli, R. J., Derian, C. K., Darrow, A. L., Tomko, K. A., Eckardt, A. J., Seiberg, M., Scarborough, R. M. and Andrade-Gordon, P. (1995) Evidence for the presence of a protease-activated receptor distinct from the thrombin receptor in human keratinocytes. Proc Natl Acad Sci U S A **92**, 9151-9155
20 Macfarlane, S. R., Seatter, M. J., Kanke, T., Hunter, G. D. and Plevin, R. (2001) Proteinase-Activated Receptors. Pharmacol Rev **53**, 245-282
21 Ossovskaya, V. S. and Bunnett, N. W. (2004) Protease-activated receptors: contribution to physiology and disease. Physiol Rev **84**, 579-621
22 Nishikawa, H. and Kawabata, A. (2003) Modulation of Gastric Function by Proteinase-Activated Receptors. Drug Dev Res **60**, 9-13
23 Noorbakhsh, F., Vergnolle, N., Hollenberg, M. D. and Power, C. (2003) Proteinase-activated receptors in the nervous system. Nat Rev Neurosci **4**, 981-990
24 Steinberg, S. F. (2005) The cardiovascular actions of protease-activated receptors. Mol Pharmacol **67**, 2-11
25 Hollenberg, M. D., Wijesuriya, S. J., Gui, Y. and Loutzenhiser, R. (2003) Proteinase-Activated Receptors (PARs) and the Kidney. Drug Dev Res **60**, 36-42
26 Fiorucci, S. and Distrutti, E. (2003) Proteinase-Activated Receptors (PARs) and Immune Function. Drug Dev Res **60**, 65-70
27 Rattenholl, A. and Steinhoff, M. (2003) Role of Proteinase-Activated Receptors in Cutaneous Biology and Disease. Drug Dev Res **59**, 408-416
28 Geppetti, P. and Trevisani, M. (2003) Proteinase-Activated Receptors (PARs) and Bronchial Smooth Muscle Functions. Drug Dev Res **60**, 24-28
29 Chen, L. B. and Buchanan, J. M. (1975) Mitogenic activity of blood components. I. Thrombin and prothrombin. Proc Natl Acad Sci U S A **72**, 131-135
30 Chen, L. B., Teng, N. N. and Buchanan, J. M. (1976) Mitogenicity of thrombin and surface alterations on mouse splenocytes. Exp Cell Res **101**, 41-46
31 Bar-Shavit, R., Kahn, A., Fenton, J. W., 2nd and Wilner, G. D. (1983) Receptor-mediated chemotactic response of a macrophage cell line (J774) to thrombin. Lab Invest **49**, 702-707
32 Bizios, R., Lai, L., Fenton, J. W., 2nd and Malik, A. B. (1986) Thrombin-induced chemotaxis and aggregation of neutrophils. J Cell Physiol **128**, 485-490
33 Daniel, T. O., Gibbs, V. C., Milfay, D. F., Garovoy, M. R. and Williams, L. T. (1986) Thrombin stimulates c-sis gene expression in microvascular endothelial cells. J Biol Chem **261**, 9579-9582
34 Hattori, R., Hamilton, K. K., Fugate, R. D., McEver, R. P. and Sims, P. J. (1989) Stimulated secretion of endothelial von Willebrand factor is accompanied by rapid redistribution to the cell surface of the intracellular granule membrane protein GMP-140. J Biol Chem **264**, 7768-7771
35 Shuman, M. A. (1986) Thrombin-cellular interactions. Ann N Y Acad Sci **485**, 228-239
36 Esmon, C. T. (1987) The regulation of natural anticoagulant pathways. Science **235**, 1348-1352
37 Hollenberg, M. D. and Compton, S. J. (2002) International Union of Pharmacology. XXVIII. Proteinase-activated receptors. Pharmacol Rev **54**, 203-217
38 Ishii, K., Chen, J., Ishii, M., Koch, W. J., Freedman, N. J., Lefkowitz, R. J. and Coughlin, S. R. (1994) Inhibition of thrombin receptor signaling by a G-protein

coupled receptor kinase. Functional specificity among G-protein coupled receptor kinases. J Biol Chem **269**, 1125-1130

39 Paing, M. M., Temple, B. R. and Trejo, J. (2004) A tyrosine-based sorting signal regulates intracellular trafficking of protease-activated receptor-1: multiple regulatory mechanisms for agonist-induced G protein-coupled receptor internalization. J Biol Chem **279**, 21938-21947

40 Swift, S., Leger, A. J., Talavera, J., Zhang, L., Bohm, A. and Kuliopulos, A. (2006) Role of the PAR1 receptor 8th helix in signaling: the 7-8-1 receptor activation mechanism. J Biol Chem **281**, 4109-4116

41 Wang, Y., Gu, Y. and Lucas, M. J. (2002) Expression of thrombin receptors in endothelial cells and neutrophils from normal and preeclamptic pregnancies. J Clin Endocrinol Metab **87**, 3728-3734

42 Sabri, A., Muske, G., Zhang, H., Pak, E., Darrow, A., Andrade-Gordon, P. and Steinberg, S. F. (2000) Signaling properties and functions of two distinct cardiomyocyte protease-activated receptors. Circ Res **86**, 1054-1061

43 Hauck, R. W., Schulz, C., Schomig, A., Hoffman, R. K. and Panettieri, R. A., Jr. (1999) alpha-Thrombin stimulates contraction of human bronchial rings by activation of protease-activated receptors. Am J Physiol **277**, L22-29

44 Nystedt, S., Emilsson, K., Larsson, A. K., Strombeck, B. and Sundelin, J. (1995) Molecular cloning and functional expression of the gene encoding the human proteinase-activated receptor 2. Eur J Biochem **232**, 84-89

45 Bohm, S. K., Kong, W., Bromme, D., Smeekens, S. P., Anderson, D. C., Connolly, A., Kahn, M., Nelken, N. A., Coughlin, S. R., Payan, D. G. and Bunnett, N. W. (1996) Molecular cloning, expression and potential functions of the human proteinase-activated receptor-2. Biochem J **314**, 1009-1016

46 Compton, S. J., Sandhu, S., Wijesuriya, S. J. and Hollenberg, M. D. (2002) Glycosylation of human proteinase-activated receptor-2 (hPAR2): role in cell surface expression and signalling. Biochem J **368**, 495-505

47 Johansson, U., Lawson, C., Dabare, M., Syndercombe-Court, D., Newland, A. C., Howells, G. L. and Macey, M. G. (2005) Human peripheral blood monocytes express protease receptor-2 and respond to receptor activation by production of IL-6, IL-8, and IL-1{beta}. J Leukoc Biol **78**, 967-975

48 Connolly, A. J., Ishihara, H., Kahn, M. L., Farese, R. V., Jr. and Coughlin, S. R. (1996) Role of the thrombin receptor in development and evidence for a second receptor. Nature **381**, 516-519

49 Schmidt, V. A., Nierman, W. C., Maglott, D. R., Cupit, L. D., Moskowitz, K. A., Wainer, J. A. and Bahou, W. F. (1998) The human proteinase-activated receptor-3 (PAR-3) gene. Identification within a Par gene cluster and characterization in vascular endothelial cells and platelets. J Biol Chem **273**, 15061-15068

50 Nakanishi-Matsui, M., Zheng, Y. W., Sulciner, D. J., Weiss, E. J., Ludeman, M. J. and Coughlin, S. R. (2000) PAR3 is a cofactor for PAR4 activation by thrombin. Nature **404**, 609-613

51 Bartha, K., Domotor, E., Lanza, F., Adam-Vizi, V. and Machovich, R. (2000) Identification of thrombin receptors in rat brain capillary endothelial cells. J Cereb Blood Flow Metab **20**, 175-182

52 Bretschneider, E., Kaufmann, R., Braun, M., Nowak, G., Glusa, E. and Schror, K. (2001) Evidence for functionally active protease-activated receptor-4 (PAR-4) in human vascular smooth muscle cells. Br J Pharmacol **132**, 1441-1446

53 Henrich-Noack, P., Riek-Burchardt, M., Baldauf, K., Reiser, G. and Reymann, K. G. (2006) Focal ischemia induces expression of protease-activated receptor1 (PAR1) and

PAR3 on microglia and enhances PAR4 labeling in the penumbra. Brain Res **1070**, 232-241

54 Guo, H., Liu, D., Gelbard, H., Cheng, T., Insalaco, R., Fernandez, J. A., Griffin, J. H. and Zlokovic, B. V. (2004) Activated protein C prevents neuronal apoptosis via protease activated receptors 1 and 3. Neuron **41**, 563-572

55 Asokananthan, N., Graham, P. T., Fink, J., Knight, D. A., Bakker, A. J., McWilliam, A. S., Thompson, P. J. and Stewart, G. A. (2002) Activation of protease-activated receptor (PAR)-1, PAR-2, and PAR-4 stimulates IL-6, IL-8, and prostaglandin E2 release from human respiratory epithelial cells. J Immunol **168**, 3577-3585

56 Hansen, K. K., Saifeddine, M. and Hollenberg, M. D. (2004) Tethered ligand-derived peptides of proteinase-activated receptor 3 (PAR3) activate PAR1 and PAR2 in Jurkat T cells. Immunology **112**, 183-190

57 Kaufmann, R., Schulze, B., Krause, G., Mayr, L. M., Settmacher, U. and Henklein, P. (2005) Proteinase-activated receptors (PARs)--the PAR3 Neo-N-terminal peptide TFRGAP interacts with PAR1. Regul Pept **125**, 61-66

58 Sabri, A., Guo, J., Elouardighi, H., Darrow, A. L., Andrade-Gordon, P. and Steinberg, S. F. (2003) Mechanisms of protease-activated receptor-4 actions in cardiomyocytes. Role of Src tyrosine kinase. J Biol Chem **278**, 11714-11720

59 Suo, Z., Wu, M., Citron, B. A., Gao, C. and Festoff, B. W. (2003) Persistent protease-activated receptor 4 signaling mediates thrombin-induced microglial activation. J Biol Chem **278**, 31177-31183

60 Mule, F., Pizzuti, R., Capparelli, A. and Vergnolle, N. (2004) Evidence for the presence of functional protease activated receptor 4 (PAR4) in the rat colon. Gut **53**, 229-234

61 Kataoka, H., Hamilton, J. R., McKemy, D. D., Camerer, E., Zheng, Y. W., Cheng, A., Griffin, C. and Coughlin, S. R. (2003) Protease-activated receptors 1 and 4 mediate thrombin signaling in endothelial cells. Blood **102**, 3224-3231

62 Grand, R. J., Turnell, A. S. and Grabham, P. W. (1996) Cellular consequences of thrombin-receptor activation. Biochem J **313**, 353-368

63 Dihanich, M., Kaser, M., Reinhard, E., Cunningham, D. and Monard, D. (1991) Prothrombin mRNA is expressed by cells of the nervous system. Neuron **6**, 575-581

64 Aronson, D. L., Ball, A. P., Franza, R. B., Hugli, T. E. and Fenton, J. W., 2nd (1980) Human prothrombin fragments F1 (alpha beta) and F2: preparation and characterization of structural and biological properties. Thromb Res **20**, 239-253

65 Corvera, C. U., Dery, O., McConalogue, K., Bohm, S. K., Khitin, L. M., Caughey, G. H., Payan, D. G. and Bunnett, N. W. (1997) Mast cell tryptase regulates rat colonic myocytes through proteinase-activated receptor 2. J Clin Invest **100**, 1383-1393

66 Yamashina, I. (1956) The action of enterokinase on trypsinogen. Biochim Biophys Acta **20**, 433-434

67 Emi, M., Nakamura, Y., Ogawa, M., Yamamoto, T., Nishide, T., Mori, T. and Matsubara, K. (1986) Cloning, characterization and nucleotide sequences of two cDNAs encoding human pancreatic trypsinogens. Gene **41**, 305-310

68 Nyaruhucha, C. N., Kito, M. and Fukuoka, S. I. (1997) Identification and expression of the cDNA-encoding human mesotrypsin(ogen), an isoform of trypsin with inhibitor resistance. J Biol Chem **272**, 10573-10578

69 Stead, R. H., Tomioka, M., Quinonez, G., Simon, G. T., Felten, S. Y. and Bienenstock, J. (1987) Intestinal mucosal mast cells in normal and nematode-infected rat intestines are in intimate contact with peptidergic nerves. Proc Natl Acad Sci U S A **84**, 2975-2979

70 Theoharides, T. C. (1990) Mast cells: the immune gate to the brain. Life Sci **46**, 607-617

71 Sawada, K., Nishibori, M., Nakaya, N., Wang, Z. and Saeki, K. (2000) Purification and characterization of a trypsin-like serine proteinase from rat brain slices that degrades laminin and type IV collagen and stimulates protease-activated receptor-2. J Neurochem **74**, 1731-1738
72 Cottrell, G. S., Amadesi, S., Grady, E. F. and Bunnett, N. W. (2004) Trypsin IV, a novel agonist of protease-activated receptors 2 and 4. J Biol Chem **279**, 13532-13539
73 Wang, Y., Luo, W., Wartmann, T., Halangk, W., Sahin-Toth, M. and Reiser, G. (2006) Mesotrypsin, a brain trypsin, activates selectively proteinase-activated receptor-1, but not proteinase-activated receptor-2, in rat astrocytes. J Neurochem **99**, 759-769
74 Feng, D. M., Veber, D. F., Connolly, T. M., Condra, C., Tang, M. J. and Nutt, R. F. (1995) Development of a potent thrombin receptor ligand. J Med Chem **38**, 4125-4130
75 Kawabata, A., Saifeddine, M., Al-Ani, B., Leblond, L. and Hollenberg, M. D. (1999) Evaluation of proteinase-activated receptor-1 (PAR1) agonists and antagonists using a cultured cell receptor desensitization assay: activation of PAR2 by PAR1-targeted ligands. J Pharmacol Exp Ther **288**, 358-370
76 Blackhart, B. D., Emilsson, K., Nguyen, D., Teng, W., Martelli, A. J., Nystedt, S., Sundelin, J. and Scarborough, R. M. (1996) Ligand cross-reactivity within the protease-activated receptor family. J Biol Chem **271**, 16466-16471
77 Hollenberg, M. D., Saifeddine, M., al-Ani, B. and Kawabata, A. (1997) Proteinase-activated receptors: structural requirements for activity, receptor cross-reactivity, and receptor selectivity of receptor-activating peptides. Can J Physiol Pharmacol **75**, 832-841
78 Hoogerwerf, W. A., Hellmich, H. L., Micci, M. A., Winston, J. H., Zou, L. and Pasricha, P. J. (2002) Molecular cloning of the rat proteinase-activated receptor 4 (PAR4). BMC Mol Biol **3**, 2
79 Hollenberg, M. D., Laniyonu, A. A., Saifeddine, M. and Moore, G. J. (1993) Role of the amino- and carboxyl-terminal domains of thrombin receptor-derived polypeptides in biological activity in vascular endothelium and gastric smooth muscle: evidence for receptor subtypes. Mol Pharmacol **43**, 921-930
80 Natarajan, S., Riexinger, D., Peluso, M. and Seiler, S. M. (1995) 'Tethered ligand' derived pentapeptide agonists of thrombin receptor: a study of side chain requirements for human platelet activation and GTPase stimulation. Int J Pept Protein Res **45**, 145-151
81 Hollenberg, M. D. (2005) Physiology and pathophysiology of proteinase-activated receptors (PARs): proteinases as hormone-like signal messengers: PARs and more. J Pharmacol Sci **97**, 8-13
82 McGuire, J. J., Saifeddine, M., Triggle, C. R., Sun, K. and Hollenberg, M. D. (2004) 2-furoyl-LIGRLO-amide: a potent and selective proteinase-activated receptor 2 agonist. J Pharmacol Exp Ther **309**, 1124-1131
83 Camerer, E., Huang, W. and Coughlin, S. R. (2000) Tissue factor- and factor X-dependent activation of protease-activated receptor 2 by factor VIIa. Proc Natl Acad Sci U S A **97**, 5255-5260
84 Sambrano, G. R., Huang, W., Faruqi, T., Mahrus, S., Craik, C. and Coughlin, S. R. (2000) Cathepsin G activates protease-activated receptor-4 in human platelets. J Biol Chem **275**, 6819-6823
85 Uehara, A., Sugawara, S., Muramoto, K. and Takada, H. (2002) Activation of human oral epithelial cells by neutrophil proteinase 3 through protease-activated receptor-2. J Immunol **169**, 4594-4603
86 Takeuchi, T., Harris, J. L., Huang, W., Yan, K. W., Coughlin, S. R. and Craik, C. S. (2000) Cellular localization of membrane-type serine protease 1 and identification of

protease-activated receptor-2 and single-chain urokinase-type plasminogen activator as substrates. J Biol Chem **275**, 26333-26342

87 Lourbakos, A., Potempa, J., Travis, J., D'Andrea, M. R., Andrade-Gordon, P., Santulli, R., Mackie, E. J. and Pike, R. N. (2001) Arginine-specific protease from Porphyromonas gingivalis activates protease-activated receptors on human oral epithelial cells and induces interleukin-6 secretion. Infect Immun **69**, 5121-5130

88 Sun, G., Stacey, M. A., Schmidt, M., Mori, L. and Mattoli, S. (2001) Interaction of mite allergens Der p3 and Der p9 with protease-activated receptor-2 expressed by lung epithelial cells. J Immunol **167**, 1014-1021

89 Seiler, S. M., Peluso, M., Michel, I. M., Goldenberg, H., Fenton, J. W., 2nd, Riexinger, D. and Natarajan, S. (1995) Inhibition of thrombin and SFLLR-peptide stimulation of platelet aggregation, phospholipase A2 and Na+/H+ exchange by a thrombin receptor antagonist. Biochem Pharmacol **49**, 519-528

90 Bernatowicz, M. S., Klimas, C. E., Hartl, K. S., Peluso, M., Allegretto, N. J. and Seiler, S. M. (1996) Development of potent thrombin receptor antagonist peptides. J Med Chem **39**, 4879-4887

91 Andrade-Gordon, P., Maryanoff, B. E., Derian, C. K., Zhang, H. C., Addo, M. F., Darrow, A. L., Eckardt, A. J., Hoekstra, W. J., McComsey, D. F., Oksenberg, D., Reynolds, E. E., Santulli, R. J., Scarborough, R. M., Smith, C. E. and White, K. B. (1999) Design, synthesis, and biological characterization of a peptide-mimetic antagonist for a tethered-ligand receptor. Proc Natl Acad Sci U S A **96**, 12257-12262

92 Zhang, H. C., Derian, C. K., Andrade-Gordon, P., Hoekstra, W. J., McComsey, D. F., White, K. B., Poulter, B. L., Addo, M. F., Cheung, W. M., Damiano, B. P., Oksenberg, D., Reynolds, E. E., Pandey, A., Scarborough, R. M. and Maryanoff, B. E. (2001) Discovery and optimization of a novel series of thrombin receptor (par-1) antagonists: potent, selective peptide mimetics based on indole and indazole templates. J Med Chem **44**, 1021-1024

93 Derian, C. K., Maryanoff, B. E., Andrade-Gordon, P. and Zhang, H. (2003) Design and Evaluation of Potent Peptide-Mimetic PAR1 Antagonists. Drug Dev Res **59**, 355-366

94 Derian, C. K., Damiano, B. P., Addo, M. F., Darrow, A. L., D'Andrea, M. R., Nedelman, M., Zhang, H. C., Maryanoff, B. E. and Andrade-Gordon, P. (2003) Blockade of the thrombin receptor protease-activated receptor-1 with a small-molecule antagonist prevents thrombus formation and vascular occlusion in nonhuman primates. J Pharmacol Exp Ther **304**, 855-861

95 Ahn, H. S., Foster, C., Boykow, G., Stamford, A., Manna, M. and Graziano, M. (2000) Inhibition of cellular action of thrombin by N3-cyclopropyl-7-[[4-(1-methylethyl)phenyl]methyl]-7H-pyrrolo[3, 2-f]quinazoline-1,3-diamine (SCH 79797), a nonpeptide thrombin receptor antagonist. Biochem Pharmacol **60**, 1425-1434

96 Kato, Y., Kita, Y., Nishio, M., Hirasawa, Y., Ito, K., Yamanaka, T., Motoyama, Y. and Seki, J. (1999) In vitro antiplatelet profile of FR171113, a novel non-peptide thrombin receptor antagonist. Eur J Pharmacol **384**, 197-202

97 Hollenberg, M. D., Saifeddine, M., Sandhu, S., Houle, S. and Vergnolle, N. (2004) Proteinase-activated receptor-4: evaluation of tethered ligand-derived peptides as probes for receptor function and as inflammatory agonists in vivo. Br J Pharmacol **143**, 443-454

98 Covic, L., Misra, M., Badar, J., Singh, C. and Kuliopulos, A. (2002) Pepducin-based intervention of thrombin-receptor signaling and systemic platelet activation. Nat Med **8**, 1161-1165

99 Covic, L., Gresser, A. L., Talavera, J., Swift, S. and Kuliopulos, A. (2002) Activation and inhibition of G protein-coupled receptors by cell-penetrating membrane-tethered peptides. Proc Natl Acad Sci U S A **99**, 643-648
100 Seeley, S., Covic, L., Jacques, S. L., Sudmeier, J., Baleja, J. D. and Kuliopulos, A. (2003) Structural basis for thrombin activation of a protease-activated receptor: inhibition of intramolecular liganding. Chem Biol **10**, 1033-1041
101 Hung, D. T., Wong, Y. H., Vu, T. K. and Coughlin, S. R. (1992) The cloned platelet thrombin receptor couples to at least two distinct effectors to stimulate phosphoinositide hydrolysis and inhibit adenylyl cyclase. J Biol Chem **267**, 20831-20834
102 Offermanns, S., Laugwitz, K. L., Spicher, K. and Schultz, G. (1994) G proteins of the G12 family are activated via thromboxane A2 and thrombin receptors in human platelets. Proc Natl Acad Sci U S A **91**, 504-508
103 Baffy, G., Yang, L., Raj, S., Manning, D. R. and Williamson, J. R. (1994) G protein coupling to the thrombin receptor in Chinese hamster lung fibroblasts. J Biol Chem **269**, 8483-8487
104 Ogino, Y., Tanaka, K. and Shimizu, N. (1996) Direct evidence for two distinct G proteins coupling with thrombin receptors in human neuroblastoma SH-EP cells. Eur J Pharmacol **316**, 105-109
105 Steinhoff, M., Buddenkotte, J., Shpacovitch, V., Rattenholl, A., Moormann, C., Vergnolle, N., Luger, T. A. and Hollenberg, M. D. (2005) Proteinase-activated receptors: transducers of proteinase-mediated signaling in inflammation and immune response. Endocr Rev **26**, 1-43
106 Wang, H. and Reiser, G. (2003) Thrombin signaling in the brain: the role of protease-activated receptors. Biol Chem **384**, 193-202
107 Macfarlane, S. R. and Plevin, R. (2003) Intracellular Signalling by the G-Protein Coupled Proteiase-Activated Receptor (PAR) Family. Drug Dev Res **59**, 367-374
108 Wang, H. and Reiser, G. (2003) The role of the Ca2+-sensitive tyrosine kinase Pyk2 and Src in thrombin signalling in rat astrocytes. J Neurochem **84**, 1349-1357
109 Schaeffer, H. J. and Weber, M. J. (1999) Mitogen-activated protein kinases: specific messages from ubiquitous messengers. Mol Cell Biol **19**, 2435-2444
110 Wang, Y., Luo, W., Stricker, R. and Reiser, G. (2006) Protease-activated receptor-1 protects rat astrocytes from apoptotic cell death via JNK-mediated release of the chemokine GRO/CINC-1. J Neurochem **98**, 1046-1060
111 Wang, H., Ubl, J. J., Stricker, R. and Reiser, G. (2002) Thrombin (PAR-1)-induced proliferation in astrocytes via MAPK involves multiple signaling pathways. Am J Physiol Cell Physiol **283**, C1351-1364
112 Tanaka, N., Morita, T., Nezu, A., Tanimura, A., Mizoguchi, I. and Tojyo, Y. (2004) Signaling mechanisms involved in protease-activated receptor-1-mediated interleukin-6 production by human gingival fibroblasts. J Pharmacol Exp Ther **311**, 778-786
113 Davis, R. J. (2000) Signal transduction by the JNK group of MAP kinases. Cell **103**, 239-252
114 Wang, Y., Luo, W. and Reiser, G. (2006) Proteinase-activated receptor-1 and proteinase-activated receptor-2 induce the release of chemokine GRO/CINC-1 from rat astrocytes via differential activation of JNK isoforms, evoking multiple protective pathways in brain. Biochem J
115 Ameyar, M., Wisniewska, M. and Weitzman, J. B. (2003) A role for AP-1 in apoptosis: the case for and against. Biochimie **85**, 747-752
116 Post, G. R., Collins, L. R., Kennedy, E. D., Moskowitz, S. A., Aragay, A. M., Goldstein, D. and Brown, J. H. (1996) Coupling of the thrombin receptor to G12 may

account for selective effects of thrombin on gene expression and DNA synthesis in 1321N1 astrocytoma cells. Mol Biol Cell **7**, 1679-1690

117 Madamanchi, N. R., Li, S., Patterson, C. and Runge, M. S. (2001) Thrombin regulates vascular smooth muscle cell growth and heat shock proteins via the JAK-STAT pathway. J Biol Chem **276**, 18915-18924

118 Huang, Y. Q., Li, J. J. and Karpatkin, S. (2000) Thrombin inhibits tumor cell growth in association with up-regulation of p21(waf/cip1) and caspases via a p53-independent, STAT-1-dependent pathway. J Biol Chem **275**, 6462-6468

119 Rahman, A., True, A. L., Anwar, K. N., Ye, R. D., Voyno-Yasenetskaya, T. A. and Malik, A. B. (2002) Galpha(q) and Gbetagamma regulate PAR-1 signaling of thrombin-induced NF-kappaB activation and ICAM-1 transcription in endothelial cells. Circ Res **91**, 398-405

120 Steinhoff, M., Vergnolle, N., Young, S. H., Tognetto, M., Amadesi, S., Ennes, H. S., Trevisani, M., Hollenberg, M. D., Wallace, J. L., Caughey, G. H., Mitchell, S. E., Williams, L. M., Geppetti, P., Mayer, E. A. and Bunnett, N. W. (2000) Agonists of proteinase-activated receptor 2 induce inflammation by a neurogenic mechanism. Nat Med **6**, 151-158

121 Masamune, A., Kikuta, K., Satoh, M., Suzuki, N. and Shimosegawa, T. (2005) Protease-activated receptor-2-mediated proliferation and collagen production of rat pancreatic stellate cells. J Pharmacol Exp Ther **312**, 651-658

122 Kim, M. S., Jo, H., Um, J. Y., Yi, J. M., Kim, D. K., Choi, S. C., Kim, T. H., Nah, Y. H., Kim, H. M. and Lee, Y. M. (2002) Agonists of proteinase-activated receptor 2 induce TNF-alpha secretion from astrocytoma cells. Cell Biochem Funct **20**, 339-345

123 Buddenkotte, J., Stroh, C., Engels, I. H., Moormann, C., Shpacovitch, V. M., Seeliger, S., Vergnolle, N., Vestweber, D., Luger, T. A., Schulze-Osthoff, K. and Steinhoff, M. (2005) Agonists of proteinase-activated receptor-2 stimulate upregulation of intercellular cell adhesion molecule-1 in primary human keratinocytes via activation of NF-kappa B. J Invest Dermatol **124**, 38-45

124 Temkin, V., Kantor, B., Weg, V., Hartman, M. L. and Levi-Schaffer, F. (2002) Tryptase activates the mitogen-activated protein kinase/activator protein-1 pathway in human peripheral blood eosinophils, causing cytokine production and release. J Immunol **169**, 2662-2669

125 Luo, W., Wang, Y., Hanck, T., Stricker, R. and Reiser, G. (2006) Jab1, a Novel Protease-activated Receptor-2 (PAR-2)-interacting Protein, Is Involved in PAR-2-induced Activation of Activator Protein-1. J Biol Chem **281**, 7927-7936

126 Molino, M., Blanchard, N., Belmonte, E., Tarver, A. P., Abrams, C., Hoxie, J. A., Cerletti, C. and Brass, L. F. (1995) Proteolysis of the human platelet and endothelial cell thrombin receptor by neutrophil-derived cathepsin G. J Biol Chem **270**, 11168-11175

127 Renesto, P., Si-Tahar, M., Moniatte, M., Balloy, V., Van Dorsselaer, A., Pidard, D. and Chignard, M. (1997) Specific inhibition of thrombin-induced cell activation by the neutrophil proteinases elastase, cathepsin G, and proteinase 3: evidence for distinct cleavage sites within the aminoterminal domain of the thrombin receptor. Blood **89**, 1944-1953

128 Molino, M., Barnathan, E. S., Numerof, R., Clark, J., Dreyer, M., Cumashi, A., Hoxie, J. A., Schechter, N., Woolkalis, M. and Brass, L. F. (1997) Interactions of mast cell tryptase with thrombin receptors and PAR-2. J Biol Chem **272**, 4043-4049

129 Bohm, S. K., Grady, E. F. and Bunnett, N. W. (1997) Regulatory mechanisms that modulate signalling by G-protein-coupled receptors. Biochem J **322**, 1-18

130 Ferguson, S. S. (2001) Evolving concepts in G protein-coupled receptor endocytosis: the role in receptor desensitization and signaling. Pharmacol Rev **53**, 1-24

131 Trejo, J., Hammes, S. R. and Coughlin, S. R. (1998) Termination of signaling by protease-activated receptor-1 is linked to lysosomal sorting. Proc Natl Acad Sci U S A **95**, 13698-13702
132 Bohm, S. K., Khitin, L. M., Grady, E. F., Aponte, G., Payan, D. G. and Bunnett, N. W. (1996) Mechanisms of desensitization and resensitization of proteinase-activated receptor-2. J Biol Chem **271**, 22003-22016
133 Yan, W., Tiruppathi, C., Lum, H., Qiao, R. and Malik, A. B. (1998) Protein kinase C beta regulates heterologous desensitization of thrombin receptor (PAR-1) in endothelial cells. Am J Physiol **274**, C387-395
134 Shapiro, M. J., Weiss, E. J., Faruqi, T. R. and Coughlin, S. R. (2000) Protease-activated receptors 1 and 4 are shut off with distinct kinetics after activation by thrombin. J Biol Chem **275**, 25216-25221
135 Dery, O., Corvera, C. U., Steinhoff, M. and Bunnett, N. W. (1998) Proteinase-activated receptors: novel mechanisms of signaling by serine proteases. Am J Physiol **274**, C1429-1452
136 Hoxie, J. A., Ahuja, M., Belmonte, E., Pizarro, S., Parton, R. and Brass, L. F. (1993) Internalization and recycling of activated thrombin receptors. J Biol Chem **268**, 13756-13763
137 Hein, L., Ishii, K., Coughlin, S. R. and Kobilka, B. K. (1994) Intracellular targeting and trafficking of thrombin receptors. A novel mechanism for resensitization of a G protein-coupled receptor. J Biol Chem **269**, 27719-27726
138 DeFea, K. A., Zalevsky, J., Thoma, M. S., Dery, O., Mullins, R. D. and Bunnett, N. W. (2000) {beta}-Arrestin-dependent Endocytosis of Proteinase-activated Receptor 2 Is Required for Intracellular Targeting of Activated ERK1/2. J. Cell Biol. **148**, 1267-1282
139 Dery, O., Thoma, M. S., Wong, H., Grady, E. F. and Bunnett, N. W. (1999) Trafficking of proteinase-activated receptor-2 and beta-arrestin-1 tagged with green fluorescent protein. beta-Arrestin-dependent endocytosis of a proteinase receptor. J Biol Chem **274**, 18524-18535
140 Paing, M. M., Stutts, A. B., Kohout, T. A., Lefkowitz, R. J. and Trejo, J. (2002) beta -Arrestins regulate protease-activated receptor-1 desensitization but not internalization or Down-regulation. J Biol Chem **277**, 1292-1300
141 Trejo, J., Altschuler, Y., Fu, H. W., Mostov, K. E. and Coughlin, S. R. (2000) Protease-activated receptor-1 down-regulation: a mutant HeLa cell line suggests novel requirements for PAR1 phosphorylation and recruitment to clathrin-coated pits. J Biol Chem **275**, 31255-31265
142 Trejo, J. (2003) Protease-activated receptors: new concepts in regulation of G protein-coupled receptor signaling and trafficking. J Pharmacol Exp Ther **307**, 437-442
143 Roosterman, D., Schmidlin, F. and Bunnett, N. W. (2003) Rab5a and rab11a mediate agonist-induced trafficking of protease-activated receptor 2. Am J Physiol Cell Physiol **284**, C1319-1329
144 Trejo, J. and Coughlin, S. R. (1999) The cytoplasmic tails of protease-activated receptor-1 and substance P receptor specify sorting to lysosomes versus recycling. J Biol Chem **274**, 2216-2224
145 Johnson, K. F. and Kornfeld, S. (1992) A His-Leu-Leu sequence near the carboxyl terminus of the cytoplasmic domain of the cation-dependent mannose 6-phosphate receptor is necessary for the lysosomal enzyme sorting function. J Biol Chem **267**, 17110-17115
146 Letourneur, F. and Klausner, R. D. (1992) A novel di-leucine motif and a tyrosine-based motif independently mediate lysosomal targeting and endocytosis of CD3 chains. Cell **69**, 1143-1157

147 Longva, K. E., Blystad, F. D., Stang, E., Larsen, A. M., Johannessen, L. E. and Madshus, I. H. (2002) Ubiquitination and proteasomal activity is required for transport of the EGF receptor to inner membranes of multivesicular bodies. J Cell Biol **156**, 843-854
148 Wang, Y., Zhou, Y., Szabo, K., Haft, C. R. and Trejo, J. (2002) Down-regulation of protease-activated receptor-1 is regulated by sorting nexin 1. Mol Biol Cell **13**, 1965-1976
149 Haft, C. R., de la Luz Sierra, M., Barr, V. A., Haft, D. H. and Taylor, S. I. (1998) Identification of a family of sorting nexin molecules and characterization of their association with receptors. Mol Cell Biol **18**, 7278-7287
150 Jacob, C., Cottrell, G. S., Gehringer, D., Schmidlin, F., Grady, E. F. and Bunnett, N. W. (2005) c-Cbl mediates ubiquitination, degradation, and down-regulation of human protease-activated receptor 2. J Biol Chem **280**, 16076-16087
151 Brass, L. F., Pizarro, S., Ahuja, M., Belmonte, E., Blanchard, N., Stadel, J. M. and Hoxie, J. A. (1994) Changes in the structure and function of the human thrombin receptor during receptor activation, internalization, and recycling. J Biol Chem **269**, 2943-2952
152 Horvat, R. and Palade, G. E. (1995) The functional thrombin receptor is associated with the plasmalemma and a large endosomal network in cultured human umbilical vein endothelial cells. J Cell Sci **108**, 1155-1164
153 Compton, S. J. (2003) Glycosylation and Proteinase-Activated Receptor Function. Drug Dev Res **59**, 350-354
154 Garcia Rodriguez, C., Cundell, D. R., Tuomanen, E. I., Kolakowski, L. F., Jr., Gerard, C. and Gerard, N. P. (1995) The role of N-glycosylation for functional expression of the human platelet-activating factor receptor. Glycosylation is required for efficient membrane trafficking. J Biol Chem **270**, 25178-25184
155 Zhang, Z., Austin, S. C. and Smyth, E. M. (2001) Glycosylation of the human prostacyclin receptor: role in ligand binding and signal transduction. Mol Pharmacol **60**, 480-487
156 Zhou, F., Xu, W., Hong, M., Pan, Z., Sinko, P. J., Ma, J. and You, G. (2005) The role of N-linked glycosylation in protein folding, membrane targeting, and substrate binding of human organic anion transporter hOAT4. Mol Pharmacol **67**, 868-876
157 Opdenakker, G., Rudd, P. M., Ponting, C. P. and Dwek, R. A. (1993) Concepts and principles of glycobiology. Faseb J **7**, 1330-1337
158 Compton, S. J., Renaux, B., Wijesuriya, S. J. and Hollenberg, M. D. (2001) Glycosylation and the activation of proteinase-activated receptor 2 (PAR(2)) by human mast cell tryptase. Br J Pharmacol **134**, 705-718
159 Vouret-Craviari, V., Grall, D., Chambard, J. C., Rasmussen, U. B., Pouyssegur, J. and Van Obberghen-Schilling, E. (1995) Post-translational and activation-dependent modifications of the G protein-coupled thrombin receptor. J Biol Chem **270**, 8367-8372
160 Dietrich, L. E. and Ungermann, C. (2004) On the mechanism of protein palmitoylation. EMBO Rep **5**, 1053-1057
161 Moffett, S., Mouillac, B., Bonin, H. and Bouvier, M. (1993) Altered phosphorylation and desensitization patterns of a human beta 2-adrenergic receptor lacking the palmitoylated Cys341. Embo J **12**, 349-356
162 Moffett, S., Adam, L., Bonin, H., Loisel, T. P., Bouvier, M. and Mouillac, B. (1996) Palmitoylated cysteine 341 modulates phosphorylation of the beta2-adrenergic receptor by the cAMP-dependent protein kinase. J Biol Chem **271**, 21490-21497
163 Ponimaskin, E. G., Heine, M., Joubert, L., Sebben, M., Bickmeyer, U., Richter, D. W. and Dumuis, A. (2002) The 5-hydroxytryptamine(4a) receptor is palmitoylated at two

different sites, and acylation is critically involved in regulation of receptor constitutive activity. J Biol Chem **277**, 2534-2546
164 Papoucheva, E., Dumuis, A., Sebben, M., Richter, D. W. and Ponimaskin, E. G. (2004) The 5-hydroxytryptamine(1A) receptor is stably palmitoylated, and acylation is critical for communication of receptor with Gi protein. J Biol Chem **279**, 3280-3291
165 Mahajan, V. B., Pai, K. S., Lau, A. and Cunningham, D. D. (2000) Creatine kinase, an ATP-generating enzyme, is required for thrombin receptor signaling to the cytoskeleton. Proc Natl Acad Sci U S A **97**, 12062-12067
166 Pai, K. S., Mahajan, V. B., Lau, A. and Cunningham, D. D. (2001) Thrombin receptor signaling to cytoskeleton requires Hsp90. J Biol Chem **276**, 32642-32647
167 Claret, F. X., Hibi, M., Dhut, S., Toda, T. and Karin, M. (1996) A new group of conserved coactivators that increase the specificity of AP-1 transcription factors. Nature **383**, 453-457
168 Deng, X. W., Dubiel, W., Wei, N., Hofmann, K. and Mundt, K. (2000) Unified nomenclature for the COP9 signalosome and its subunits: an essential regulator of development. Trends Genet **16**, 202-203
169 Schwechheimer, C. (2004) The COP9 signalosome (CSN): an evolutionary conserved proteolysis regulator in eukaryotic development. Biochim Biophys Acta **1695**, 45-54
170 Fu, H., Reis, N., Lee, Y., Glickman, M. H. and Vierstra, R. D. (2001) Subunit interaction maps for the regulatory particle of the 26S proteasome and the COP9 signalosome. Embo J **20**, 7096-7107
171 Tomoda, K., Kubota, Y. and Kato, J. (1999) Degradation of the cyclin-dependent-kinase inhibitor p27Kip1 is instigated by Jab1. Nature **398**, 160-165
172 Bianchi, E., Denti, S., Granata, A., Bossi, G., Geginat, J., Villa, A., Rogge, L. and Pardi, R. (2000) Integrin LFA-1 interacts with the transcriptional co-activator JAB1 to modulate AP-1 activity. Nature **404**, 617-621
173 Bae, M. K., Ahn, M. Y., Jeong, J. W., Bae, M. H., Lee, Y. M., Bae, S. K., Park, J. W., Kim, K. R. and Kim, K. W. (2002) Jab1 interacts directly with HIF-1alpha and regulates its stability. J Biol Chem **277**, 9-12
174 Chauchereau, A., Georgiakaki, M., Perrin-Wolff, M., Milgrom, E. and Loosfelt, H. (2000) JAB1 interacts with both the progesterone receptor and SRC-1. J Biol Chem **275**, 8540-8548
175 Stalheim, L., Ding, Y., Gullapalli, A., Paing, M. M., Wolfe, B. L., Morris, D. R. and Trejo, J. (2005) Multiple independent functions of arrestins in the regulation of protease-activated receptor-2 signaling and trafficking. Mol Pharmacol **67**, 78-87
176 Stamnes, M. A., Craighead, M. W., Hoe, M. H., Lampen, N., Geromanos, S., Tempst, P. and Rothman, J. E. (1995) An integral membrane component of coatomer-coated transport vesicles defines a family of proteins involved in budding. Proc Natl Acad Sci U S A **92**, 8011-8015
177 Blum, R., Feick, P., Puype, M., Vandekerckhove, J., Klengel, R., Nastainczyk, W. and Schulz, I. (1996) Tmp21 and p24A, two type I proteins enriched in pancreatic microsomal membranes, are members of a protein family involved in vesicular trafficking. J Biol Chem **271**, 17183-17189
178 Schimmoller, F., Singer-Kruger, B., Schroder, S., Kruger, U., Barlowe, C. and Riezman, H. (1995) The absence of Emp24p, a component of ER-derived COPII-coated vesicles, causes a defect in transport of selected proteins to the Golgi. Embo J **14**, 1329-1339
179 Fiedler, K., Veit, M., Stamnes, M. A. and Rothman, J. E. (1996) Bimodal interaction of coatomer with the p24 family of putative cargo receptors. Science **273**, 1396-1399

180 Nickel, W., Sohn, K., Bunning, C. and Wieland, F. T. (1997) p23, a major COPI-vesicle membrane protein, constitutively cycles through the early secretory pathway. Proc Natl Acad Sci U S A **94**, 11393-11398
181 Blum, R., Pfeiffer, F., Feick, P., Nastainczyk, W., Kohler, B., Schafer, K. H. and Schulz, I. (1999) Intracellular localization and in vivo trafficking of p24A and p23. J Cell Sci **112**, 537-548
182 Dominguez, M., Dejgaard, K., Fullekrug, J., Dahan, S., Fazel, A., Paccaud, J. P., Thomas, D. Y., Bergeron, J. J. and Nilsson, T. (1998) gp25L/emp24/p24 protein family members of the cis-Golgi network bind both COP I and II coatomer. J Cell Biol **140**, 751-765
183 Anantharaman, V. and Aravind, L. (2002) The GOLD domain, a novel protein module involved in Golgi function and secretion. Genome Biol **3**, research0023
184 Ciufo, L. F. and Boyd, A. (2000) Identification of a lumenal sequence specifying the assembly of Emp24p into p24 complexes in the yeast secretory pathway. J Biol Chem **275**, 8382-8388
185 Emery, G., Rojo, M. and Gruenberg, J. (2000) Coupled transport of p24 family members. J Cell Sci **113**, 2507-2516
186 Contreras, I., Ortiz-Zapater, E. and Aniento, F. (2004) Sorting signals in the cytosolic tail of membrane proteins involved in the interaction with plant ARF1 and coatomer. Plant J **38**, 685-698
187 Majoul, I., Straub, M., Hell, S. W., Duden, R. and Soling, H. D. (2001) KDEL-cargo regulates interactions between proteins involved in COPI vesicle traffic: measurements in living cells using FRET. Dev Cell **1**, 139-153
188 Barr, F. A., Preisinger, C., Kopajtich, R. and Korner, R. (2001) Golgi matrix proteins interact with p24 cargo receptors and aid their efficient retention in the Golgi apparatus. J Cell Biol **155**, 885-891
189 Carney, G. E. and Bowen, N. J. (2004) p24 proteins, intracellular trafficking, and behavior: Drosophila melanogaster provides insights and opportunities. Biol Cell **96**, 271-278
190 Wen, C. and Greenwald, I. (1999) p24 proteins and quality control of LIN-12 and GLP-1 trafficking in Caenorhabditis elegans. J Cell Biol **145**, 1165-1175
191 Springer, S., Chen, E., Duden, R., Marzioch, M., Rowley, A., Hamamoto, S., Merchant, S. and Schekman, R. (2000) The p24 proteins are not essential for vesicular transport in Saccharomyces cerevisiae. Proc Natl Acad Sci U S A **97**, 4034-4039
192 Gommel, D., Orci, L., Emig, E. M., Hannah, M. J., Ravazzola, M., Nickel, W., Helms, J. B., Wieland, F. T. and Sohn, K. (1999) p24 and p23, the major transmembrane proteins of COPI-coated transport vesicles, form hetero-oligomeric complexes and cycle between the organelles of the early secretory pathway. FEBS Lett **447**, 179-185
193 Bockaert, J. and Pin, J. P. (1999) Molecular tinkering of G protein-coupled receptors: an evolutionary success. Embo J **18**, 1723-1729
194 Yun, J., Tomida, A., Andoh, T. and Tsuruo, T. (2004) Interaction between glucose-regulated destruction domain of DNA topoisomerase IIalpha and MPN domain of Jab1/CSN5. J Biol Chem **279**, 31296-31303
195 Burger-Kentischer, A., Finkelmeier, D., Thiele, M., Schmucker, J., Geiger, G., Tovar, G. E. and Bernhagen, J. (2005) Binding of JAB1/CSN5 to MIF is mediated by the MPN domain but is independent of the JAMM motif. FEBS Lett **579**, 1693-1701
196 Kim, B. C., Lee, H. J., Park, S. H., Lee, S. R., Karpova, T. S., McNally, J. G., Felici, A., Lee, D. K. and Kim, S. J. (2004) Jab1/CSN5, a component of the COP9 signalosome, regulates transforming growth factor beta signaling by binding to Smad7 and promoting its degradation. Mol Cell Biol **24**, 2251-2262

197 Kleemann, R., Hausser, A., Geiger, G., Mischke, R., Burger-Kentischer, A., Flieger, O., Johannes, F. J., Roger, T., Calandra, T., Kapurniotu, A., Grell, M., Finkelmeier, D., Brunner, H. and Bernhagen, J. (2000) Intracellular action of the cytokine MIF to modulate AP-1 activity and the cell cycle through Jab1. Nature **408**, 211-216
198 Seeger, M., Kraft, R., Ferrell, K., Bech-Otschir, D., Dumdey, R., Schade, R., Gordon, C., Naumann, M. and Dubiel, W. (1998) A novel protein complex involved in signal transduction possessing similarities to 26S proteasome subunits. Faseb J **12**, 469-478
199 Uhle, S., Medalia, O., Waldron, R., Dumdey, R., Henklein, P., Bech-Otschir, D., Huang, X., Berse, M., Sperling, J., Schade, R. and Dubiel, W. (2003) Protein kinase CK2 and protein kinase D are associated with the COP9 signalosome. Embo J **22**, 1302-1312
200 Naumann, M., Bech-Otschir, D., Huang, X., Ferrell, K. and Dubiel, W. (1999) COP9 signalosome-directed c-Jun activation/stabilization is independent of JNK. J Biol Chem **274**, 35297-35300
201 Li, S., Liu, X. and Ascoli, M. (2000) p38JAB1 binds to the intracellular precursor of the lutropin/choriogonadotropin receptor and promotes its degradation. J Biol Chem **275**, 13386-13393
202 Ascoli, M. (2005) Learning new tricks from an old dog: the processing of the intracellular precursor of the luteinizing hormone receptor (LHR) into the mature cell-surface LHR is a regulated process. Endocrinology **146**, 3221-3223
203 Cottrell, G. S., Amadesi, S., Schmidlin, F. and Bunnett, N. (2003) Protease-activated receptor 2: activation, signalling and function. Biochem Soc Trans **31**, 1191-1197
204 Somasundaram, P., Ren, G., Nagar, H., Kraemer, D., Mendoza, L., Michael, L. H., Caughey, G. H., Entman, M. L. and Frangogiannis, N. G. (2005) Mast cell tryptase may modulate endothelial cell phenotype in healing myocardial infarcts. J Pathol **205**, 102-111
205 Hirano, K., Yufu, T., Hirano, M., Nishimura, J. and Kanaide, H. (2005) Physiology and pathophysiology of proteinase-activated receptors (PARs): regulation of the expression of PARs. J Pharmacol Sci **97**, 31-37
206 Lundberg, A. H., Eubanks, J. W., 3rd, Henry, J., Sabek, O., Kotb, M., Gaber, L., Norby-Teglund, A. and Gaber, A. O. (2000) Trypsin stimulates production of cytokines from peritoneal macrophages in vitro and in vivo. Pancreas **21**, 41-51
207 Vliagoftis, H., Schwingshackl, A., Milne, C. D., Duszyk, M., Hollenberg, M. D., Wallace, J. L., Befus, A. D. and Moqbel, R. (2000) Proteinase-activated receptor-2-mediated matrix metalloproteinase-9 release from airway epithelial cells. J Allergy Clin Immunol **106**, 537-545
208 Foletta, V. C., Segal, D. H. and Cohen, D. R. (1998) Transcriptional regulation in the immune system: all roads lead to AP-1. J Leukoc Biol **63**, 139-152
209 Duden, R. (2003) ER-to-Golgi transport: COP I and COP II function (Review). Mol Membr Biol **20**, 197-207
210 Milligan, G. (2004) G protein-coupled receptor dimerization: function and ligand pharmacology. Mol Pharmacol **66**, 1-7
211 Corpet, F. (1988) Multiple sequence alignment with hierarchical clustering. Nucleic Acids Res **16**, 10881-10890
212 Chavrier, P. and Goud, B. (1999) The role of ARF and Rab GTPases in membrane transport. Curr Opin Cell Biol **11**, 466-475
213 Gommel, D. U., Memon, A. R., Heiss, A., Lottspeich, F., Pfannstiel, J., Lechner, J., Reinhard, C., Helms, J. B., Nickel, W. and Wieland, F. T. (2001) Recruitment to Golgi membranes of ADP-ribosylation factor 1 is mediated by the cytoplasmic domain of p23. Embo J **20**, 6751-6760

214 Wieland, F. and Harter, C. (1999) Mechanisms of vesicle formation: insights from the COP system. Curr Opin Cell Biol **11**, 440-446
215 Jenne, N., Frey, K., Brugger, B. and Wieland, F. T. (2002) Oligomeric state and stoichiometry of p24 proteins in the early secretory pathway. J Biol Chem **277**, 46504-46511

8. ABBREVIATION

aa	amino acid(s)
AP	activating peptide
AP-1	activator protein-1
APC	activated protein C
β_2-AR	β_2-adrenergic receptor
ARF1	ADP-ribosylation factor 1
BSA	bovine serum albumin
$[Ca^{2+}]_i$	intracellular calcium concentration
CAT	chloramphenicol acetyltransferase
CNS	central nervous system
COP	coat protein
DMSO	dimethyl sulfoxide
DAG	diacylglycerol
EL	extracellular loop
ELISA	enzyme-linked immunosorbent assay
ER	endoplasmic reticulum
ERK 1/2	extracellular signal regulated kinase 1/2
FCS	fetal calf serum
GAPDH	glyceraldehyde-3-phosphate dehydrogenase
GEF	guanine nucleotide exchange factor
GPCR	G protein-coupled receptor
GRK	G protein-coupled receptor kinase
GRO/CINC-1	growth-regulated oncogene/cytokine-induced neutrophil chemoattractant-1
GST	glutathione *S*-transferase
HA	haemagglutinin epitope
HIF-1 α	hypoxia-inducible factor-1 α
IL	interleukin
IP_3	inositol 1,4,5-trisphosphate
IP	immunoprecipitation
Jab1	Jun activation domain-binding protein 1
JNK	c-Jun N-terminal kinase

LHR	lutropin/choriogonadotropin receptor
MAPK	mitogen-activated protein kinase
MIF	migration inhibitory factor
MT-SP1	membrane-type serine protease 1
NF-κB	nuclear factor-κB
NHA	normal (primary) human astrocytes
PAO	phenylarsine oxide
PAR	protease-activated receptor
PFA	paraformaldehyde
PKA	protein kinase A
PKC	protein kinase C
PLC-β	phospholipase C-β
PNGase F	peptide *N*-glycosidase F
PRSS	protease, serine
RgpB	arginine-specific gingipains-R
RT-PCR	reverse transcription-polymerase chain reaction
Sf9	*Spodoptera frugiperda* 9
siRNA	small interfering RNA
SRC-1	steroid receptor coactivator-1
TNF-α	tumor necrosis factor-α
tPA	tissue plasminogen activator
TRag	Ala-parafluoroPhe-Arg-Cha-Cit-Tyr-NH_2
TRAP	thrombin receptor agonist peptide
WT	wild-type
ZPAD	Z-Phe-Ala-diazomethylketone

9. APPENDIX

I Publications

1. **Luo W.**, Wang Y., Reiser G. (2005) Two types of protease-activated receptors (PAR-1 and PAR-2) mediate calcium signaling in rat retinal ganglion cells RGC-5. **Brain Res** 1047: 159-67.

We characterized the functional expression of PAR-1 and PAR-2 in RGC-5 cells.

2. **Luo W.**, Wang Y., Hanck T., Stricker R., Reiser G. (2006) Jab1, a novel protease-activated receptor-2 (PAR-2)-interacting protein, is involved in PAR-2-induced activation of activator protein-1. **J Biol Chem** 281: 7927-36.

We identified Jab1 as a novel PAR-2-interacting protein, and delineated its physiological function in the PAR-2 signalling pathway.

3. Wang Y., **Luo W.**, Stricker R., Reiser G. (2006) Protease-activated receptor-1 protects rat astrocytes from apoptotic cell death via JNK-mediated release of the chemokine GRO/CINC-1. **J Neurochem**, 98: 1046-60.

We investigated the biological functions of JNK in the PAR-1 signalling pathway, and delineated a novel mechanism underlying the PAR-1-mediated protection in astrocytes.

4. Wang Y., **Luo W.**, Wartmann T., Halangk W., Sahin-Tóth M., Reiser G. (2006) Mesotrypsin, a brain trypsin, activates selectively proteinase-activated receptor-1, but not proteinase-activated receptor-2, in rat astrocytes. **J Neurochem**, 99: 759-69.

We identified a novel specific PAR-1 agonist in the brain.

5. Wang Y., **Luo W.**, Reiser G. Proteinase-activated receptor-1 and proteinase-activated receptor-2 induce the release of chemokine GRO/CINC-1 from rat astrocytes via differential activation of JNK isoforms, evoking multiple protective pathways in brain. **Biochem J**. 2006 Aug 30; [Epub ahead of print].

We distinguished the functions of different JNK isoforms in the PAR-1 and PAR-2 signalling pathways.

6. **Luo W.,** Wang Y., Reiser G. Regulation of post-Golgi transport of the protease-activated receptor-2 by p24A and p23. In preparation.

II Conference abstracts

1. **Luo W** and Reiser G. *Expression of protease-activated receptors (PARs) and PAR-mediated calcium signaling in rat RGC-5 cells.* Molecular Mechanisms of Neurodegeneration and Neuroprotection—Experimental Approaches and the Diseased

Brain, annual Meeting of the Study Group Neurochemistry of the German Society of Biochemistry and Molecular Biology (GBM) in Leipzig, Germany, Sep. 9-11th, 2004. **Int. J. Devl Neuroscience** 22, p588, 2004.

2. Wang Y., **Luo W.,** Stricker R., Reiser G. *Protease-activated receptors (PARs)-induced IL-8-like chemokine GRO/CINC-1 release from rat astrocytes.* Molecular Mechanisms of Neurodegeneration and Neuroprotection—Experimental Approaches and the Diseased Brain, annual Meeting of the Study Group Neurochemistry of the German Society of Biochemistry and Molecular Biology (GBM) in Leipzig, Germany, Sep. 9-11th, 2004. **Int. J. Devl Neuroscience** 22, p598, 2004.
3. **Luo W.**, Wang Y., Reiser G. *Two types of protease-activated receptors (PAR-1 and PAR-2) mediate calcium signalling in rat retinal ganglion (RGC-5) cells.* 6th Meeting of the German Neuroscience Society-30th Göttingen Neurobiology Conference and Joint symposium of the DFG Neuroscience Graduate Schools in Göttingen, Germany, Feb. 16-20th, 2005.
4. Wang Y., **Luo W.,** Stricker R., Reiser G. *The mechanism of IL-8-like chemokine (GRO/CINC-1) release from rat astrocytes mediated by protease-activated receptor-1.* 6th Meeting of the German Neuroscience Society-30th Göttingen Neurobiology Conference and Joint symposium of the DFG Neuroscience Graduate Schools in Göttingen, Germany, Feb. 16-20th, 2005.
5. **Luo W.**, Wang Y., Stricker R., Hanck T., Reiser G. *Identification and characterization of human protease-activated receptor (PAR-2) interacting proteins.* VII. European Meeting on Glial Cell Function in Health and Disease in Amsterdam, Netherlands. May 17-20th, 2005.
6. Wang Y., **Luo W.,** Stricker R., Reiser G. *Different mechanisms of GRO/CINC-1 release from rat astrocytes mediated by protease-activated receptor 1 and 2.* VII. European Meeting on Glial Cell Function in Health and Disease in Amsterdam, Netherlands. May 17-20th, 2005.
7. **Luo W.**, Wang Y., Stricker R., Hanck T., Reiser G. *A proteasome subunit regulates a novel human protease-activated receptor-2 (PAR-2)-mediated inflammatory response pathway.* Neural signal transduction in health and disease-cytokines, mitochondrial dysfunction and transport processes, annual Meeting of the Study Group Neurochemistry of the German Society of Biochemistry and Molecular Biology (GBM) in Leipzig, Germany, Oct. 6-8th, 2005. **Int. J. Devl Neuroscience** 24, p218, 2006.

8. Wang Y., **Luo W.,** Hanck T., Stricker R., Reiser G. *Protease-activated receptor (PAR)-1 and –2 differently mediate release of the chemokine GRO/CINC-1 from rat astrocytes.* Neural signal transduction in health and disease-cytokines, mitochondrial dysfunction and transport processes, annual Meeting of the Study Group Neurochemistry of the German Society of Biochemistry and Molecular Biology (GBM) in Leipzig, Germany, Oct. 6-8th, 2005. **Int. J. Devl Neuroscience** 24, p218, 2006.

III DNA sequences published in the GenBank™

1. **AY336105**, human PAR-2 cDNA sequence
   Our sequence shows the alternative human PAR-2 cDNA.
2. **AY594282**, human HUEL cDNA sequence
   Our sequence shows the alternative human HUEL cDNA.

IV Curriculum Vitae

Name: Weibo LUO
Birthday: June 21, 1976
Place of Birth: Zhejiang, China
Nationality: China

Education and Experience

Sep. 1995 – June 1999 Zhejiang University, Hangzhou, China
Bachelor of Science in Biochemistry and Microbiology
Thesis: Studies on mitochondrial DNA of *Macrobrachium nipponese*.

Sep. 1999 – July 2002 Shanghai Institute of Materia Medica, Chinese Academy of Sciences, Shainghai, China
Master of Science in Pharmacology
Thesis: The mechanisms of magnesium lithospermate B on attenuating hypoxia-reoxygenation-induced endothelial cell injury.

Aug. 2002 – Feb. 2003 Institute of Medical Psychology, Otto-von-Guericke-Universität Magdeburg, Magdeburg, Germany
Supported by Deutsche Forschungsgemeinschaft (Graduiertenkolleg 253/3 für "Biologische Grundlagen von Erkrankungen des Nervensystems")
Project: Repair of internal axon damage following optic nerve crush.

Feb. 2003 - present Insitute of Neurobiochemistry, Otto-von-Guericke-Universität Magdeburg, Magdeburg, Germany
Supported by Deutsche Forschungsgemeinschaft (Graduiertenkolleg 253/3 für "Biologische Grundlagen von Erkrankungen des Nervensystems")

Project:

1) Identification and characterization of human PAR-2-interacting partner proteins.

2) The expression of protease-activated receptors in retinal ganglion cells (RGC-5 cells).

20. 04. 2007, Magdeburg

Weibo LUO